Norwegian University
of Life Sciences

Master's Thesis 2017 60 ECTS
Faculty of Chemistry, Biotechnology and Food Science

Risk assessment of BRCA1 variants with unknown clinical significance

Jonas Langerud
Biotechnology

RISK ASSESSMENT OF BRCA1 VARIANTS WITH UNKNOWN CLINICAL SIGNIFICANCE

A functional study of BRCA1 missense variants found in breast cancer patients

Oslo University Hospital,
Department of Medical Genetics

and

The Norwegian University of Life Sciences (NMBU),
Department of Chemistry, Biotechnology and Food Sciences

Acknowledgments

The work described in this thesis was performed at the Oslo University Hospital, Department of Medical Genetics, as a part of the Norwegian University of Life Sciences (NMBU) Master program in Biotechnology, at the Department of Chemistry, Biotechnology and Food Sciences (IKBM).

First and foremost, I want to thank my supervisors Dr. Philos Nina Iversen[1] and Sarah Ariansen[2] for their excellent guidance. Your knowledge, patience and support has been invaluable to this work. I would also like to thank Department Engineer Marit Sletten and PhD Mari Tinholt, their skill and prowess in the laboratory has been an inspiration. I owe a great deal of gratitude to Deeqa Ahmed and Magnhild Fjeldvær for their help in the laboratory and for sharing their expertise in the intricate field of variant classification. Moreover, I would like to thank Elisabeth Jarhelle for providing the plasmids utilised in this study, and for helpful correspondence. Additionally, I would like to thank my supervisor at NMBU Tor Erling Lea[3]. A special thanks to Lovise Olaug Mæhle[4] for inviting me to spend a day with her, and for the opportunity to observe on the genetic counselling of a patient. The insight into how the work on this thesis could directly affect patients was deeply appreciated. Furthermore, to all the wonderful people at the Department of Medical Genetics that helped me along the way, either with your expertise or with your words of encouragement, thank you.

I want to express my gratitude to my fellow student Mona Hellenes, who have provided me with much encouragement and support throughout this work. Also, I would like to thank my family and friends for their patience and support. A very special thanks to Hedda Johannesen, it would not be an overstatement to say that this work would be far less without your support, encouragement and help.

Oslo, May 2017

Jonas Langerud

---

[1] Scientist, Dept. of Medical Genetics, Oslo University Hospital.
[2] Laboratory manager, Cancer Genetic Unit, Section for Genetic Diagnostic Laboratories, Dept. of Medical Genetics, Oslo University Hospital.
[3] Professor, Dept. of Chemistry, Biotechnology and Food Sciences, Norwegian University of Life Sciences.
[4] Doctor, Section of Hereditary Cancers, Dept. of Medical Genetics, Oslo University Hospital.

Sammendrag

Brystkreft er den mest utbredte kreftformen blant kvinner og er ansvarlig for 14 % av kreftrelaterte dødsfall i verden. Omlag 10 % av krefttilfellene kan tilskrives sykdomsgivende kimcellevarianter, av disse stammer 30 % av tilfellene fra skadelige varianter i tumorsuppressorgen *BRCA1* og *BRCA2*. Basesubstitusjoner i *BRCA1* er særlig problematiske fra et klinisk ståsted, da effekten de har på proteinets funksjonalitet ofte er ukjent. Mange patogene varianter i *BRCA1* ligger i det BRCA1 C-terminale (BRCT) domenet, et domene nødvendig for nøkkelfunksjoner som homolog rekombinasjon, protein-protein interaksjon og transaktivering (TA). Vi undersøkte transaktiveringsegenskapene til 12 *BRCA1* BRCT basesubstitusjonsvarianter med ukjent klinisk signifikans (VUS), på et funksjonelt assay. For å oppnå dette modifiserte vi en dobbel-luciferase transaktiverings analysemetode (TA-metode), til å gi økt prøvemengde og sensitivitet. Vi ønsket også å beskrive brystkreftcellelinjene MDA-MB-231, MDA-MB-436, SUM102 og MCF-7, ved å studere effekten av Doxorubicin og Carboplatin på cellenes levedyktighet sett i forhold til endogent *BRCA1* og *TP53* status.

Ved å etablere TA-aktivitetsgrenseverdier for høy- og lav-risiko grupper utfra kontroller bestående av kjente patogene og benigne varianter, fant vi at variantene p.Thr1700Thr, p.Gly1709Arg, p.Pro1776Ser, p.Glu1826Leu og p.Arg1835Gln, falt innenfor lavrisiko gruppen. Variantene p.Asp1692Ala, p.Gly1706Arg og p.Val1838Gly viste en fullstendig mangel på TA-aktivitet som samsvarer med patogenitet, og ble dermed plassert i høy-risikogruppen. De fire variantene p.Arg1699Gln, p.Ala1708Val, p.Lys1711Gln og p.Met1783Thr viste intermediær TA-aktivitet. Ved å kombinere våre funn med tilgjengelige data, og tolke dette i samsvar med retningslinjene utarbeidet av American College of Medical Genetics and Genomics (ACMG), foreslår vi følgende klassifisering av variantene: p.Thr1700Thr, p.Pro1776ser, p.Met1783Thr, p.Glu1826Leu og p.Arg1835Gln er sannsynlig benigne (klasse 2) varianter. p.Asp1692Ala, p.Arg1699Gln, p.Gly1706Arg, p.Ala1708Val og p.Val1838Gly er sannsynlig patogene (klasse 4), der p.Arg1699Gln og p.Ala1708Val sannsynligvis representerer patogene varianter med moderat penetrans. Variantene p.Gly1709Arg og p.Lys1711Gln forblir klassifisert som VUSer (klasse 3). Vi kan konstantere at TA-metoden i stor grad er uavhengig av valg av modellcellelinjer og det endogene *BRCA1* og *TP53* uttrykket, men at forlenget inkubasjonstid gir en signifikant økning i sensitivitet.

Vi oppdaget også at de trippel negative brystkreftcellelinjene MDA-MB-231 og MDA-MB-436, med manglende p53 aktivitet, viste lav sensitivitet ved behandling med Doxorubicin, noe som kan indikere en rolle for p53 i utviklingen av cytostatika resistens. Trippelnegative brystkreftceller viste en økt sensitivitet ved behandling med Carboplatin, sammenlignet med Doxorubicin. Det ble påvist at cellelinjen MDA-MB-436 var bærer av c.604_610dupCGTGTGG, en ny *TP53* variant med et tidlig stoppkodon og sannsynligvis et ødelagt p53 protein. Cellelinjen SUM102 viste høy sensitivitet under behandling med både Carboplatin og Doxorubicin, men inneholdt villtype *BRCA1* og *TP53*, noe som kan indikere at den kan ha vært bærer av skadelige varianter i andre gener involvert i DNA reparasjonsmekanismer. Den luminale og hormonreseptor positive cellelinjen MCF-7 viste lav sensitivitet til behandling med Doxorubicin, men økt sensitivitet til Carboplatin med særlig effekt ved økt behandlingstid.

Abstract

Breast cancer is the most prevalent cancer in women, and is responsible for 14 % of cancer related deaths worldwide. Approximately 10 % of all breast cancers can be attributed to deleterious germline variants. Deleterious variants in tumour suppressor gene *BRCA1* are known to cause hereditary breast and ovarian cancer syndrome (HBOC), and together with *BRCA2* they account for 30 % of hereditary morbidity. Missense variants in *BRCA1* pose a challenge in clinical care, as their effect on protein functionality largely remains unknown. Many of the pathogenic variants found in *BRCA1* are located in the *BRCA1* C-terminal (BRCT) domain, a domain that is known to be vital for key functions such as homologous repair, protein-protein interactions and transactivation (TA). This led to an investigation of the transactivation ability of 12 *BRCA1* variants of unknown clinical significance (VUSs) located in the BRCT domain, on a functional assay to assess their impact on BRCA1. To accomplish this, a modified version of the dual luciferase transactivation activity assay (TA-assay) was utilised, to yield increased sensitivity and sample size. Additionally, the breast cancer cell lines MDA-MB-231, MDA-MB-436, SUM102 and MCF-7 was characterised by investigating the effects of Doxorubicin and Carboplatin treatment on cell viability, with respect to endogenous *BRCA1* and *TP53* status.

By establishing the TA-activity thresholds for high and low risk groups utilising known benign and pathogenic variants as controls, we found that the variants p.Thr1700Thr, p.Gly1709Arg, p.Pro1776Ser, p.Glu1826Leu and p.Arg1835Gln were within the low risk category. The p.Asp1692Ala, p.Gly1706Arg and p.Val1838Gly variants displayed a complete lack of TA-activity consistent with pathogenic variants, and were categorised as high risk. Variants p.Arg1699Gln, p.Ala1708Val, p.Lys1711Gln and p.Met1783Thr were found to have intermediate TA-activity. By combining our findings with available data, and interpreting them in accordance with the American College of Medical Genetics and Genomics (ACMG) guidelines for variant classification, we proposed the following classification of the variants: p.Thr1700Thr, p.Pro1776ser, p.Met1783Thr, p.Glu1826Leu and p.Arg1835Gln as likely benign (class 2) variants. p.Asp1692Ala, p.Arg1699Gln, p.Gly1706Arg, p.Ala1708Val and p.Val1838Gly were likely pathogenic (class 4), while p.Arg1699Gln and p.Ala1708Val likely represented pathogenic variants with moderate penetrance. Variants p.Gly1709Arg and p.Lys1711Gln remained classified as VUSs (class 3). We also report that the TA-assay results were independent in choice of model cell line and endogenous *BRCA1* and *TP53* status. However, increased incubation time yielded a significant increase in sensitivity.

We found that triple negative breast cancer (TNBC) cells MDA-MB-436 and MDA-MB-231 lacking p53 functionality, displayed decreased sensitivity to doxorubicin, suggesting a role for p53 in drug resistance. The TNBC cell lines displayed higher sensitivity to Carboplatin treatment than Doxorubicin, supporting the notion that treatment of TNBCs with platinum-based cytostatic presents with favourable results. The MDA-MB-436 cells were shown to be homozygous for the novel *TP53* variant c.604_610dupCGTGTGG, that resulted in an early stop codon and likely abolished p53 activity. The wild type *BRCA1* and *TP53* cell line SUM102 displayed high sensitivity to both cytostatic, and it could be that the cells harboured deleterious variants in other DNA damage response genes. The luminal, hormone receptor positive MCF-7 cells proved resistant to the effects of Doxorubicin, but displayed higher sensitivity to Carboplatin, although with a greater dependency on exposure time.

Abbreviations

A – Adenine
aa – amino acid
Ala – Alanine
AlignGVGD – Align Grantham Variation/Grantham Deviation
Arg – Arginine
Asp – Asparagine
ATM – Ataxia telangiectasia mutated
ATR - Ataxia telangiectasia and Rad3 related
BRCA1 – Breast cancer susceptibility gene 1
BRCA2 – Breast cancer susceptibility gene 2
BRCT – BRCA1 C-terminal
C – Cytosine
cdc25c – Gene that encodes M-phase inducer phosphatase 3
cDNA – Complementary DNA
CDK1 – Cyclin-dependent kinase 1
CHK2 – Checkpoint kinase 2, alternate name CHEK2
CMV – Cytomegalovirus
Ct – Threshold cycle
CtIP – CtBP-interacting protein
DBD – DNA binding domain
DBS – Double-stranded breaks
DDR – DNA damage response
DHX9 – RNA helicase A
DMEM – Dulbecco's modified eagle medium
DNA – Deoxyribonucleic acid
DPBS – Dulbecco's phosphate buffered saline
EMT – Epithelial mesenchymal transition
ER-α – Oestrogen receptor α
ER^- – Oestrogen receptor negative
EtOH – Ethanol
G – Guanine
GADD45 – Growth arrest and DNA damage 45
Gln – Glutamine
Gly – Glycine
HBOC – Hereditary breast and ovarian cancer syndrome
$HER2^-$ - Human epidermal growth factor 2 negative
HR – Homologous recombination
HSV-TK – Herpes simplex virus thymidine kinase
IC_{50} – Half maximal inhibitory concentration
Ile – Isoleucine
LAR II – Luciferase Assay Reagent II
Leu – Leucine

Lys – Lysine
MAF – Maximal allele frequency
Met – Methionine
MPAF – Maximal pathogenic allele frequency
MPF – M-phase promoting factor
NHEJ – Non-homologous end-joining
NRF2 – Nuclear factor-like 2
$p21^{cip1/WAF1}$ – cyclin-dependent kinase inhibitor 1
p53 – Tumour protein 53, encoded by TP53
PALB2 – Partner and localiser of BRCA2
PBA – Phosphopeptide binding activity
PBS – Phosphopeptide binding specificity
PCR – Polymerase Chain Reaction
Phe – phenylalanine
PLB – Passive lysis buffer
PR^- – Progesterone receptor negative
Pro – Proline
PS – Phosphatase sensitivity
RING – Really Interesting New Gene
RIPA – Radioimmunoprecipitation assay buffer
RNA – Ribonucleic acid
ROS – Reactive oxygen species
RT-qPCR – Real-Time Quantitative PCR
SCP – Small colony phenotype
Ser – Serine
SIFT – Separating Intolerant From Tolerant
SSA – Single-strand annealing
T – Thymine
TA – Transactivation
Thr – Threonine
TP53 – Tumour protein 53, encodes p53
Trp – Tryptophan
Val – Valine
VUS – Variant of unknown clinical significance

Table of Contents

1 Introduction

1.1 Hereditary breast and ovarian cancer syndrome (HBOC)

Breast cancer is not a new disease, and the oldest documented cases of breast cancer can be traced back to the ancient Egyptians around 3,500 BCE (Lukong 2017; Mukherjee 2010). Despite its ancient origins, breast cancer continues to plague humanity to this day, and it is the most prevalent cancer in women worldwide, representing 29 % of all new cancer cases and 14 % of cancer related deaths (Siegel *et al.* 2013). According to the Norwegian Directorate of Health (2014), breast cancer represents 22 % of female cancers, with approximately 3,000 new individuals diagnosed in Norway every year. Roughly 10 % of breast cancer incidents can be attributed to pathogenic germline variants. These germline variants are inherited in an autosomal dominant manner, and result in what is known as hereditary breast and ovarian cancer syndrome (HBOC) (van Marcke *et al.* 2016). The syndrome confers a 50-80 % lifetime risk of developing breast cancer, and a 30-50 % risk of ovarian cancer (Roy *et al.* 2011). In addition, HBOC associates with an increased risk of tumour development in other tissues exposed to elevated hormone levels, such as, the fallopian tubes, pancreas and the prostate (Roy *et al.* 2011). HBOC often presents with a high occurrence of cancers in affected families, usually with an early onset of disease, bilateral tumour affliction and an increased incidence of male breast cancer. Several genes have been identified as factors pertaining to HBOC, with varying risk and penetrance. Monoallelic variants in the high penetrance (> 40 % lifetime risk of cancer development) genes *Breast cancer susceptibility gene 1* and *2* (*BRCA1* and *BRCA2*) are estimated to account for 30 % of hereditary morbidity, whereas the additional genes presented in Table 1 explains 40 % (Katsuki & Takata 2016; van Marcke *et al.* 2016). According to the Cancer Registry of Norway, the prevalence of breast cancer has increased noticeably over the last decades, from approximately 0.4 % in the late 1950s, to 1.2 % over the last five years. No singular explanation exists for the elevated prevalence of breast cancer cases, but it can in part be attributed to the introduction of organised screening of women between the ages 50 – 69 in the mammography program (Cancer Registry of Norway 2016). The five-year survival rate for localised breast cancer is estimated at 89 %, with a significantly poorer prognosis of 27 %, in cases presenting distant metastasis (Norwegian Directorate of Health 2014). Thus, it highlights the importance of early diagnosis and efficient screening of breast cancer related genes in patients at risk. This thesis will focus on *BRCA1*, to determine the risk of cancer development associated with a selection of missense variants found within this gene.

A pedigree from a family carrying the *BRCA1* variant p.Val1838Gly is displayed in Figure 1, presenting an inheritance pattern typical of HBOC. The family represented in the pedigree is known to the Oslo University Hospital, Department of Medical Genetics and the variant was also included in this study.

Table 1. Genes associated with increased risk of breast cancer. Related syndromes, function of gene, predisposition to other forms of cancer and penetrance are listed (modified from: Katsuki and Takata (2016); van Marcke *et al.* (2016)).

Gene	Syndrome	Functions	Predisposition to other cancers	Penetrance
BRCA1	HBOC	Homologous recombination	Ovarian, prostate, pancreatic, melanoma.	High
BRCA2	HBOC	Homologous recombination	Ovarian, prostate, pancreatic, melanoma.	High
PTEN	Cowden syndrome, PTEN hamartoma	Suppresses AKT signalling	Thyroid, endometrial, colon, renal, lipoma, trichilemmoma.	High
TP53	Li-Fraumeni	Regulates cell cycle, apoptosis, senescence	Predisposes virtually all neoplasms.	High
CDH1	Hereditary diffuse gastric cancer syndrome	Maintains cell adherence	Diffuse gastric cancer	High
STK11	Peutz-Jeghers syndrome	Regulates cell polarity	Digestive tract, pancreas, ovarian, endometrial, cervix, testis, lung.	High
NBS1	Nijmegen breakage syndrome	Cell cycle checkpoint after DNA damage		High
NF1	Neurofibromatosis type 1	Negative regulator of Ras signalling		High
ATM	Ataxia telangiectasia	Cell cycle checkpoint and DSB repair	Ataxia telangiectasia syndrome if homozygous	Moderate
CHK2	Li-Fraumeni syndrome	Activation of cell cycle checkpoint after DNA damage	Predisposes virtually all neoplasms.	Moderate
BRIP1 (FANCJ)	Fanconi anaemia	Interstrand crosslink repair	Acute myeloid leukaemia	Moderate
FANCM	Fanconi anaemia	Interstrand crosslink repair	Acute myeloid leukaemia	Moderate
PALB2	Fanconi anaemia	Interstrand crosslink repair, homologous recombination	Pancreas	Moderate
RAD51C	Fanconi anaemia-like syndrome	Interstrand crosslink repair, homologous recombination		Moderate

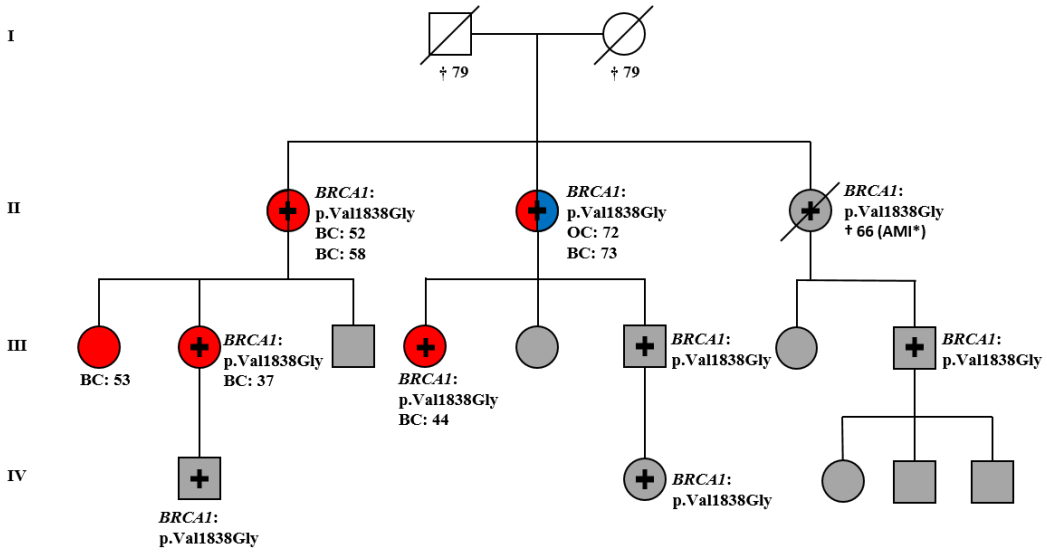

Figure 1. Pedigree displaying the inheritance pattern of *BRCA1* missense variant p.Val1838Gly. The variant was included in this thesis, and the family represented in the pedigree is known to the Oslo University Hospital, Department of Medical Genetics. Black crosses indicated carriers of variant p.Val1838Gly. Red and blue symbolise breast cancer (BC) and ovarian cancer (OC), respectively, with age at diagnosis. Grey signifies individuals tested for *BRCA1* variants. Upward slash were deceased individuals, and † mark age at death. (*AMI: Acute myocardial infarction).

1.2 *Breast cancer susceptibility gene 1*

In 1990, a linkage study was performed on a cohort of families with characteristics typical of familial breast cancer, resulting in the identification of the first breast and ovarian cancer susceptibility gene, a tumour suppressor later termed *BRCA1*, which was mapped to chromosome 17q21 (Hall et al. 1990). A few years later *BRCA1* was cloned and identified as a 1.863 amino acids (aa), nuclear phosphoprotein (~220 kDa) (Miki *et al.* 1994). BRCA1 (Figure 2) contains an N-terminal Really Interesting New Gene (RING) domain with E3-ubiquitin ligase activity, as well as a negatively charged BRCA1 C-terminal domain (BRCT), predicted to have transactivation activity (Miki *et al.* 1994). The C-terminal of BRCA1 consists of two BRCT repeats at aa 1646-1736 and aa 1760-1855 (Millot *et al.* 2012), and further reference made to the BRCT-domain will include both repeats. BRCA1 also includes a nuclear export signal (aa 81-99), two nuclear localisation signals (aa 503-508 and aa 607-617), in addition to a coiled-coil domain, various binding sites and phosphorylation targets for a variety of protein interaction partners. The prediction that the BRCA1 BRCT-domain confer transactivation activity, was confirmed when a GAL4 DNA binding domain was fused to the C-terminus of BRCA1 (aa 1560-1863), and the protein complex could transactivate transcription of a luciferase reporter gene in both yeast and mammalian cells (Monteiro *et al.* 1996). Another important function of BRCA1 is the interaction with homologous repair (HR)-related proteins

such as Abraxas, CtIP and BRIP1 (also known as BACH1) (Leung & Glover 2011). This interaction is facilitated by the BRCT domains ability to recognise and bind to pSer-X-X-Phe motifs, where pSer is phosphorylated serine (Wu *et al.* 2015).

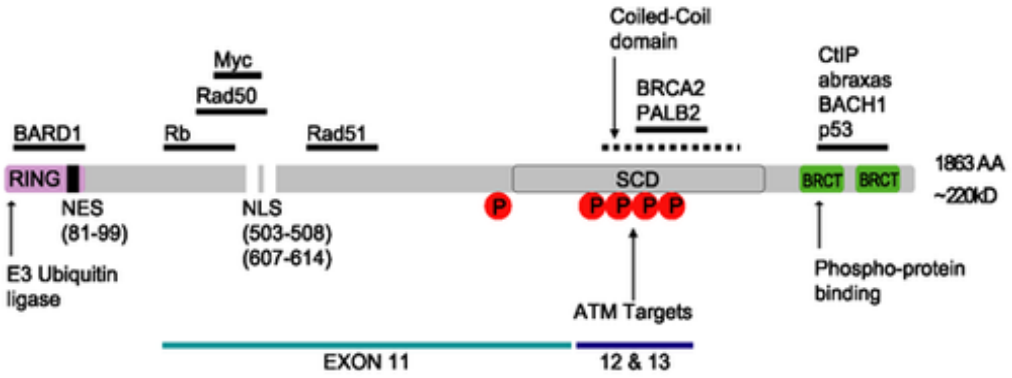

Figure 2. Schematic representation of BRCA1 displaying the N-terminal RING domain with E3 Ubiquitin ligase activity and the two BRCT domains vital for transactivation activity. Additionally, protein interaction sites and phosphorylation targets (red circles), nuclear export (NES) and nuclear localisation signals (NLS) are indicated. Numbers in parenthesis are amino acids (Clark *et al.* 2012).

1.3 Breast cancer subtypes and *BRCA1* status

Through the centuries a multitude of attempts have been made at describing and classifying tumours, from ancient Hippocrates's famous "humours" and Galen's "black bile" to the 21st centuries molecular classification system. In a study conducted by Perou *et al.* (2000), they classified breast tumours based on a microarray analysis of over 8000 genes. They constructed a system dividing breast tumours into four groups; Luminal A, Luminal B, HER2-positive ($HER2^+$) and basal-like. Separation of these groups were determined based on the status of oestrogen (ER)- and progesterone (PR)-receptors, as well as HER2 status. In addition to these molecular subgroups, tumours were characterised based on size, lymph node status and histological grade (G1=low, G2=medium, G3=high) (Vuong *et al.* 2014). Histological grading of breast cancers follows the Nottingham grading system (Amin *et al.* 2017) that describe a tumour by the following features: Tubule formation i.e. differentiation of breast cells, Nuclear grade i.e. morphology of tumour cell nucleus, and Mitotic rate i.e. how many proliferating cells are present. Each of these features are assigned a grade from 1-3, where 1 is most normal and 3 is most abnormal. A score is calculated by combining the scores for each feature, dividing the tumours into three groups (G1-G3, Table 2).

Table 2. Histological grading of tumours into three groups, G1, G2 and G3. Score refers to the Nottingham grading system, and are accumulated from three categories; Tubule formation, Nuclear grade and Mitotic rate (Amin et al. 2017).

Score	Grade	Description
3-5	G1	Well differentiated, low grade tumour.
6-7	G2	Moderate differentiation, intermediate grade tumour.
8-9	G3	Poor differentiation, high grade tumour.

Characteristic of the Luminal A subgroup is that it is ER^+ and PR^+, while being $HER2^-$ and graded G1 histologically. Luminal B is somewhat like A; ER^+, $PR^{+/-}$ and $HER2^{+/-}$, but are graded G3 histologically, often resulting in a more aggressive cancer phenotype. The $HER2^+$ tumours are usually graded G3 and are independent of ER and PR status, often overlapping with the Luminal B type and resulting in a poor prognosis. Basal-like tumours are so named because they exhibit similar characteristics as the cells located at the basal layer of the mammary glands. They are usually triple negative (ER^-, PR^-, $HER2^-$) and are histologically graded G3, resulting in the most aggressive form of breast cancer, with a short relapse time (Rakha & Ellis 2009).

As for carriers of deleterious *BRCA1* variants, the majority are affected by triple-negative basal-like cancers (TNBC) (Atchley *et al.* 2008; Couch *et al.* 2015). While various drugs have been established that successfully targets ER^+ and $HER2^+$ tumours (such as Tamoxifen, Fulvestrant and Herceptin), treatment of TNBCs have proven to be more challenging. However, since TNBCs often associate with *BRCA1* loss-of-function and subsequent loss of homologous recombination (discussed below, 1.4.1) (Crown *et al.* 2012), a new type of drug has been developed, namely PARP1-inhibitors. Several PARP1-inhibitors have displayed promising results in both response rate and recurrence, and are currently under clinical testing, while some has already been approved by the US Food and Drug Administration (FDA) for clinical use (Brown *et al.* 2016; Liang & Tan 2010).

1.4 BRCA1 function

BRCA1 is associated with numerous functions in the cell (Figure 3), ranging from DNA-repair via homologous repair (HR), to transcription and cell-cycle control, with links to cell differentiation. Due to the scope of this thesis and the fact that these functions are complex features, the following section will contain a brief introduction to some examples of the BRCA1 roles, with emphasis on the BRCT-domain.

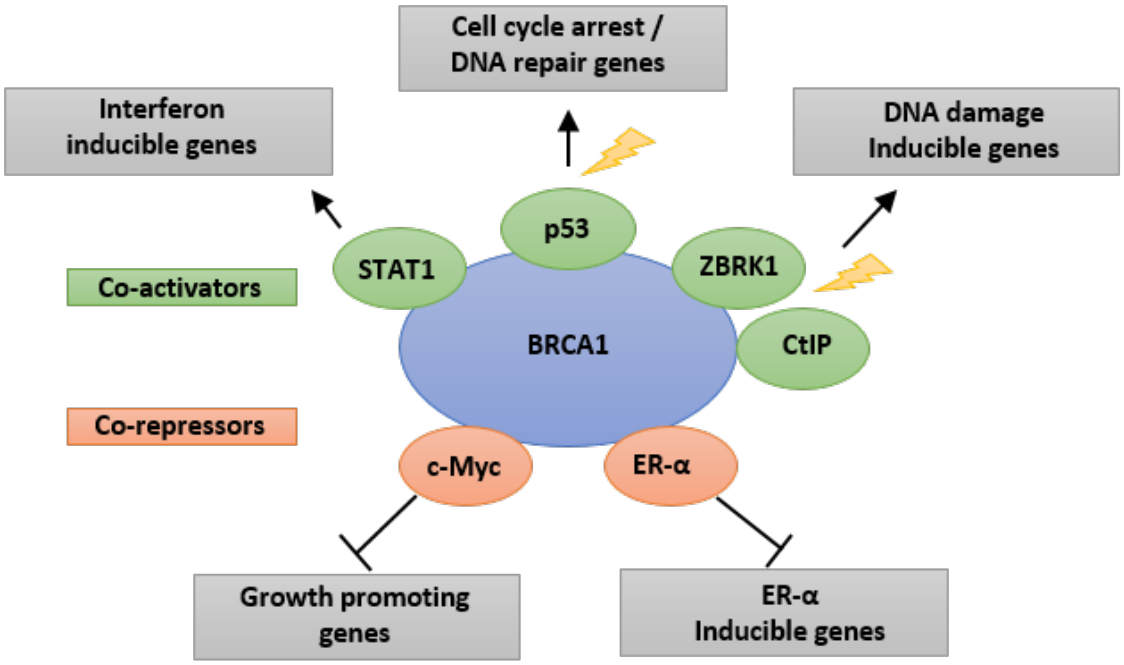

Figure 3. Schematic representation of BRCA1 interaction partners and its functionality. BRCA1 co-activate transcription of interferon inducible genes, cell cycle arrest/DNA repair genes and genes induced by DNA damage (yellow lightning), through interaction with STAT1, p53 and ZBRK1, respectively. BRCA1 and CtIP dissociates after DNA damage, and BRCA1 associates with ZBRK1 to stimulate transcription. BRCA1 function as a co-repressor of growth promoting genes and ER-α inducible genes through interaction with c-Myc and ER-α. Modified from Mullan et al. (2006).

1.4.1 BRCA1 role in DNA damage response (DDR)

Repair of double-stranded breaks (DSB) in DNA via HR occurs during the S and G2 cell-cycles. HR is essential for maintaining genomic stability because it introduces few errors due to the availability of a sister chromatid for use as template for repair of the damaged strand. The alternative mechanisms for DNA repair, such as non-homologous end-joining (NHEJ) and single-strand annealing (SSA), are highly error-prone and are considered mutagenic pathways that can result in chromatid rearrangements and genomic instability (Prakash *et al.* 2015).

During HR (Figure 4) BRCA1 associates with several proteins to facilitate repair of DSB. Deleterious variants in the BRCA1 BRCT domain may halt the interactions between BRCA1 and either Abraxas, BRIP1 or CtIP, and has been correlated with diminished HR activity as well as increased susceptibility to tumour formation (Shakya *et al.* 2011). It has also been reported that RAD51 mediated HR is accomplished through BRCA1 interaction with PALB2, that binds to the BRCA1 coiled-coil domain (Sy *et al.* 2009; Zhang *et al.* 2009). However, deleterious variants in the BRCA1 BRCT-domain have been shown to render BRCA1 unstable (Williams *et al.* 2003). Thereby, prohibiting recruitment of RAD51 regardless of an initially undamaged PALB2 binding site (Johnson *et al.* 2013). It is worth noting that genes encoding the above-mentioned proteins are associated with breast cancer in addition to other HR related genes such as *CHK2*, *ATM* and *ATR*, underscoring how important HR is in breast cancer tumourigenesis.

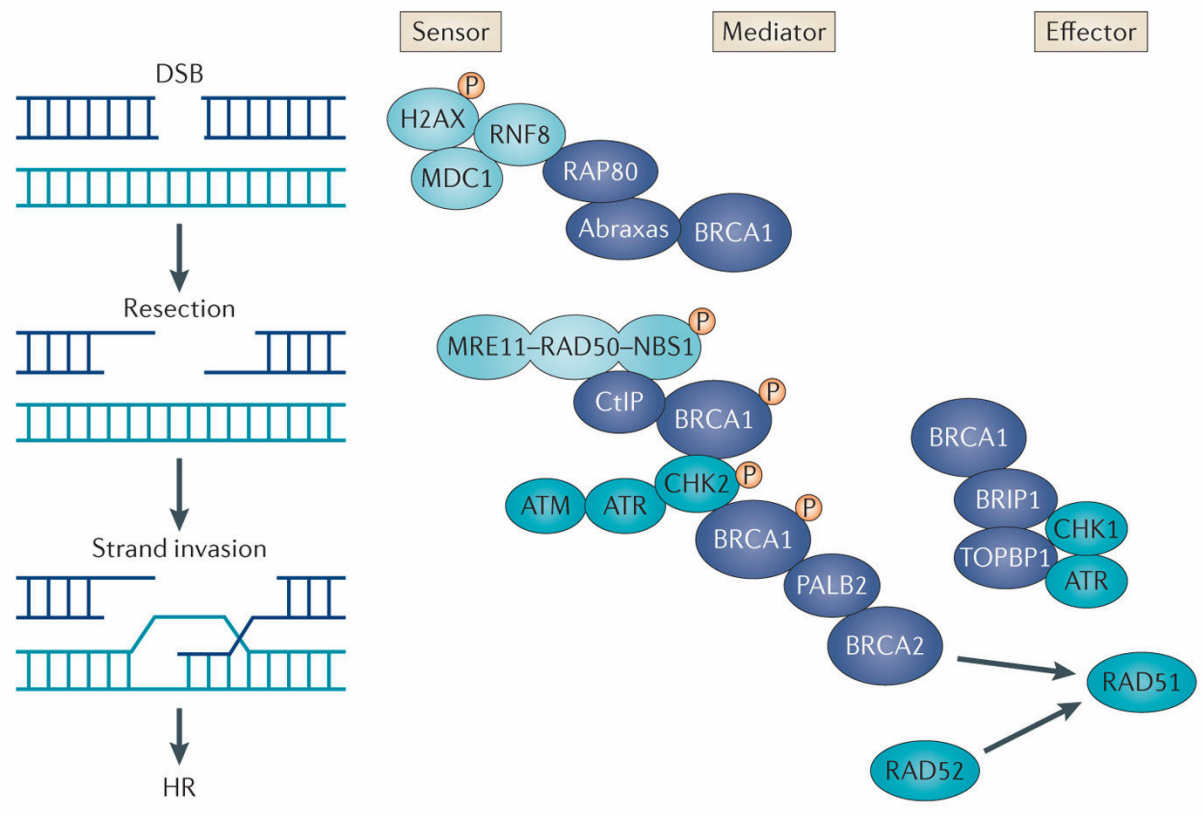

Figure 4. Illustration of the various protein complexes involved in different stages of homologous recombination (Roy *et al.* 2011). Sensors (light blue) detect DNA damage and recruit mediator (dark blue) and effector (turquois) proteins to help repair the damage. BRCA1 including macromolecules are essential for the HR pathway. Note that several of the genes listed in Table 1 (*BRCA1*, *BRCA2, NBS1, ATM, CHK2, BRIP1, PALB2* and *RAD51)* where deleterious mutations predispose to increased breast cancer risk, are involved in the HR pathway. Underscoring the importance of HR-mediated repair in breast related tumourigenesis.

1.4.2 Interaction with transcription factors

It has been revealed that BRCA1 interacts with several transcription factors in both a co-activating and co-repressive manner (Mullan *et al*. 2006). It is probable that BRCA1 does not possess a true transcriptional activity, i.e. it does not necessarily bind directly to DNA in order to facilitate transcription (Carvalho *et al.* 2007a). However, BRCA1 has been shown to regulate p53-responsive promoters such as $p21^{cip1/WAF1}$, as well as changing the transcription activity of p53 by direct binding to p53 (human p53 is encoded by the gene TP53). Both wild type p53 and a functional BRCA1 BRCT-domain are necessary for the transactivation of p53-responsive elements, like $p21^{cip1/WAF1}$ (Ouchi *et al.* 1998). A study demonstrated that while p53 regulates many proapoptotic genes, overexpression of BRCA1 redirected p53 away from these, and instead activated DNA repair and cell cycle arrest related genes (MacLachlan *et al.* 2002). While deleterious variants in *TP53* are common in many tumours, they are more abundant in cancers with pathogenic *BRCA1* germline variants (Schuyer & Berns 1999). This implies that cells without wild type *BRCA1* and *TP53* have a selective advantage in regard to chromosomal instability induced by BRCA1 insufficient HR, and loss of p53 mediated apoptosis or cell-cycle arrest (Roy *et al.* 2011). It is notable that breast cancer patients with deleterious variants in the BRCT domain lack transactivation activity, further pointing to the importance of the mechanism in the BRCA1 tumour suppression ability (Monteiro *et al.* 1996). Another aspect of the BRCA1 role in regulation of transcription, is as a component in the transcriptional mechanism, by its connection to the RNA polymerase II holoenzyme complex via the BRCT-domain binding to RNA helicase A (*DHX9*) (Anderson *et al.* 1998; Neish *et al.* 1998). Deleterious variants in the BRCT-domain of *BRCA1* has been shown to disrupt the interaction between BRCA1 and RNA polymerase II (Scully *et al.* 1997). It has been suggested that BRCA1 aid in enhancing nucleotide excision repair (NER) and transcription coupled repair (TCR) via its connection to the RNA polymerase II holoenzyme complex (Moisan *et al*. 2004). Moisan *et al.* illustrated that BRCA1 negatively regulates phosphorylation of Cdk-activating kinase through interaction with the BRCT domain, which in turn is thought to regulate NER and TCR. Further indicating the importance of BRCA1 as a vital part of the DNA damage response apparatus of the cell.

1.4.3 Role in cell cycle control

BRCA1 has proven to be a contributing factor in control of the cell cycle checkpoints (Figure 5). BRCA1 can upregulate activity of $p21^{cip1/WAF1}$ in a p53-independent manner (Somasundaram *et al.* 1997). $p21^{cip1/WAF1}$ is known as cyclin-dependent kinase inhibitor 1, and regulates the progression through G1/S-phase (Gartel & Radhakrishnan 2005). However, cells containing variants in the *BRCA1* BRCT-domain associated with tumour development, lack the ability to prevent S-phase progression (Somasundaram *et al.* 1997). BRCA1 also regulates various genes associated with the G2/M checkpoint, such as *14-3-3σ*, *cdc25C* and *GADD45*, all of which affect the activity of cyclin-dependent kinase 1 (CDK1)-cyclin B kinase complex (MacLachlan *et al.* 2000; Yarden *et al.* 2002). This is notable as CDK1-cyclin B, also known as M-phase promoting factor (MPF), permits the transition to M-phase. As an example, BRCA1 regulation of GADD45 is known to block activation of MPF and entry into M-phase due to its ability to sequester CDK1 in the cytoplasm during DDR (Mullan *et al.* 2006; Wang *et al.* 1999).

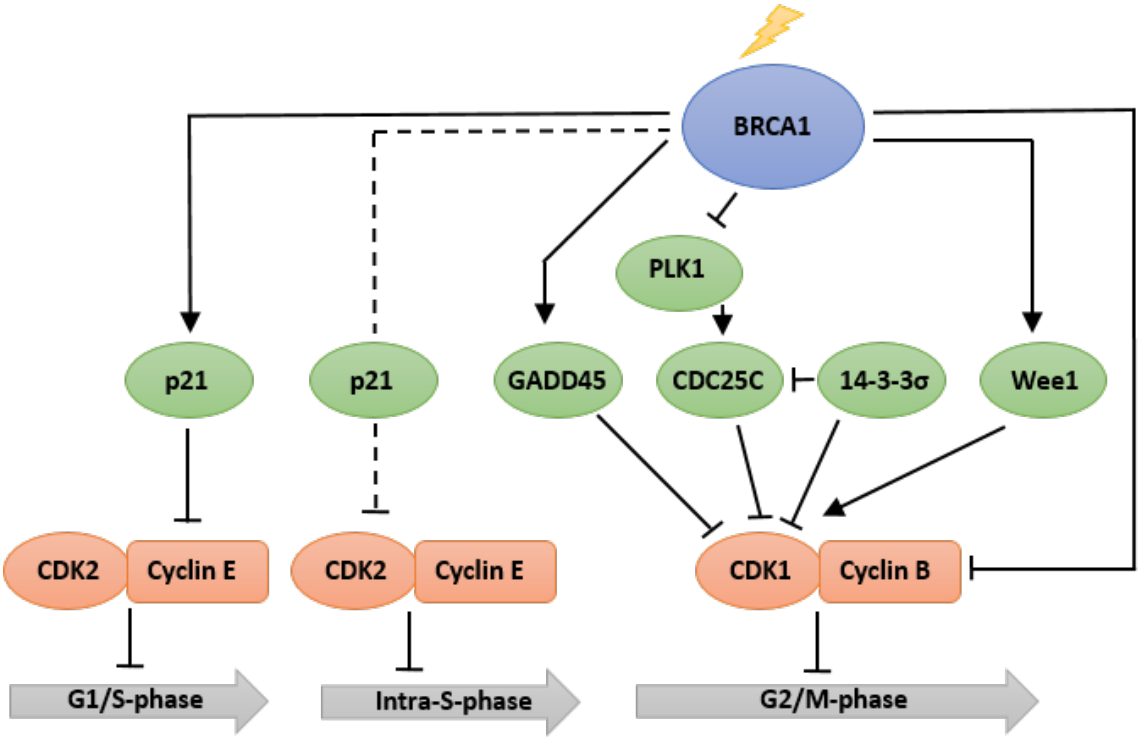

Figure 5. Displaying the interaction between BRCA1 and various proteins involved in cell cycle control. BRCA1 interacts with $p21^{cip1/WAF1}$, resulting in cell cycle arrest in the G1/S and S phase. Through activation of GADD45, BRCA1 is able to sequester CDK1 in the cytoplasm and inhibits transition through the G2/M phase. BRCA1 also promote G2/M cell cycle arrest through interaction with PLK1, 14-3-3σ and Wee1. Yellow lightning indicates DNA damage. Modified from Mullan et al. (2006).

1.4.4 Interaction with oestrogen receptor-α

Incidence of breast cancer is correlated with factors such as late menopause, nulliparity and early onset menarche, all of which results in increased life-time exposure to oestrogen (Hulka & Moorman 2008). The association between BRCA1 and oestrogen receptor-α (ER-α) is an important feature in the growth regulation mechanism of breast biology, and was elucidated by Fan *et al.* (2001), showing that the RING-domain of BRCA1 binds to ER-α, and that the BRCT-domain subsequently repressed the transcription ability of ER-α. A result of the abnormal cell metabolism in proliferating cancer cells, is increased levels of reactive oxygen species (ROS), which is known to cause damage to macromolecules. BRCA1 functions as a regulator of ROS via regulation of transcription factor NRF2, which is responsible for regulation of critical anti-oxidant genes (Kang *et al.* 2011). Therefore, it is reasonable to assume that loss of BRCA1 functionality potentially results in increased DNA damage (Wang & Di 2014). An aspect of the BRCA1 - ER-α interaction is the de-differentiation via epithelial mesenchymal transition (EMT), promoted by the transcription repressor SLUG (Figure 6). EMT results in the cells loss of cell-cell adhesion and cell polarity, while gaining invasive and migratory abilities. BRCA1 promotes differentiation by supressing the activity of SLUG. It has been suggested that mutant BRCA1 together with increased oestrogen levels may promote cell de-differentiation, as well as increased risk of DNA damage due to elevated ROS, which then leads to tumourigenesis (Wang & Di 2014). As mentioned above, deleterious variants in *BRCA1* usually result in triple-negative basal-like tumours. It is a seemingly paradoxical notion that ER might play an important role in the development of a tumour devoid of it. Some explanations for this could be that, based on observations that ER^+ cells disappear during development of ER^- tumours, it may be that while oncogenic ER^- cells gradually outgrow ER^+ cells, the ER^+ cells provide mitogenic stimulation to the ER^-, thereby contributing to their tumourigenesis (Wang & Di 2014). Another hypothesis attempting to explain this phenomenon is that ER^+ cells, because of tumourigenesis, de-differentiate and consequently lose the ability to express ER (Wang & Di 2014). Evidence for this was based on a study on MCF-7 cells where over-expression of transcription factors such as SLUG resulted in a reduction of ER expression, and increased cell mobility (Simoes *et al.* 2011).

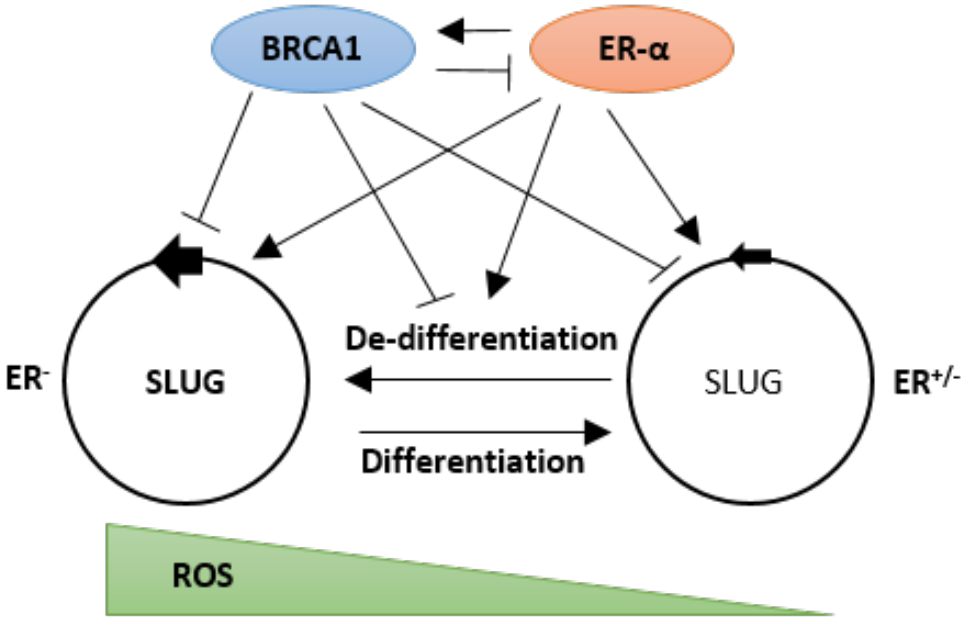

Figure 6. Illustration of the relationship between BRCA1, oestrogen receptor-α and transcription factor SLUG as well as different levels of reactive oxygen species (ROS). BRCA1 inhibits de-differentiation of the cell, whereas ER-α promotes de-differentiation, and subsequently increases the levels of ROS in the cell. Modified from Wang and Di (2014).

1.5 Deleterious *BRCA1* variants

Many of the inherited *BRCA1* variants associated with cancer have been found within either the BRCA1 N-terminal RING-domain or in the BRCT-domain (Figure 7), indicating the importance of these domains in the tumour suppressor function of BRCA1 pertaining to breast and ovarian cancer (Couch & Weber 1996; Friedman *et al.* 1994). A study by Cressman *et al.* (1999) on mice with *BRCA1*$^{+/-}$ and *Trp53*$^{+/-}$ *(Trp53* is the mouse orthologue of human tumour suppressor gene *TP53),* have shown to possess slightly increased tumour formation compared to *Trp53*$^{+/-}$ only mice. The fact that these mice continued to express *BRCA1* ruled out epigenetic silencing of the wild type allele. Thus, suggesting that haploinsufficiency promotes enough genomic instability to result in tumourigenic behaviour, and that complete loss of wild type functionality is not necessary in *BRCA1*-related tumourigenesis. This contrasts with the Knudson two-hit hypothesis, which postulate that tumour suppressor genes must acquire a deleterious variant in both alleles, before becoming tumourigenic due to loss of heterozygosity and wild type function.

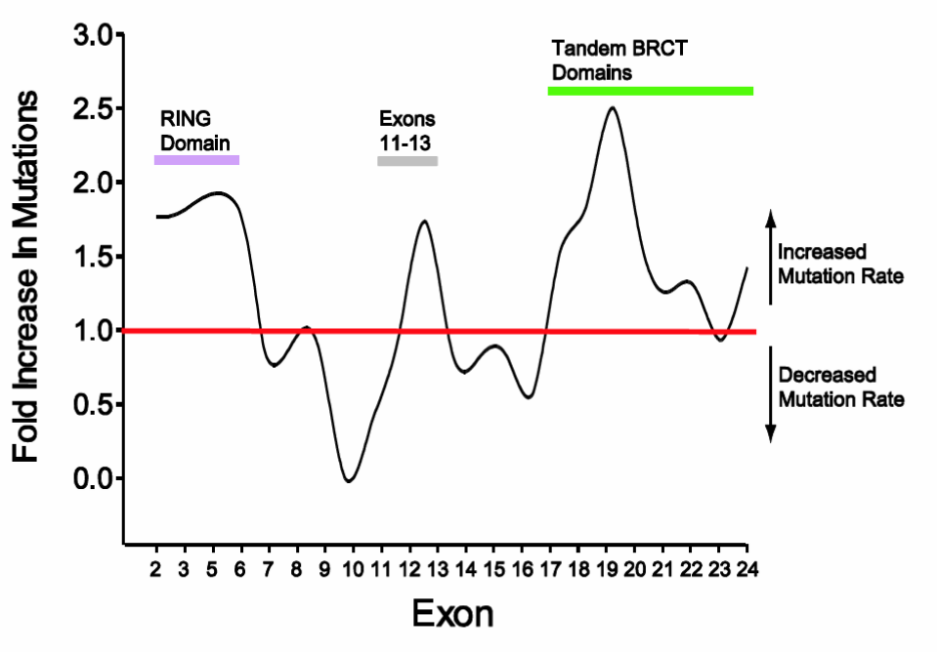

Figure 7. Displaying the fold increase of clinically relevant variants in *BRCA1*. The RING and BRCT domains in addition to exons 11-13 are highly important for the functions of BRCA1. The red line indicates the total average mutation rate per codon (Clark *et al*. 2012).

Biallelic deleterious variants in *BRCA1* result in embryonic lethality in mice, and are considered lethal in general (Gowen *et al.* 1996; Hohenstein *et al.* 2001). However, at least two cases exist where a human patient possess biallelic deleterious variants in *BRCA1* (Domchek *et al.* 2013; Sawyer *et al.* 2015). In both, the patient presented with either breast- or ovarian cancer, as well as congenital abnormalities. An explanation for this is that some rare hypomorphic variants render BRCA1 partially functional, resulting in a distinct subtype of Fanconi anaemia (Sawyer *et al.* 2015).

The Maximal Pathogenic Allele Frequency (MPAF) for *BRCA1* is estimated at 0.1 %, and the prevalence at 0.25 % for the general population (Song *et al.* 2016). However, due to founder effects the estimates vary significantly between populations (Janavicius 2010). For instance, the four known Norwegian *BRCA1* founder variants (c.1556delA, c.3228delAG, c.697delGT and c.1016dupA) contribute to 51.9 % of the total *BRCA1* variant carriers in the Norwegian population (Personal communication Ariansen, S., 2017). Whereas three founder variants contribute to 98-99 % of identified *BRCA1/2* variants in the Ashkenazi Jewish population (Janavicius 2010). The Norwegian population possess a rather heterogeneous distribution of *BRCA1* founder variants due to genetic drift as a result of the dramatic population loss, and subsequent genetic isolation following the bubonic plague ~650 years ago (Møller *et al.* 2007).

Approximately 98 % of the pathogenic variants in *BRCA1* are truncating, i.e. frameshift indels and splice variants, with missense variants contributing to only 2 % of the disease-causing variants (Maxwell *et al.* 2016). The reason for the increased frequency of indels in *BRCA1* is due to the accumulation of repeated Alu sequences (Karami & Mehdipour 2013). Since most of the pathogenic *BRCA1* variants that have been identified result in protein truncation, it is understandable that missense and in-frame indels are challenging to classify as the impact on the proteins functionality is uncertain (Szabo *et al.* 2004). Because each missense variant is rare, segregation and association studies become challenging due to low sample numbers and the need to match each case to ethnicity (Szabo *et al.* 2004). Despite the fact that they are infrequent, variants in *BRCA1* with unknown clinical significance account for more than 35 % of the total number of discovered variants (Carvalho *et al.* 2007a), and therefore present a significant challenge in regard to risk assessment.

1.6 Classification of *BRCA1* variants

Deleterious variants in *BRCA1* have high penetrance and greatly elevates life-time risk of cancer. Thus, it is important to ascertain whether a variant is of pathogenic or benign nature, in order to provide the best possible care for the patient. Classification of variants are recommended to follow the guidelines formulated by the American College of Medical Genetics and Genomics (ACMG) (Richards *et al.* 2015), and this subchapter is based on this document. It is important to note that these are guidelines and recommendations only, and while forming the basis for variant classification in Norwegian hospitals, they do allow for individual consideration of the criteria and weightings. It is therefore possible that the classification of a variant may differ between institutions, despite there being a consensus on the foundation of which classification is done. Variants found in patients at the Oslo University Hospital, Department of Medical Genetics, are routinely re-evaluated to account for updated knowledge of the discovered variants. The ACMG classification scheme aims to classify variants in a numerical system (1-5) where; 1-benign, 2-likely benign, 3-variant of unknown significance (VUS), 4-likely pathogenic and 5-pathogenic, based on various criteria and weightings.

1.6.1 ACMG classification criteria

Table 3 and Table 4 display the ACMG criteria recommended for use in classification of variants as pathogenic or benign, respectively. Note that the numbering of each criterion does in no way confer a weighting, but instead serves to differentiate between types of evidence.

Table 3. List of ACMG classification criteria recommended for classification of a variant as pathogenic (Richards *et al.* 2015). The conditions stretch from very strong evidence to supporting evidence, and are listed thereafter.

Very strong evidence of pathogenicity	
PVS1	Used in cases where a null variant is present in a gene where loss of function (LOF) is a known cause of disease. This is used in cases where nonsense variants, frameshift, aberrant splicing and exon deletions are present.
Strong evidence of pathogenicity	
PS1	Used if the change in amino acid is the same as in a previously reported pathogenic variant, regardless of the nucleotide substitution.
PS2	*De novo* variant in genes known to cause disease, found in patient with no family history where both maternity and paternity is confirmed.
PS3	Deleterious effect confirmed by a well-established functional assay, either in *in vivo* or *in vitro.*
PS4	If the variant in question confer with a significantly increased prevalence in affected individuals in comparison to a control group. However, the confidence interval of the estimated risk ratio or odds ratio may not include 1.0. This is because 1.0 indicate no discernible difference from variants that does *not* confer with increased risk, thereby rendering the comparison invalid. It is important to note that many missense variants are characteristic, and limited, to certain families, absence of the variant in a race-matched population is therefore not sufficient evidence in favour of pathogenicity.
Moderate evidence of pathogenicity	
PM1	If the variant in question is found in a mutational hot spot or a critical domain necessary for protein function, where no benign variation has been confirmed.
PM2	Applies if the variant in question is absent in controls from the Exome Aggregation Consortium (ExAC), 1000 Genomes or the Exome sequencing project databases.
PM3	If the disorder in question is of a recessive nature, variants found in *trans* with known pathogenic variants indicate pathogenicity.
PM4	If the variant results in a changed protein length due to an in-frame indel or loss of stop codon in a non-repeat part of the gene.
PM5	Used if the variant results in an amino acid change dissimilar from a previously established variant found at the same location.
PM6	Variants assumed to be *de novo,* where no maternity or paternity has been established.
Supporting evidence of pathogenicity	
PP1	Used if the variant is found in a gene known to cause the disease in question, co-segregate in multiple affected members of a family. If the segregation data is sufficiently strong, this point can be utilised as stronger evidence.
PP2	Missense variant found in a disease-causing gene where missense variations are the predominant cause of affliction.
PP3	Multiple *in silico* prediction software agree on the deleterious effect of the suspected variant. However, since most of these software utilise the same algorithm as a basis, the evidence of multiple *in silico* assessments are to be regarded as one piece of evidence. If the results between software differ, they should be disregarded in classification of the variant.
PP4	Used if the patient present with a phenotype or family history that is highly similar for a disease with a singular genetic cause.
PP5	The variant in question is reported pathogenic from a highly reputable source, but evidence is unavailable for independent on-site evaluation.

Table 4. List of ACMG classification criteria recommended for classification of a variant as benign (Richards *et al.* 2015). The conditions stretch from stand-alone evidence to supporting evidence, and are listed thereafter.

Stand-alone evidence in support of benign impact	
BA1	The variant has an allele frequency of > 5 % in the ExAC, 1000 Genomes or Exome Sequencing Project databases.
Strong evidence supporting benign impact	
BS1	Used if the variant in question is known to possess a higher allele frequency than what is expected for the disease.
BS2	This criterion is used if the disease is associated with full penetrance and early onset. A healthy adult present with a homozygous variant in a gene known to predispose for a recessive disease, or is heterozygous for a variant in a gene known to be dominant. If linked to the X chromosome, a healthy adult presenting with a hemizygous variant will fulfil the criteria.
BS3	No change in effect confirmed by a well-established functional assay, either in *in vivo* or *in vitro.*
BS4	There is no segregation of the variant in family members affected by the disease in question.
Supporting evidence of benign impact	
BP1	If the pathogenicity related to the gene in question is mainly associated with truncations, missense variants may be regarded as supporting evidence of a benign nature.
BP2	If the disorder is dominant and fully penetrant, variants found in *trans* with a pathogenic variant suggests a benign nature. Variants found *in cis* to a known pathogenic variant, in either recessive or dominant afflictions, can be considered as supporting evidence of benignity.
BP3	Used if the variant results in an in-frame indel in a repetitive region without functional impact.
BP4	Multiple *in silico* prediction software agree on the benign effect of the suspected variant. As with the PP3 criteria, since most of these software utilise the same algorithm as a basis, the evidence of multiple *in silico* assessments are to be regarded as one piece of evidence. If the results between software differ, they should be disregarded in the variant classification.
BP5	Applies if the variant in question is present in a case with an alternate molecular basis for the illness. Care must be taken as certain afflictions may increase in severity in the presence of multiple pathogenic variants, and in such cases observation of the variant in question would not support a benign interpretation.
BP6	Mirrors PP5, the variant in question is reported benign from a highly reputable source, but evidence is unavailable for independent on-site evaluation.
BP7	The variant is synonymous, with no prediction in alternative splicing from established algorithms in addition to the nucleotide not being highly conserved.

1.6.2 Weighting of ACMG classification criteria

To use the above-mentioned criteria (Table 3 and Table 4) for classification of variants in the 1 – 5 tier system, the weightings listed in Table 5 have been proposed by the ACMG.

Table 5. List of weightings of the criteria listed in Tables 3 and 4, recommended by the ACMG for classification of variants to classes 1-5.

Classification	Criteria weighting
Class 1, benign	Classification of a variant as a class 1 benign variant confers a certainty of ≥ 99 % of benignity, and is defined as: 1 stand-alone piece of evidence or ≥ 2 strong.
Class 2, likely benign	Classification of a variant to the class 2 category of likely benign variants requires a certainty of > 90 % and is defined as either: 1 strong and 1 supporting, or ≥ 2 supporting pieces of evidence.
Class 3, VUS	If a variant fail to meet any of the above criteria or weightings, or if the evidence is contradictory, the variant should be classified as a variant of uncertain significance.
Class 4, likely pathogenic	To classify a variant as a class 4 variant, meaning a > 90 % certainty of effect, one of the following combinations must be attained: 1 very strong and 1 moderate, 1 strong and 1-2 moderate, 1 strong and ≥ 2 supporting, ≥ 3 moderate, 2 moderate and ≥ 2 supporting or 1 moderate and ≥ 4 supporting.
Class 5, pathogenic	To classify a variant as a class 5 pathogenic variant, which is synonymous with a ≥ 99 % certainty of effect, either of the following criteria must be met: At least one PVS1 piece of evidence, combined with at least one of the following; ≥ 1 strong, ≥ 2 moderate, 1 moderate and 1 supporting or ≥ 2 supporting pieces of evidence.

1.7 The breast cancer patient program

Suspicion of breast cancer usually starts with the patient noticing a change in their breast physiology, followed by evaluation by a General Practitioner (GP). If the GP determines that there is a reason for further inquiry, the patient will be included in the breast cancer patient program, and evaluated using mammography, needle biopsy and/or ultrasound (Norwegian Directorate of Health 2014). In the case of malignancy, the patient will be referred to a treatment; otherwise the patient involvement in the breast cancer patient program is ended. Treatment of breast cancer is dependent on the type of tumour and development stage, but the primary actions include surgery, neoadjuvant and adjuvant treatment with hormonal therapy, chemotherapy or radiation treatment (Norwegian directorate of Health 2016).

1.7.1 Who are tested for *BRCA1* variants

According to the guidelines for the breast cancer patient program, specified by the Norwegian directorate of Health (2016), patients can be referred to genetic counselling if one or more of the following requirements are met:

- Breast cancer before the age of 50.
- Ovarian cancer, no matter the age.
- Breast cancer and a close relative with prostate cancer, age < 55.
- Breast cancer and close relative with ovarian cancer.
- Two close relatives with breast cancer, average age < 55.
- Three close relatives with breast cancer, any age.
- Male breast cancer.
- Bilateral breast cancer, age < 60.
- Women < 60 years of age with triple negative (ER^-, PR^- and $HER2^-$) breast cancer.

However, genetic testing can be permitted to patients that do not fulfil these requirements, if the treating physician can document that a genetic test will have a deciding effect on treatment (Norwegian directorate of Health 2016). For cases where there are sufficient reasons to warrant genetic testing, it is recommended that relatives of the patient who have suffered from, or currently have cancer should be included in the testing. If such individuals are unavailable for screening, first-degree relatives or second-degree relatives via a male member, can be tested instead. Healthy individuals are referred to genetic counselling prior to testing, as well as

afterwards for all individuals where a deleterious variant or VUS is uncovered (Norwegian directorate of Health 2016). A strict interpretation of the guidelines pertaining to family history is not recommended if the objective is the discovery of pathogenic variant carriers. A study performed on a Norwegian cohort revealed that patient history detects less than 50 % of *BRCA1/2* variant carriers (Møller *et al.* 2007). Screening only for founder- and known variants are also of increasingly limited value in a Norwegian population that is becoming increasingly multi-ethnic. This is due to the fluctuating distribution of *BRCA1* variants regarding ethnicity and municipality (Janavicius 2010; Møller *et al.* 2007).

1.7.2 Prophylactic treatment of pathogenic *BRCA1* variant carriers

The Norwegian directorate of Health (2016) state that females with a confirmed deleterious *BRCA1* variant must be informed of risk reducing prophylactic mastectomy and breast reconstruction surgery, as it reduces the risk of breast cancer by 90-98 %, and is currently the safest option. They also suggest annual follow-up with mammography and MR as an alternative, if surgery is undesired. Women above the age of 35 carrying a deleterious *BRCA1* variant, who no longer wish to bear a child, should additionally consider a salpingo-oophorectomy (removal of the fallopian tubes and ovaries). The timing of a potential surgical treatment should be carefully considered with each patient, as the risk of developing breast cancer increases following the age of 25 (Norwegian directorate of Health 2016).

1.7.3 *BRCA1* status and cytostatic treatment

Cytostatic cancer treatment is usually reserved for patients with large tumours and/or aggressive phenotypes. Multiple chemotherapy regimens are applied in adjuvant treatment, but therapies containing anthracyclines such as Doxorubicin (sold as Adriamycin, Figure 8A), have resulted in higher survival rates in high-risk groups (Norwegian directorate of Health 2016). Doxorubicin is a DNA intercalating agent, and functions by invading DNA strands and forming bonds with the aromatic rings of nucleotides. A study by Spencer *et al.* (2008) revealed that cells with nucleotide excision repair (NER) and HR deficiencies were sensitive to the effects of Doxorubicin. Patients with deleterious *BRCA1/2* variants and/or triple-negative breast cancers treated with platinum-based cytostatic, have shown an increased response rate. As a result, treatment of such cases with Carboplatin (Figure 8B) is recommended (Norwegian directorate of Health 2016). Carboplatin is thought to function in the same manner as its predecessor

Cisplatin, by forming inter- and intra-strand crosslinks between nucleotides (Go & Adjei 1999). Thereby halting DNA replication and killing the fastest replicating and/or HR deficient cells. Carboplatin has also shown to be less toxic than Cisplatin, despite requiring higher doses to function (Perez 2004).

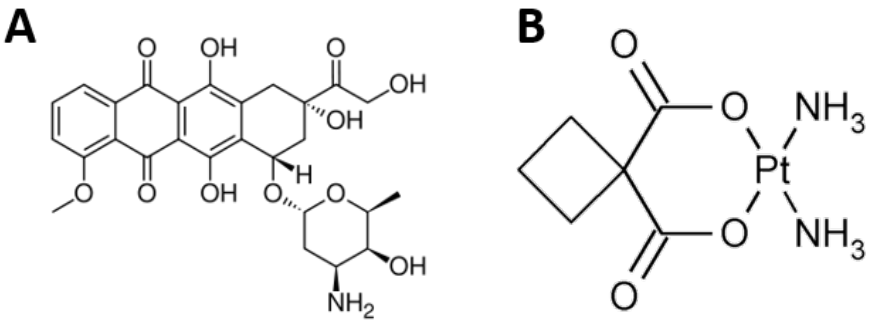

Figure 8 A) Chemical structure of the cytostatic, DNA intercalating drug Doxorubicin. Doxorubicin (and other anthracyclines such as Epirubicin) are used in regular chemotherapeutic treatment regimens of breast cancers. **B)** Chemical structure of the cytostatic, DNA cross-linking agent Carboplatin. Carboplatin is recommended for treatment of patients with triple negative basal-like tumours, as they often present with high tolerance to other cytostatic, such as Doxorubicin.

1.8 Introduction to the transactivation assay

The transactivation assay measures the relative transactivation activity between the BRCA1 wild type and variant-containing BRCT domains. As stated above, it is unlikely that BRCA1 has a *bona fide* transcription activity. Therefore, the transactivation (TA)-assays main goal is to ascertain the integrity of the BRCT-domain, as it has proven to be crucial in BRCA1 key functions such as HR-mediated DNA repair, interaction with transcription factors and cell cycle control (Carvalho *et al.* 2007a). The assay is based on the fusion of the BRCA1 BRCT-domain to a GAL4 DNA Binding Domain (DBD). The GAL4 DBD used in this assay originates from *Saccharomyces cerevisiae* and is a well characterised and heterogeneous DBD often used in similar assays (Carvalho *et al.* 2007b; Monteiro *et al.* 1996). A plasmid containing the GAL4 DBD:BRCT fusion protein is co-transfected into mammalian cells along with two reporter plasmids. A plasmid with a Firefly luciferase gene enables the GAL4 DBD:BRCT fusion protein to bind to the GAL4 promoter upstream of the Firefly luciferase gene, and trans-actively induce expression Firefly luciferase. The second plasmid contains the *Renilla*-luciferase gene, and serves as an internal control for normalising differences in cell number and transfection efficiencies. Renilla is continuously expressed due to a Herpes simplex thymidine kinase

promoter (HSV-TK) upstream of the reporter gene. A schematic illustration of the principle behind the method is displayed in Figure 9.

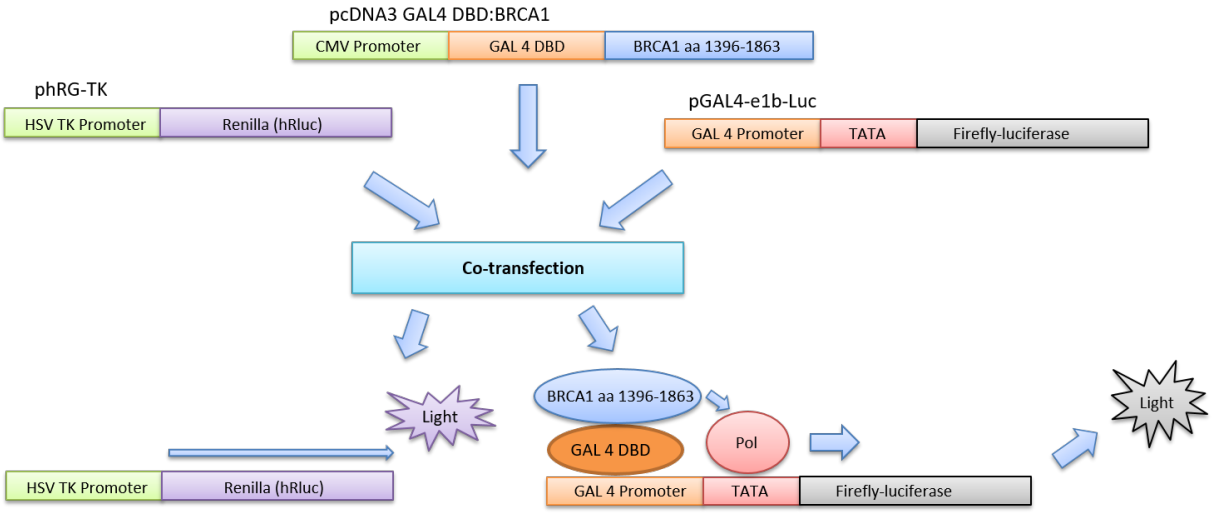

Figure 9. A schematic of the transactivation assay (TA-assay). Variant plasmid pcDNA3 GAL4 DBD:BRCA1 are co-transfected with reporter plasmids pGAL4-e1b-Luc and phRG-TK into mammalian cells. Expression of the variant plasmid creates a fusion protein with a GAL4 DBD and the BRCA1 BRCT-domain, which bind to the GAL4 specific promoter on the pGAL4-e1b-Luc reporter plasmid and induce expression of Firefly luciferase, in the absence of deleterious variants. The phRG-TK reporter plasmid continuously expresses the Renilla luciferase protein due to the HSV-TK promoter, and function as an internal control for the experiment. Correction for transfection efficiency and unequal cell number is done by taking the ratio between the light emitted by Firefly and Renilla.

Firefly- and Renilla-luciferase are enzymes that, because of convergent evolution, have different structural forms and substrate requirements despite having a similar bioluminescent effect (Figure 10). The firefly and the Renilla luciferase originate from *Photinus pyralis* and *Renilla reniformis,* respectively. This dissimilar evolutionary origin provides the ability to individually measure the luminescence emitted by each of these enzymes, within the same system without interference. Depending on the effect of the variant present in the BRCT-domain, differing results can be expected (Figure 11). For benign variants, the level of TA-activity will be close to or similar to that of the wild type. Deleterious variants will display a greatly reduced or complete lack of TA-activity. A study by Carvalho *et al.* (2007b) suggested that the relationship between cancer risk and the level of TA-activity is of a discrete nature rather than continuous. The same study proposed that variants with TA $\geq$ 50 % can be classified as *low risk* and TA $\leq$ 45 % as *high risk*. Variants in-between could be considered to be of intermediate or undetermined risk.

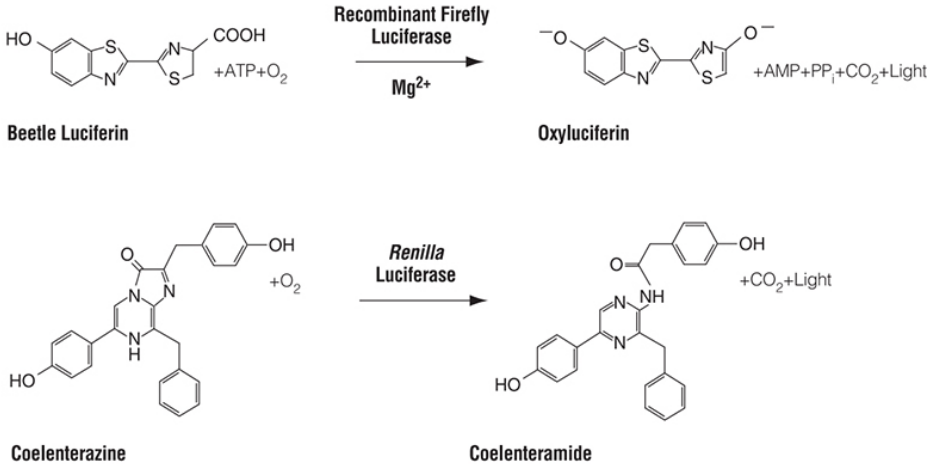

Figure 10. Due to convergent evolution, the dissimilar substrate reactions of Firefly and Renilla luciferase enables detection of bioluminescence from each enzyme within the same system. At the top; the luciferase reaction corresponding to recombinant Firefly luciferase. At the bottom; the Renilla Luciferase reaction (Dual-Luciferase® Reporter Assay System Technical Manual TM040).

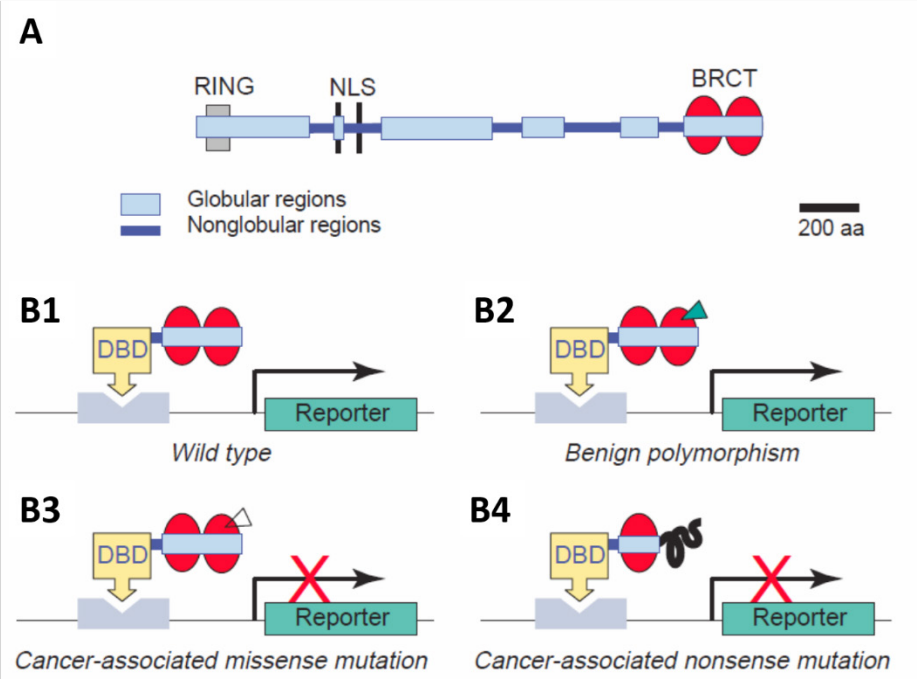

Figure 11. A simplified illustration of the TA-assay (Monteiro 2000). **A)** Display a schematic illustration of the BRCA1 gene with its N-terminal RING-domain (grey box), Nuclear Localisation Signals (black bars) and the two C-terminal BRCT-domains (red circles). **B1-B4)** Illustrates the principle of the method; the BRCA1 BRCT-domain is fused to a GAL4 DNA Binding Domain (DBD), and is thus able to bind to a GAL4-specific promoter, and trans activate expression of the reporter gene (Firefly-luciferase). **B1)** Wild type BRCT give normal transactivation of reporter. **B2)** BRCT containing a benign polymorphism, activates reporter in a wild type-like fashion. **B3)** BRCT-domain carrying a deleterious missense variant demonstrating non, or greatly reduced transactivation of the reporter gene. **B4)** BRCT-domain containing a nonsense variant results in lack of transactivation activity. Expression of reporter gene is abolished.

2 Aims

Pathogenic variants in *BRCA1* are known to cause HBOC. Therefore, it was important to correctly characterise variants found in this gene, in order to provide the best possible care for each individual patient. Some of the variants found during diagnostic screening of *BRCA1* were challenging to classify, because they were rare and little was known about their impact on BRCA1 functionality. This thesis aimed to establish a functional assay that efficiently ascertained the impact of VUSs found in the BRCT-domain of *BRCA1*. The TA-assay was well described in the literature, and previous studies revealed a high correlation between its results and variant pathogenicity. Additionally, this thesis aimed to characterise a selection of breast cancer cells that were regularly used by the Iversen, N. research group, regarding *BRCA1* and *TP53* status and response to various cytostatic treatments.

The aims were as follows:

1. Incorporation of *BRCA1* variants in plasmids for use in the TA-assay via *in vitro* mutagenesis. Amplification and purification of plasmids, and verification of plasmid sequences.
2. Establishing, and optimisation of the TA-assay in multiple cell-lines to; increase efficiency, sensitivity and sample number yield, while maintaining reliability.
3. Comparing the results of the TA-assay and patient mRNA samples with reports from predictive software, and previously published results pertaining to the variants in question, to classify the variants as either pathogenic or benign.
4. Determine the possible effects of variants on splicing, and *BRCA1* expression levels in mRNA samples obtained from patients carrying the *BRCA1* variants.
5. Characterisation of breast cancer cell-lines, used in functional experiments at the Department of Medical Genetics. Specifically; *BRCA1* and *TP53* variant status and expression levels of *BRCA1,* as well as cell viability during exposure to cytostatic drugs.

3 Methods

A complete list of instruments, software, kits, reagents and disposables used in this master thesis were listed in the Appendix, Section A, pages i-iii. Primers, cycling parameters and nucleic acid sequences were listed in Section B, pages iv – xi. Buffers and solutions were listed in Section C, page xii.

3.1 *BRCA1* variants found in patients included in the study

The variants included in this study were found in patients during routine diagnostics at the Oslo University Hospital, Department of Medical Genetics. A total of 18 missense variants in the BRCT domain were chosen for functional studies (Table 6). Prior to this work, twelve variants were classified as VUSs (class 3), and six variants were classified as either benign (class 1), likely benign (class 2), likely pathogenic (class 4) or pathogenic (class 5). Variants in classes other than class 3 were considered controls. Two plasmids containing variants *in cis* were included as they presented an opportunity to look for possible additive effects.

Table 6. List of BRCA1 variants investigated in the TA-assay. The two variants at the end are variants inserted *in cis* during in vitro mutagenesis, and were utilised during investigation of potential additive effects. Nomenclature follows HGVS standards, c.1 corresponds to first nucleotide of ATG.

Class	HGVS variant	HGVS protein	Exon
1	c.4956G>A	p.Met1652Ile	16
1	c.5252G>A	p.Arg1751Gln	20
2	c.5411T>A	p.Val1804Asp	23
3	c.5100A>G	p.Thr1700Thr	18
3	c.5116G>A	p.Gly1706Arg	18
3	c.5131A>C	p.Lys1711Gln	18
3	c.5326C>T	p.Pro1776Ser	21
3	c.5348T>C	p.Met1783Thr	22
3	c.5477A>T	p.Glu1826Leu	24
3	c.5504G>A	p.Arg1835Gln	24
3	c.5075A>C	p.Asp1692Ala	18
3	c.5096G>A	p.Arg1699Gln	18
3	c.5123C>T	p.Ala1708Val	18
3	c.5125G>A	p.Gly1709Arg	18
3	c.5513T>G	p.Val1838Gly	24
4	c.4964C>T	p.Ser1655Phe	16
4	c.5309G>T	p.Gly1770Val	21
5	c.5095C>T	p.Arg1699Trp	18
3 (2)	c.5075A>C/c.5411T>A	p.Asp1692Ala/p.Val1804Asp	18/23
1 (3)	c.5252G>A/c.5477A>T	p.Arg1751Gln/p.Glu1826Leu	20/24

3.1.1 *In Silico* assessment of *BRCA1* variants

Alamut Visual was used to perform an *in silico* assessments on the impact of *BRCA1* missense variants on BRCA1 functionality. Alamut contains several programs for prediction of variant effects, and was divided in two main groups, variant sequence effect on protein (both nucleotide and amino acid) and variant effect on splicing. Additionally, Alamut supplies links to relevant databases containing allele frequencies (Exome Sequencing Project (ESP), 1000 Genomes and Exome Aggregation Consortium (ExAC)), reported variants and polymorphisms (dbSNP) and variants associated with diseases (ClinVar and HGMDp). The prediction tools included in Alamut for determination of variant effect on protein include: Sorting intolerant from tolerant (SIFT), Mutation taster and Align GVGD. SIFT was founded on multiple sequence alignment, and predicts whether a variant is tolerated or deleterious based on evolutionary conservation (Ng & Henikoff 2001). Align GVGD combines Grantham variation (GV, multiple alignment with score based on evolutionary conservation) and Grantham deviation (GD, biophysical distance between amino acids at position) scores to categorise variants in 1 of 7 groups (C0, C15, C25, C35, C45, C55 and C65), where C0 is neutral and C65 is deleterious (Tavtigian *et al.* 2006). Mutation taster evaluates the impact of the amino acid change and return the variant as either "polymorphism" or "disease causing". For prediction of variant effect on splicing, Alamut employ four prediction software: SpliceSiteFinder-like (SSF), MaxEntScan, NNsplice and GeneSplicer (Houdayer 2011). These programs return scores for reference and variant sequence, and a change in these scores of ~10-20 % should be reported by at least 3 of them to be considered likely predictions.

3.2 Plasmid methods

3.2.1 Plasmids

Two luciferase reporter plasmids and one GAL4 DBD:BRCA1 wild type plasmid (Figure 12) were used for assessing TA-activity of *BRCA1* variants. All three plasmids were kindly provided by Elisabeth Jarhelle, with permission from Alvaro N. A. Monteiro.

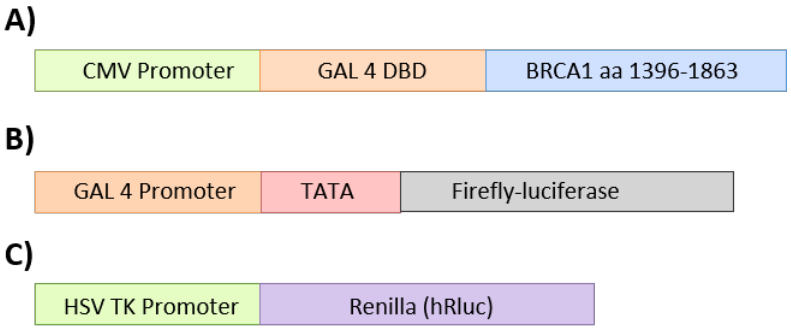

Figure 12. A schematic illustration of the plasmids utilised in the TA-assay **A)** Illustration of the pcDNA3 GAL4 DBD:BRCA1 containing a CMV promoter and a GAL4 DBD:BRCA1 fusion protein. **B)** The reporter plasmid pGAL4-e1b-Luc containing a GAL4 promoter, a TATA box and the Firefly-luciferase gene. **C)** The internal control reporter plasmid phRG-TK containing a HSV-TK promoter and the Renilla-luciferase gene.

The pcDNA3 GAL4 DBD:BRCA1 (Figure 12A) contained a construct consisting of a GAL4 DNA binding domain (DBD) and the BRCA1 BRCT domain (aa 1396-1863). A *Cytomegalovirus* (CMV) promoter, which is a strong eukaryote promoter, was placed upstream of the fusion protein to facilitate constitutive high expression. The pcDNA3 vector contained an Ampicillin resistance gene, enabling selection during amplification and transformation. The GAL4 DBD:BRCA1 insert sequence and a schematic representation of the pcDNA3 GAL4 DBD:BRCA1 plasmid is presented in the Appendix, Section B. Reporter plasmid pGAL4-e1b-Luc (Figure 12B) contained a GAL4 promoter upstream of a TATA-box and the *Firefly luciferase* gene. The second reporter plasmid, phRG-TK (Figure 12C), contained a *Renilla luciferase* gene. *Renilla* luciferase was expressed in a continuous and reliable fashion due to a HSV-TK promoter upstream of the gene that was constantly active.

3.2.2 *In vitro* mutagenesis

In vitro mutagenesis (Figure 13) was used to implement *BRCA1*-BRCT variants (Table 6) in to the wild type plasmid pcDNA3 GAL4 DBD:BRCA1, for use in functional studies. Primers (Appendix Section B) were designed according to the QuikChange II XL Site-Directed Mutagenesis Kit procedure by Agilent Technologies, and provided by Eurofins (MWG Synthesis, GmbH). Mutagenesis of all variants were performed per manufacturer's procedure. Sample reactions and cycling parameters used for production of all variants were displayed in the Appendix, Section B.

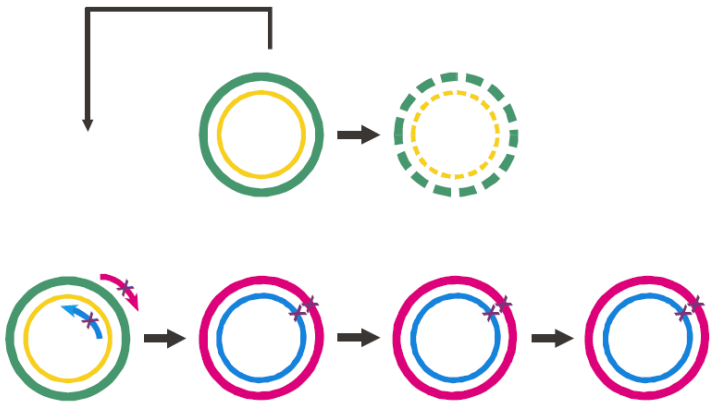

Figure 13. A simplified illustration of in vitro mutagenesis. Mutagenic primers bound to wild-type plasmid and induced the desired variation. Methylated and hemi-methylated parental plasmid DNA were digested by endonuclease Dpn I. Green and yellow lines represented parental plasmid DNA. Blue and violet arrows illustrated mutagenic primers, and blue and violet lines were successfully mutated plasmid DNA. Fragmented green and yellow lines indicated digestion by Dpn I.

3.2.3 Transformation

Transformation of plasmids and colony growth were performed as described in the suppliers' manual "TOPO® Cloning Reaction and Transformation" with some volume modification.

Protocol per sample: one microlitre of plasmid DNA was added to 10 µL of One Shot® TOP10 Chemically Competent *Escherichia coli* (*E. coli*) and gently mixed. After incubation on ice for 25 minutes the sample was heat shocked for thirty seconds at 42 °C and immediately put on ice. 100 µL of room temperature Super Optimal broth with Catabolite repression (SOC)-medium was added to the sample. The sample vial was then incubated at 37 °C at 200 rpm for one hour. After incubation, 100 µL of the cell culture was spread on a selective Lysogeny Broth-plate containing 100 µg/mL ampicillin (LB-A) plate, and incubated at 37 °C

overnight. The next day, single colonies were picked and incubated in LB-A broth at 37 °C overnight, before plasmids were isolated. The volume of the final cell culture depended on the isolation procedure; 5 mL for Miniprep, or 150 mL for Maxiprep.

3.2.4 Isolation and quantification of plasmids

Isolation of plasmid DNA was performed using both the Zappy™ Plasmid Miniprep Kit and the ZymoPure™ Plasmid Maxiprep Kit for verification of mutagenesis and use in functional assays, respectively. Quantification and measure of plasmid purity was done with the NanoDrop® ND1000. Plasmid purity was determined by the 260/280 ratio (DNA absorb light at 260 nm wavelength, whereas proteins absorb strongly at 280 nm). A ratio of 1.8 was considered pure for DNA, and values between 1.7 and 1.9 were deemed satisfactory. Isolation and quantification were performed as described in the manufacturers procedure.

3.3 Cell methods

In this study, Human Embryonic Kidney cells 293T (HEK293T, Figure 14A) and the human breast adenocarcinoma cell-lines MDA-MB-231 (Figure 14B) and MDA-MB-436 (Figure 14C) were used in the TA-assay. HEK293T was known to yield high transfection efficiencies and was therefore useful as a model cell-line. MDA-MB-231 and MDA-MB-436 were harder to transfect, but provided an opportunity to study the variants in a more accurate environment. In addition to the above-mentioned cell lines, breast cancer cells MCF-7 (Figure 14D) and SUM102 (Figure 14E) were included in the cell characterisation studies with MDA-MB-231 and MDA-MB-436 cell lines. Table 7 display characteristics such as subtype, hormone receptor and HER2 status for the breast cancer cells included in the characterisation studies. All cell lines were originally derived from pleural effusions of Caucasian females afflicted with breast cancer and represent three tumour types, metastatic adenocarcinoma, adenocarcinoma and invasive ductal carcinoma (a specific form of adenocarcinoma).

Table 7. Breast cancer cell lines used in the characterization studies displaying subtype, oestrogen receptor (ER), progesterone receptor (PR) and HER2 status, as well as source and tumour type. The table is a modified rendition from Kao *et al.* (2009).

Cell line	Subtype	ER	PR	HER2	Source	Tumour type
MDA-MB-231	Basal B	-	-	-	Pleural effusion	Metastatic adenocarcinoma
MDA-MB-436	Basal B	-	-	-	Pleural effusion	Adenocarcinoma
MCF-7	Luminal	+	+	-	Pleural effusion	Metastatic adenocarcinoma
SUM102	Basal B	-	-	-	Pleural effusion	Invasive ductal carcinoma

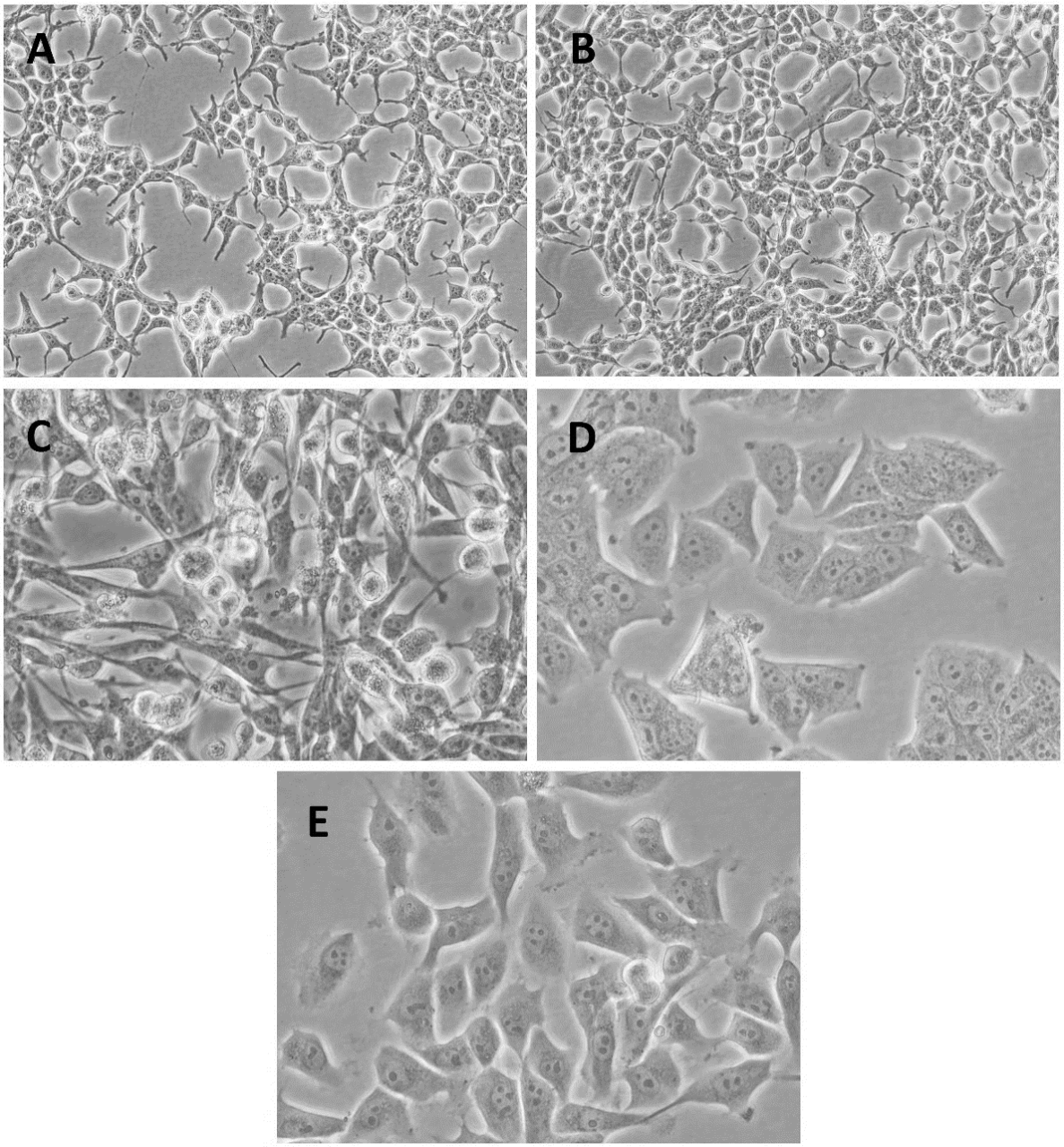

Figure 14. Displaying the cell lines used on the TA-assay and characterisation studies. **A)** Human embryonic kidney cells HEK293T. **B)** MDA-MB-231, a triple negative basal metastatic adenocarcinoma. **C)** MDA-MB-436, a triple negative basal adenocarcinoma. **D)** MCF-7, a luminal, ER/PR^{+} and HER2^{-} metastatic adenocarcinoma **E)** SUM102, a triple negative basal invasive ductal carcinoma.

3.3.1 Cultivation of cell lines

Nunc™ Cell Culture Treated EasYFlasks™ (T25 and T75) were used for all handling of cells. Dulbecco's Modified Eagle Medium (DMEM) with 10 % foetal bovine serum (FBS) was used for growth and passaging of cell lines HEK293T, MDA-MB-231 and MDA-MB-436. Roswell Park Memorial Institute (RPMI) 1640 with 10 % FBS was used with MCF-7 cells, and HuMEC Basal Serum-Free medium with added HuMEC Supplement Kit was used with SUM102 cells. FBS was added to most mediums as it contains growth factors necessary for cell proliferation, and because FBS neutralises trypsin, which is toxic to the cells, but is used to dissociate cell-cell and cell-flask adhesion during passaging.

Inoculation and passaging of cell lines

A vial containing approximately one million cells was gently thawed in a water bath at 37 °C. The cells were transferred to a T25 culture flask and re-suspended in preheated medium, and incubated at 37 °C with 5 % CO_2 for five hours to allow the cells to adhere to the flask. Cryopreserved cells were stored a in medium containing the cryoprotective agent dimethyl sulfoxide (DMSO). DMSO is detrimental to cell viability due to its ability to dissolve the cell membrane. DMSO containing medium was therefore replaced with fresh medium once the cells had adhered to the flask (~5 hours).

Passaging of cells was performed by removing old medium, and gently washing the cells with Dulbecco's phosphate-buffered saline (DPBS), before 1 mL trypsin was added to loosen cell adhesion. Cells were then suspended in fresh medium and passaged to a new culture flask.

Cell confluency was determined visually with a Nikon eclipse Ts2-FL microscope. The cells were kept below 90 % confluence to avoid overgrowth, which could result in changes in cell morphology and behaviour. This was particularly important regarding the SUM102 cells, who readily changes morphology if they become too confluent. An exception to this are the MDA-MB-436 cells who required a high level of confluency, thus, these cells were always kept at high confluence (> 80 %). All cell lines depended on cell-to-cell contact to maintain proper growth, so care was taken to avoid over-dilution.

Passaging of SUM102 was performed using HuMEC with 5 % FBS to neutralize trypsin, however, FBS is detrimental to SUM102, therefore, medium containing FBS was replaced with HuMEC with added supplement after passaging.

3.3.2 Viability of cells exposed to cytostatic drugs

Assessment of cell viability during exposure to the cytostatic drugs Doxorubicin and Carboplatin in breast cancer cell lines MDA-MB231, MDA-MB436, SUM102 and MCF-7, was done by studying the proliferation rates of cells exposed to varying concentrations of the drugs. 6,000 cells were added to each well in a 96-well plate, and incubated at 37 °C with 5 % CO_2 overnight. The cells were treated with six concentrations of Doxorubicin (0-10 µM) and Carboplatin (0-400 µM), separately, and incubated for 24-hours at 37 °C with 5 % CO_2. Cells treated with Carboplatin were incubated for 72 and 120 hours additionally, but the number of cells were reduced to 3,000 per well, to avoid overgrowth. To measure viability, 20 µL Wst-1 Cell proliferation reagent was added to each well. Wst-1 is a tetrazolium salt that was cleaved to a soluble formazan via a reaction reliant on NAD(P)H production in living cells. The plates were then incubated at 37 °C with 5 % CO_2 for 30 minutes prior to spectrophotometric analysis. The quantity of formazan is correlated with the cells metabolic activity, and can therefore be used as an indirect quantification of cell viability. The plates were read at 450 nm, and at 745 nm as reference, on the VersaMax plate reader utilising the SoftMax Pro 6.4 software. Seven parallels were measured for every concentration of cytostatic in all cell lines, and wells containing only media and drug were measured as blank samples.

3.3.3 Reverse transfection

Transfection is the process in which foreign genetic material is introduced into a host organism using recombinant DNA technology. Reverse transfection refers to the procedure of adding cells to the transfection reaction second to the transfecting reagents, whereas regular transfection is performed by growing cells in plates until they reach the desired confluence prior to adding transfection reagents. Reverse transfection was used because it was consistent with a high-throughput assay, as the additional plating and growing of cells necessary in regular transfection was no longer required. An added benefit of reverse transfection was the increased cell surface available, which may result in higher transfection efficiency.

Lipofectamine 3000

Lipofectamine 3000 is a lipid based transfection agent comprised of two components; Lipofectamine 3000 and the helper-lipid P3000. An illustration of lipid based transfection is displayed in Figure 15.

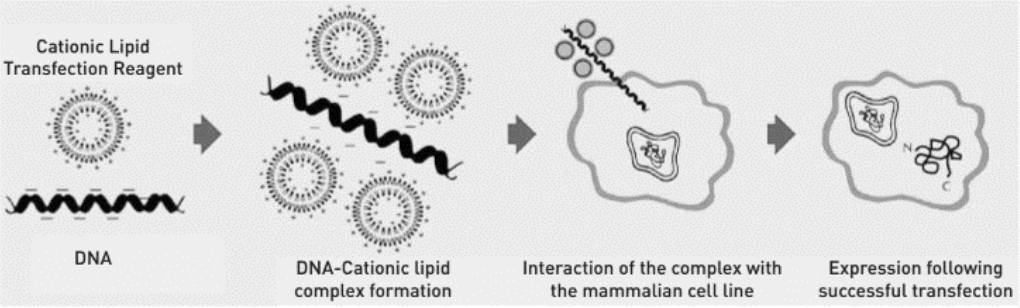

Figure 15. A schematic illustration of cationic lipid mediated transfection. The positively charged head groups of the lipids interact with the negatively charged phosphate backbone of DNA. This interaction forms a DNA-cationic lipid complex that can enter the cell through endocytosis (Thermo Fischer Scientific).

Transfection procedure

The pcDNA3 GAL4 DBD:BRCA1 plasmids were co-transfected into HEK293T, MDA-MB-231 or MDA-MB-436 cells together with two reporter plasmids; phRG-TK (*Renilla*) and pGAL4-e1b-Luc (*Firefly*), to investigate the effects of *BRCA1* variants on TA-activity.

Transfection was done using Lipofectamine 3000, according to the manufacturers procedure. The amount of, and ratio between the plasmids, were taken from Jarhelle *et al.* (2016), and scaled down from a 6-well plate to a 96-well plate setup. The ratios between the Lipofectamine 3000 kit reagents and plasmid-amount previously found by the Iversen, N. research group for a similar experiment, were tested and deemed suitable. The NucleoCounter® NC-100™ was used for cell quantification in all transfection experiments.

96-well plate experiment

The transfection experiment described by Jarhelle *et al.* (2016) was scaled to a 96-well experiment, in order to increase efficiency and sample number per setup.

Wild type and variant plasmids were transfected in six parallels. For every experiment, transfection with reporter plasmids pGAL4-e1b-Luc (Firefly) and phRG-TK (Renilla) only, was included as a measure of background expression. Three parallels of cells transfected with reporter plasmids and pMaxGFP were included to verify successful transfection, as well as three parallels of non-transfected cells. A reaction mixture of plasmids and helper lipid P3000 was prepared (Table 8), and mixed with a Lipofectamine 3000 dilution (Table 9), before 15 minutes of room temperature incubation and subsequent addition of 30 µL of OptiMem, bringing the total transfection mixture volume to 50 µL pr. well (20 µL plasmid and Lipofectamine 3000 mixture + 30 µL OptiMem).

Table 8. Reaction mixes used in 96-well transfection of HEK293T, MDA-MB-231 and MDA-MB-436 cells. pcDNA3 GAL4 DBD:BRCA1 was the plasmid containing either wild type or variant BRCA1 BRCT domain. Samples refer to the mixture containing either wild type or variant plasmid. GFP was the mixture containing the Green Fluorescent Protein, and Reporters contained reporter plasmids Firefly and Renilla only. The volumes listed per column were for one well.

		HEK293T			MDA-MB-231/436		
Plasmid/reagent	**Conc. (µg/µL)**	**Samples (µL)**	**GFP (µL)**	**Reporters (µL)**	**Samples (µL)**	**GFP (µL)**	**Reporters (µL)**
OptiMem	-	8.5	8.8	9.0	8.1	8.4	8.6
pGAL4-e1b-Luc (Firefly)	0.20	0.5	0.5	0.5	0.5	0.5	0.5
phRG-TK (Renilla)	0.02	0.5	0.5	0.5	0.5	0.5	0.5
pcDNA3 GAL4 DBD:BRCA1	0.20	0.5	-	-	0.5	-	-
pMaxGFP	0.50	-	0.2	-	-	0.2	-
P3000	-	0.2	0.2	0.2	0.42	0.42	0.42

Table 9. Lipofectamine 3000 dilutions in OptiMem used in 96-well transfection of the cell lines HEK293T, MDA-MB-231 and MDA-MB-436. Volumes listed were for one well.

Cell line	OptiMem (µL)	Lipofectamine 3000 (µL)
HEK293T	10	0.35
MDA-MB231/436	10	0.50

A DMEM suspension of $4x10^5$ cells/mL of HEK293T and MDA-MB231 cells, and $4.5x10^5$ of MDA-MB436 cells were prepared using the NucleoCounter® NC-100™ for quantification of cell numbers. To each well 50 µL of transfection mixture was added, before 100 µL of cell suspension were transferred to the well. The plate was incubated at 37 °C with 5 % CO_2 for 24 or 48 hours before harvesting. The experiment was repeated three-four times for each variant and incubation time.

12-well plate experiment

The transfection procedure described for a 96-well experiment was scaled to a 12-well plate setup in order to yield the amount of protein and RNA needed to perform protein- and RNA-based assays. The 12-well experiment was performed similar to the 96-well experiment, but in one parallel and without GFP.

A reaction mixture of plasmids and helper lipid P3000 was prepared (Table 10), and mixed with a Lipofectamine 3000 dilution (Table 11), before incubation for 15 minutes at room temperature.

Table 10. Reaction mixes used in 12-well transfection of HEK293T, MDA-MB-231 and MDA-MB-436 cells. pcDNA3 GAL4 DBD:BRCA1 was the plasmid containing either wild type or variant BRCA1 BRCT domain. Samples refer to the mixture containing either wild type or variant plasmid. GFP was the mixture containing the Green Fluorescent Protein and Reporters contained reporter plasmids Firefly and Renilla only. The volumes listed per column were for one well.

		HEK293T			MDA-MB231/436		
Plasmid/reagent	**Conc. (µg/µL)**	**Samples (µL)**	**GFP (µL)**	**Reporters (µL)**	**Samples (µL)**	**GFP (µL)**	**Reporters (µL)**
OptiMem	-	42.5	44	45.0	40.5	42	43.0
pGAL4-e1b-Luc (Firefly)	0.20	2.5	2.5	2.5	2.5	2.5	2.5
phRG-TK (Renilla)	0.02	2.5	2.5	2.5	2.5	2.5	2.5
pcDNA3 GAL4 DBD:BRCA1	0.20	2.5	-	-	2.5	-	-
pMaxGFP	0.50	-	1	-	-	1	-
P3000	-	1	1	1	2.1	2.1	2.1

Table 11. Lipofectamine 3000 dilutions in OptiMem used in 96-well transfection of the cell lines HEK293T, MDA-MB-231 and MDA-MB-436. Volumes listed were for one well.

Cell line	OptiMem (µL)	Lipofectamine 3000 (µL)
HEK293T	50	1.75
MDA-MB-231/436	50	2.50

A DMEM suspension of $2x10^5$ cells/mL of HEK293T and MDA-MB-231 cells, and $2.5x10^5$ of MDA-MB436 cells were prepared using the NucleoCounter® NC-100™ for quantification of cell numbers. To each well, a 100 µL of transfection mixture was added, before 1 mL of cell suspension was transferred to the well. The plate was incubated at 37 °C with 5 % CO_2 for 48 hours before harvesting.

3.3.4 Cell harvesting

Cell lysate to TA-assay

Harvesting of cells for use in the TA-assay was performed with the Dual Luciferase® Reporter Assay System Kit in accordance with manufacturers protocol. Following 96-well plate transfection and incubation, medium was carefully removed from each well. Cells were then lysed in 20 µL of 1x PLB (Passive Lysis Buffer), and put on an orbital shaker for 15 minutes with gentle shaking to ensure complete coverage of the cells. Lysates were stored in 96-well plates at -80 °C before measuring luciferase intensity.

TA-assay cell lysate used in Western blot

Protein lysates were prepared for use in total protein assay and western blotting. Following 12-well plate transfection and incubation, medium was carefully removed from the wells and cells

were washed with cold DPBS, taking care not to dislodge the cells from the plate. 150 µL RIPA buffer (with 100x Halt™ Protease & Phosphatase inhibitor cocktail) was added to each well. The plate was incubated on ice for 5 minutes and cells were mixed with lysis buffer and detached from the plate with a cell scrape. Lysates were transferred to Eppendorf tubes and stored at -20 °C for use in downstream applications.

TA-assay cell lysate used in mRNA analysis on qPCR

RNA lysates were prepared for use in cDNA synthesis and subsequent qPCR. Following 12-well plate transfection and incubation, medium was carefully removed from the well and cells were washed with cold DPBS, taking care not to dislodge the cells from the plate. 300 µL RNAqueous buffer was added to each well and thoroughly mixed by pipetting. The plate was stored at -80 °C prior to RNA isolation. RNA isolation was performed using the RNAqueous™ Phenol-free total RNA isolation kit (Thermo Fisher Scientific) following manufacturers procedure. RNA was quantified and the purity was measured on the NanoDrop® ND1000, a 260/280 ratio of 2.1 ± 0.2 was deemed satisfactory. RNA isolates were stored at -80 °C, prior to cDNA synthesis and downstream applications.

Cell lysate used in measure of endogenous expression of *BRCA1* in cell lines

RNA lysates were prepared for use in cDNA synthesis and Real-Time quantitative polymerase chain reaction (qPCR) for studies on endogenous expression of *BRCA1* in the HEK293T, MDA-MB-231, MDA-MB-436, SUM102 and MCF-7 cell lines. Approximately 200,000 HEK293T cells were seeded in a 12-well plate and incubated at 37 °C with 5 % CO_2 for 48 hours prior to harvesting. After incubation, medium was carefully removed from the well. The cells were washed with cold DPBS, taking care not to dislodge the cells from the plate. Cells were lysed in 300 µL of RNAqueous lysis buffer and mixed thoroughly by pipetting. Cell lysis were transferred to tubes and stored at -80 °C for use in downstream applications. The remaining cell lines were grown in T25 bottles until confluent, and carefully washed with cold DPBS. Cells were lysed in 1200 µL of RNAqueous lysis buffer, and mixed thoroughly by pipetting. Cell lysis were transferred to Eppendorf tubes in 600 µL aliquots and stored at -80 °C.

3.4 Nucleic acid methods

3.4.1 Isolation and quantification of nucleic acids

DNA isolation

DNA was extracted from HEK293T, MDA-MB-231, MDA-MB-436, SUM102 and MCF-7 cell lines for use in sequencing of endogenous *BRCA1* and *TP53*. Cell pellets from all cell lines were taken from -80 °C and thawed at room temperature. DNA extraction was done using the QIAamp Mini DNA Kit following the manufacturers protocol, with some adjustments to the lysis step; PBS was added to the pellets, bringing the total volume up to 200 µL, and then suspended. 100 µL of buffer ATL and AL and 20 µL of proteinase K was added. Samples were then vortexed and incubated at 56 °C for 10 minutes, before 100 µL of 100 % EtOH was added. Quantification and measurement of DNA purity was done on NanoDrop® ND1000.

RNA isolation

RNA isolation was performed on cell lysates from cell lines and cells transfected in the 12-well TA-assay, using the RNAqueous™ Phenol-free total RNA isolation kit (Thermo Fisher Scientific) following manufacturers procedure. RNA was quantified and purity measured on the NanoDrop® ND1000, a 260/280 ratio of 2.1 ± 0.2 was deemed satisfactory. RNA isolates were stored at -80 °C, prior to cDNA synthesis and downstream applications.

3.4.2 cDNA synthesis

Complementary DNA (cDNA) was synthesised using the High Capacity cDNA Reverse Transcription Kit in accordance with manufacturer instructions. In short, RNA was diluted in nuclease-free water in 96-well plates to assure equal input. The cDNA reaction mixture (appendix section B) was added in a 1:1 ratio to the RNA dilutions (25 µL of each), and the plate was run on a 2720 Thermal Cycler using the program listed in Appendix, Section B.

3.4.3 qPCR

Quantification of relative *BRCA1* expression in cell lines and expression levels of *GAL4 DBD:BRCA1* fusion construct mRNA was done using qPCR (Figure 16) on the QuantStudio™ 12K Flex Real-Time System. Reference gene *GAPDH* were tested for use as reference genes. cDNA was diluted 1:5 prior to setup to avoid inhibitory effects. Reaction mixtures for *BRCA1* and *GAPDH* are given in Appendix, Section B. cDNA and reaction mixtures were prepared in a 96-well plate, before transfer in triplicates of 10 µL to a 384-well plate and run on the Applied Biosystems™ QuantStudio™ 12K Flex Real-Time System, using cycling parameters listed in Appendix B. The Relative gene expression was calculated using the comparative ΔCt method

(equations 1-3). A fictive sample with a *BRCA1* Ct-value set to 40, representing no expression of *BRCA1*, was used as reference sample.

$$\Delta Ct = Ct_{Target\ gene} - Ct_{Reference\ gene} \quad (1)$$

$$\Delta\Delta Ct = \Delta Ct_{Target\ sample} - \Delta Ct_{Reference\ sample} \quad (2)$$

$$RQ = 2^{-\Delta\Delta Ct} \quad (3)$$

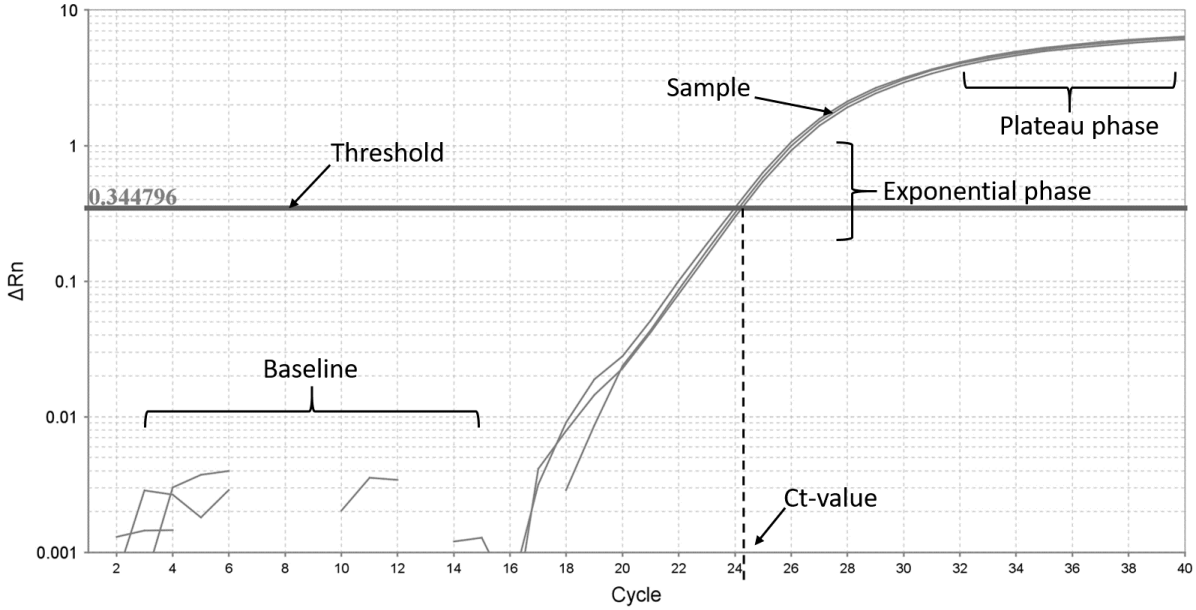

Figure 16. Diagram of the qPCR plot indicating the nomenclature used in calculating expression. Threshold is an arbitrary fluorescence level set in the exponential phase and above any baseline signals. The threshold cycle (Ct) is the cycle in which the measured sample fluorescence crosses the threshold.

Verification of efficiency and specificity of the qPCR

Primers for qPCR were chosen that would bind specifically to *BRCA1* mRNA in cell lines and the *GAL4 DBD:BRCA1* fusion construct mRNAs. The relative expression of *BRCA1* in cell lines and cells transfected in the TA-assay, was measured using the comparative Ct method. Unlike the absolute quantification method, comparative Ct does not rely on the construction of a standard curve with known copy numbers. Instead it measures expression relative to a target gene. A requirement for performing this method is that PCR efficiency is equal for both target and reference gene. To assess the PCR efficiency of the assay, a five-fold dilution series was analysed. In short, cDNA from cell line MDA-MB-231 and MCF-7 was diluted 1:2 and used as the maximum concentration of the series. Four subsequent five-fold dilutions were performed to give a series consisting of; 1, 5, 25, 125 and 625 relative quantities of cDNA. PCR efficiency was calculated using equation 4.

$$Efficiency\ (\%) = 10^{\frac{-1}{a}} - 1 * 100\ \% \quad (4)$$

Where *a* is the slope of the trendline generated by the standard curve.

The reference gene included in the test were *GAPDH*. The criteria for the qPCR reactions are shown in equations 5 and 6.

$$90\ \% < Efficiency\ (\%) < 105\ \% \quad (5)$$

$$\Delta_{slope} < 0.1 \quad (6)$$

Since the qPCR reaction for *BRCA1* was based on SYBR® green, a reagent that binds to and detects all dsDNA, it was necessary to verify the specificity of the reaction. This was performed using a melting curve analysis. Since denaturation of DNA occurs at different temperatures depending on sequence, a specific PCR will yield a single peak, while unspecific assays display multiple. This is because of hyperchromicity, were dissociation of dsDNA increases the absorbance intensity. The reference genes are commercially available assays with primers and probes placed in exon-intron junctions, and have been tested for specificity.

3.4.4 Sanger sequencing

Plasmid verification

Verification of wild type and the genotype variant plasmids were performed by Sanger sequencing with the BigDye Terminator v.3.1 Cycle Sequencing Kit (Figure 17). Sequencing primers, reaction mix and cycling parameters are listed in Appendix, Section B. Primers were selected to give complete coverage of the insert along with the flanking regions of the plasmid vector. Sequencing PCR products were purified with Agencourt CleanSEQ – Dye Terminator Removal Kit (Figure 18) on the BioMek FX robot, according to manufacturer's procedure. Sequence files were analysed with SnapGene v.3.3.2, and aligned to *BRCA1* reference sequence NM_007294.3 and the pcDNA3 GAL4 DBD:BRCA1 plasmid sequence provided by Elisabeth Jarhelle (2017) (Appendix, Section B). Plasmid sequencing was performed twice on each plasmid, after *in vitro* mutagenesis, and after production of plasmid stock solutions.

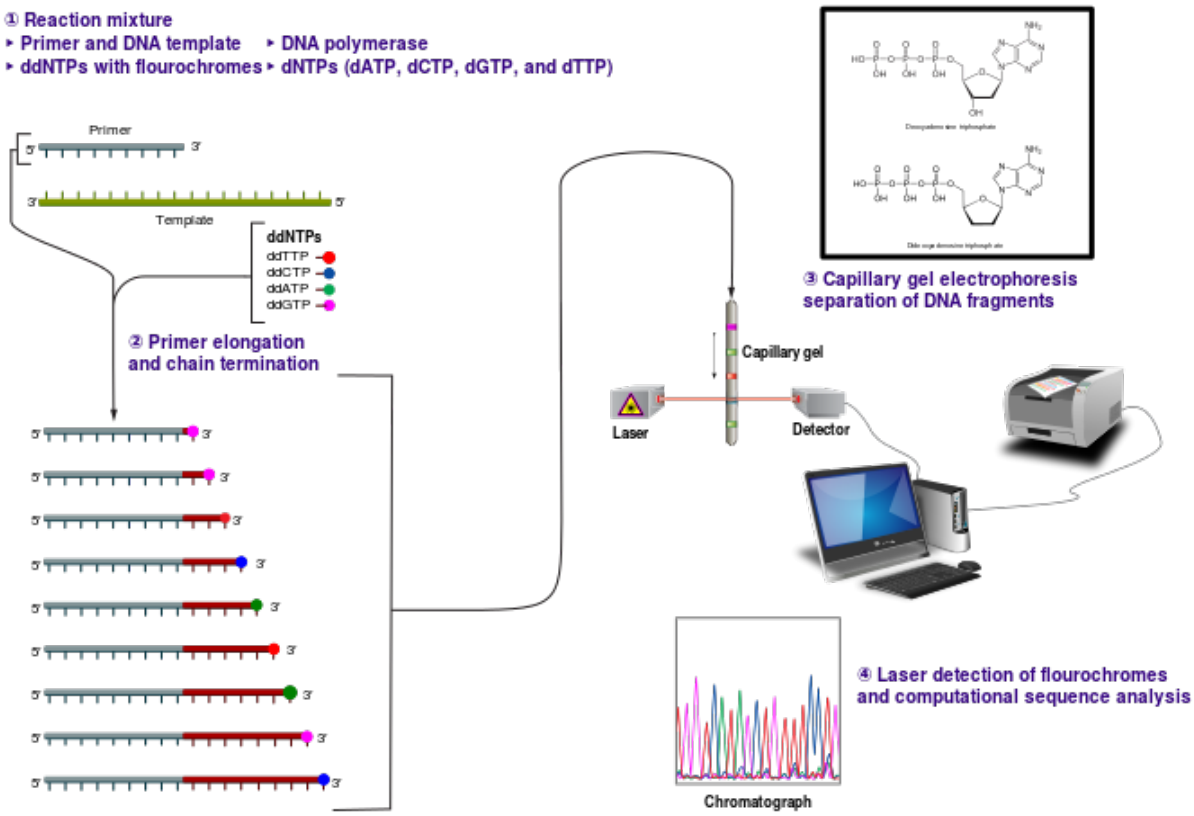

Figure 17. Principle of Sanger sequencing using BigDye Terminator. The method follow the principle of a standard PCR, but incorporation of fluorescently labelled ddNTPs terminate elongation, resulting in fluorescently labelled DNA fragments of unequal length. These fragments are separated using capillary gel electrophoresis, detected via laser and presented as electropherograms. (Estevezj - Own work, CC BY-SA 3.0, https://commons.wikimedia.org/w/index.php?curid=23264166)

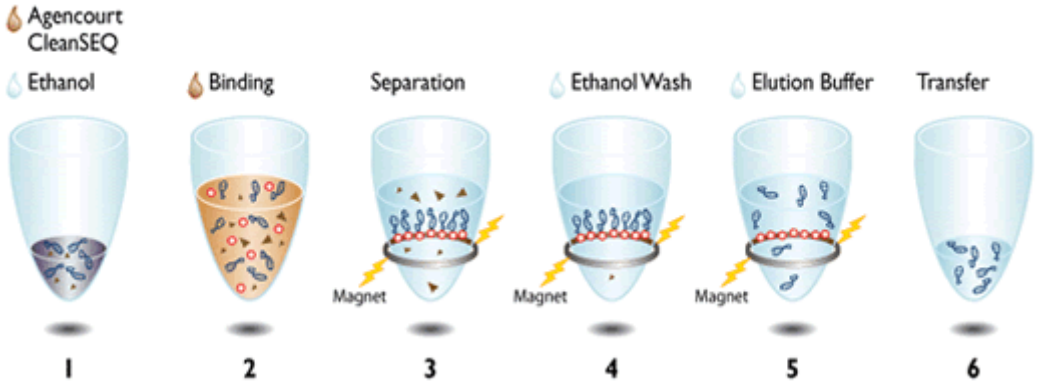

Figure 18. Illustration of the Agencourt CleanSEQ Dye Terminator Removal procedure, used in purification prior to analysis on a DNA sequencer. **1)** Magnetic, DNA binding CleanSEQ beads and ethanol is added to the sample. **2)** Sequencing PCR products bind to CleanSEQ beads. **3)** Application of a magnetic field separate beads carrying sequencing product from undesired substances. **4)** Sequencing product is washed in ethanol. **5)** Elution buffer releases sequencing product from beads. **6)** Purified sequencing product is transferred to clean tube.

Cell lines

Sanger sequencing of *BRCA1* and *TP53* was performed per the method utilised during routine diagnostic sequencing of these genes at the Oslo University Hospital, Department of Medical Genetics. Sequencing was performed using the BigDye Terminator v.3.1 Cycle Sequencing Kit. Sequencing primers, reaction mixes and cycling parameters are listed in Appendix, section B. Purification of PCR and sequencing PCR products were done on a BioMek FX robot with Agencourt® AMPure® XP (Figure 19) and Agencourt® CleanSEQ – Dye Terminator Removal Kit, respectively and per manufacturer instructions. Sequence files were analysed using SeqPilot v.4.3.0.

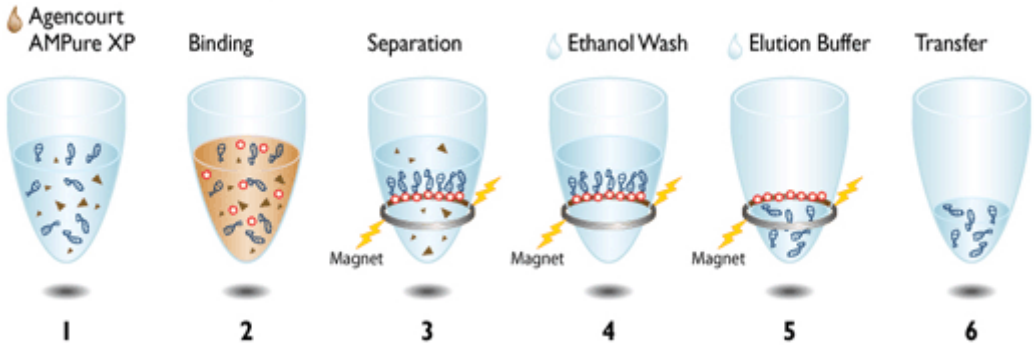

Figure 19. Illustration of the Agencourt AMPure XP procedure, used in purification of PCR products prior to sequencing PCR. **1)** Magnetic, DNA binding AMPure XP beads are added to the sample. **2)** PCR products bind to AMPure XP beads. **3)** Application of a magnetic field separate beads carrying PCR product from undesired substances. **4)** PCR product is washed in ethanol. **5)** Elution buffer releases PCR product from beads. 6) Purified PCR product is transferred to clean plate.

3.5 Protein techniques

3.5.1 Luciferase measurement

TA-activity of BRCA1 variants were measured using the Dual Luciferase® Reporter Assay System. Lysates from transfected and harvested cells, were thawed at room temperature. The Luciferase Assay Reagent II (LAR II) and Stop&Glo® were prepared as described in the manufacturers procedure. For each sample of HEK293T and MDA-MB-231, 5 µL of cell lysate was transferred to a white half area, µclear® 96-well plate. For the MDA-MB-436 samples, 10 µL of lysate were used. Light emission was measured with a BioTek® Synergy H1 luminometer with an auto-injection system. 50 µL of LAR II was then added to the sample, and Firefly-luciferase light emission was recorded. 50 µL of Stop&Glo® was added to inhibit Firefly-luciferase and simultaneously activate light emission by *Renilla*-luciferase, before measuring the light emission. This was repeated for all six parallels of every sample and control in each experiment.

3.5.2 Total protein

Total protein was measured using the PIERCE® BCA Protein Assay Kit to normalise sample protein levels prior to western blotting, and for determining the correct amount of protein added. A two-fold standard dilution series with five concentrations of Albumin (0.125-2 µg/µL) were prepared. RIPA buffer with added 100x Halt™ Protease & Phosphatase inhibitor cocktail was used for dilution and as blank. The BCA Working Reagent (WR) was prepared by mixing reagent A and reagent B in a 50:1 ratio. Standards and samples were measured in triplicate. 5 µL of each standard and sample were transferred to a flat-bottom 96-well plate, and 200 µL of WR reagent was added to each well. The plate was mixed on an orbital shaker for 30 seconds, before incubation at 37 °C for 30 minutes. Absorbance was measured at 570 nm with the VersaMax microplate reader. Sample concentrations were calculated using the SoftMax Pro 6.4 software with a quadratic fit standard curve (Figure 20).

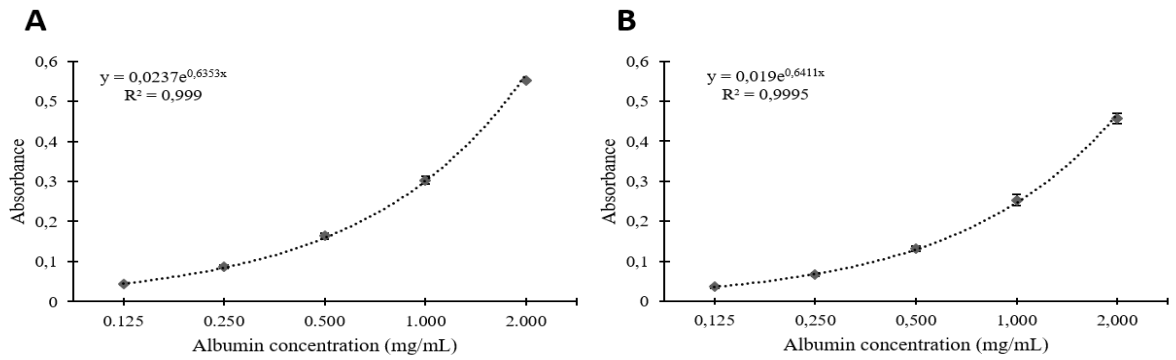

Figure 20. Standard curves displaying absorbance at 570 nm as a function of albumin concentration. The curves are used in total protein measurement for use in normalisation of protein levels prior to western blot analysis. Equation for the quadratic fit trendline from one representative experiment is displayed along with the R^2-value (n=3). **A)** HEK293T RIPA-lysate. **B)** MDA-MB-231 RIPA-lysate.

3.5.3 Western blot

Western blotting was used to ascertain the presence of GAL4 DBD:BRCA1 fusion protein, and that variation in TA-activity was a result of the variant in question, and not a product of fluctuations in sample protein levels. Samples were normalised using total protein measures. Western blotting was performed on 10 % precast Mini-PROTEAN® TGX™ gels (Bio-Rad Laboratories, Inc.), with 10 µg of sample protein added. Gels were blotted onto 0.2 µM Nitrocellulose Membranes (Bio-Rad Laboratories, Inc.) and blocked with 5 % BSA for one hour. Primary staining of the blots was done with two different antibodies mapped to the BRCA1 BRCT domain. The first was BRCA1 (C-20):sc-642, a rabbit polyclonal antibody that was applied in a 1:2000 dilution. The second was BRCA1 (D-9):sc-6954, a mouse monoclonal antibody used in a 1:1000 dilution. Staining was performed overnight at 4 °C. Staining with secondary antibodies was done with the m-IgGκ BP-HRP: sc-516102 antibody in a 1:1000 dilution, for 1 hour at room temperature.

The predicted size of the fusion protein GAL4 DBD:BRCA1 was 69.6 kDa (estimated using SnapGene v3.3.2). Blots were developed using the Amersham™ ECL™ Prime Western Blotting Detection Reagent kit (GE Healthcare UK). Exposure of the blots was performed on the ImageQuant™ LAS 4000, with ImageQuant™ TL 1D v8.1.

3.5.4 Statistical methods

Statistical significance of TA-assay results of *BRCA1* variants *in cis,* and the effects of incubation time on TA-assay, were calculated using the unpaired t-test. Data were considered independent and normally distributed, and probability values $P < 0.05$ were considered significant.

4 Results

4.1 Verification of TA-assay plasmids

Plasmid pcDNA3 GAL4 DBD:BRCA1 was sequenced using Sanger sequencing to ensure correct incorporation of each variant (Figure 21). Wild type plasmid was also sequenced to confirm that no variants were present. Each plasmid was sequenced twice, after mutagenesis and after amplification to create plasmid stocks.

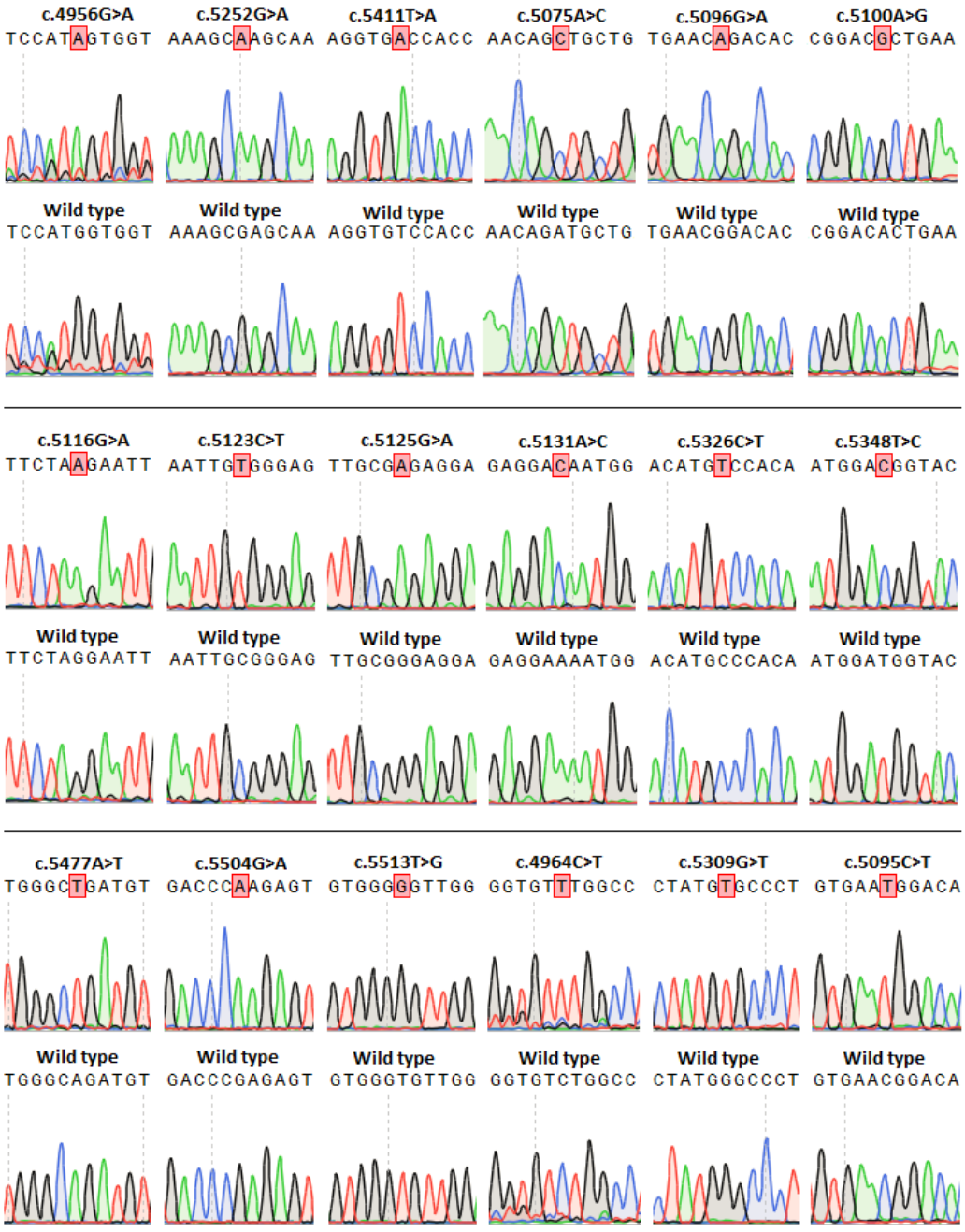

Figure 21. Electropherograms displaying the correct implementation of *BRCA1* variants in the pcDNA3 GAL4 DBD:BRCA1 plasmid compared to the wild type sequence.

4.2 Effect of *BRCA1* variants in the transactivation assay

The TA-assay was used to assess the effect of *BRCA1* variants on the integrity of the BRCT-domain. This was accomplished by measuring the ability of a fusion protein containing the BRCA1 BRCT-domain to transactivate expression of firefly luciferase.

4.2.1 Transactivation activity of *BRCA1* variants

The TA-assay was performed on 18 *BRCA1* variants found in patients during routine diagnostics at the Oslo University Hospital, Department of Medical Genetics. Analysis on the TA-assay was done in HEK293T and MDA-MB-231 cells with 48-hours incubation time, for all variants included. The results from both cell-lines are displayed in Figure 22, and reveal a high degree of similarity between the two cell lines. The largest discrepancies are in variants displaying high TA-activity (TA > 70 %), whereas variants presenting lower TA-activity (TA < 60 %) have a high degree of similarity. Variants classified as benign (class 1, p.Met1652Ile, p.Arg1751Gln) or likely benign (class 2, p.Val1804Asp) prior to this study, were used as controls representing normal/wild type variants. The wild type controls displayed TA-activities ranging from 44-102 %, and were used to estimate the range of wild-type TA-activity. Three variants with prior classifications as likely pathogenic (class 4, p.Ser1655Phe and p.Gly1770Val) and pathogenic (class 5, p.Arg1699Trp) displayed a TA-activity ranging from 0.7-14 %, and were used as controls for estimating the range of TA-activity in deleterious variants. Variants of uncertain clinical significance (Class 3) were divided into three groups based on a strict interpretation of the TA-assay controls; low-risk (TA > 44 %), high-risk (TA < 14 %) and intermediate (14 % < TA < 44 %). Variants included in the low-risk category were; p.Gly1709Arg, p.Thr1700Thr, p.Pro1776Ser, p.Glu1826Leu and p.Arg1835Gln. Variants p.Asp1692Ala, p.Val1838Gly and p.Gly1706Arg were considered high-risk. Two variants, p.Arg1699Gln and p.Ala1708Val, displayed TA-activities slightly above the estimated 14 % threshold for pathogenicity (16.1-19.9 % and 15.7-16.0 % in MDA-MB-231 and HEK293T, respectively), and was therefore placed in the intermediate category along with variants p.Lys1711Gln and p.Met1783Thr (TA-activities 36.8-41.6 % and 27.2-31.9 % in MDA-MB-231 and HEK293T, respectively). However, both variants p.Arg1699Gln and p.Ala1708Val failed to display TA-activities significantly different from the pathogenic control p.Arg1699Trp in the MDA-MB-231 cell-line (p-values 0.12 and 0.18 for p.Arg1699Gln and p.Ala1708Val, respectively).

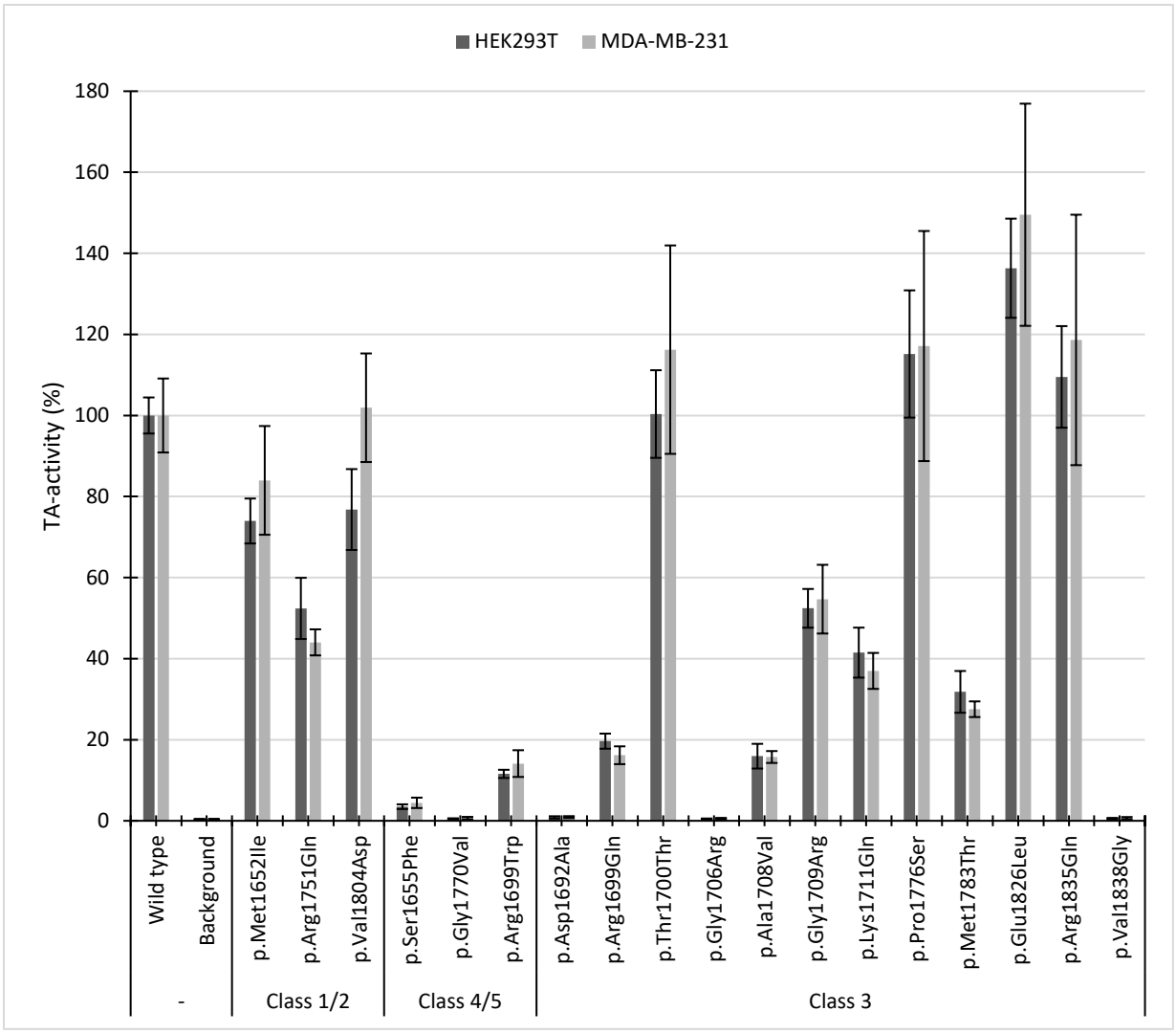

Figure 22. TA-activity of *BRCA1* BRCT variants measured after 48-hour incubation in HEK293T (dark grey) and MDA-MB-231 (light grey) cells. Class 1-5 represent classification prior to this study. Variants in classes 1-2 and 4-5 were used as benign and pathogenic controls, respectively, and class 3 was variants of unknown clinical significance. TA-activity is displayed as mean percentage of wild type for three-four experiments, conducted in sextuplicate, with error bars representing standard deviation ($n \geq 18$). The background is cells transfected with reporter plasmids pGAL4-e1b-Luc (firefly) and phRG-TK (Renilla) only.

4.2.2 Transactivation activity of *BRCA1* variants *in cis*

Two plasmids, each containing two different *BRCA1* variants *in cis*, were included in the study on the TA-assay as they presented the opportunity to look for additive effects. Both plasmids were analysed in HEK293T and MDA-MB-231 cells.

Effect of *in cis* variants p.Asp1692Ala and p.Val1804Asp on TA-activity

TA-activity of the plasmid containing variants p.Asp1692Ala and p.Val1804Asp was compared to the activity of plasmids containing only one of these variants (Figure 23). Variant p.Val1804Asp display TA-activity (102 %) comparable to that of the wild type plasmid in MDA-MB-231, and slightly reduced TA-activity (77 %) in HEK293T cells, while variant p.Asp1692Ala practically abolish the TA-activity of the BRCT-domain in both cell-lines. Combining variants p.Val1804Asp and p.Asp1692Ala displayed significantly reduced TA-activities in both HEK293T and MDA-MB-231 (p-values < 0.0001), compared to p.Ala1692Asp alone. While the TA-activity of p.Asp1692Ala were low to begin with (0.86 % in HEK293T and 0.91 % in MDA-MB-231), inclusion of p.Val1804Asp reduced the TA-activities to 0.48 % in HEK293T and 0.61 % in MDA-MB-231.

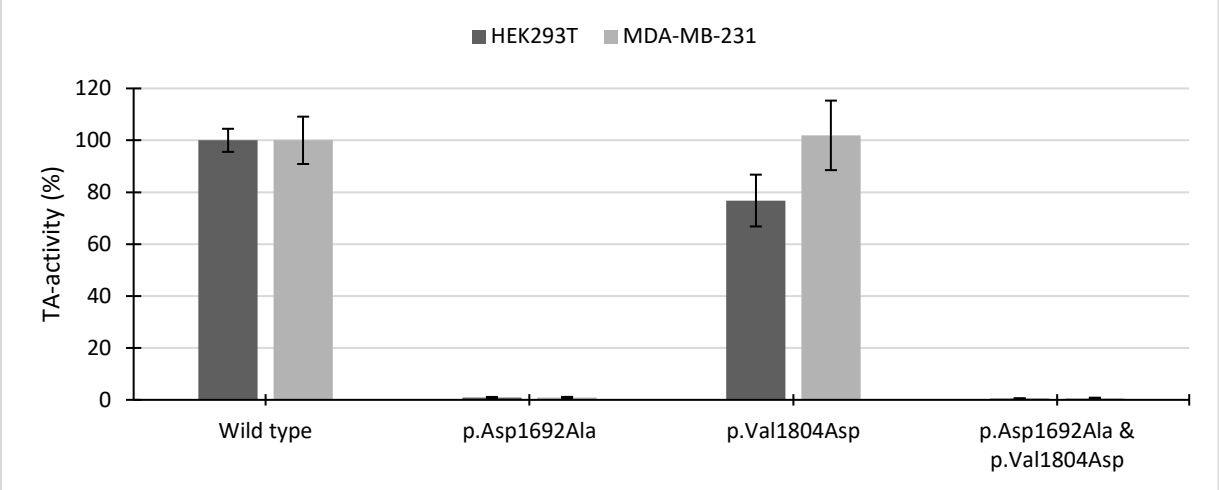

Figure 23. TA-activity as mean percentage of wild type for plasmids containing the variants p.Asp1692Ala, p.Val1804Asp and both variants *in cis*. Analysed using HEK293T and MDA-MB-231 cells with 48-hour incubation time and three-four experiments in sextuplicate. Error bars represent standard deviation ($n \geq 18$).

Effect of *in cis* variants p.Arg1751Gln and p.Glu1826Leu on TA-activity

TA-activity of the plasmid containing both variant p.Arg1751Gln and p.Glu1826Leu was compared to the activity of plasmids containing only one these variants (Figure 24). Variant p.Arg1751Gln had TA-activity of 52 % and 44 % of wild type activity in cell-lines HEK293T and MDA-MB-231, respectively. Variant p.Glu1826Leu display increased TA-activity in both

cell-lines; 136 % in HEK293T and 150 % in MDA-MB-231. The plasmid containing both variants had a TA-activity of 76 % in HEK293T and 78 % in MDA-MB-231. The difference in TA-activity between the three plasmids was significant in both cell-lines (p-value < 0.0001), and p.Glu1826Leu seemed to rescue some of the loss in TA-activity caused by p.Arg1751Gln.

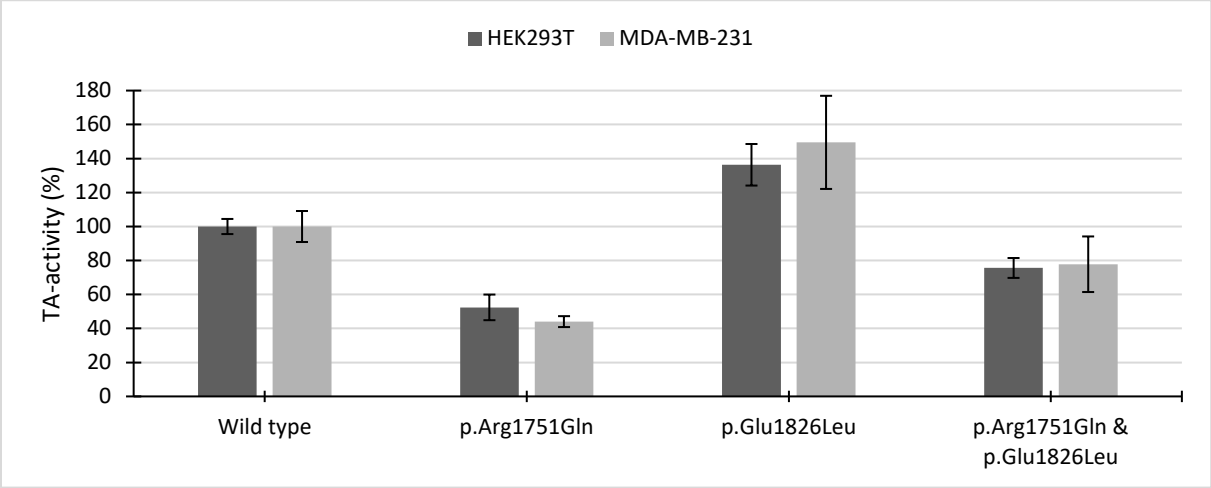

Figure 24. TA-activity as mean percentage of wild type for plasmids containing the variants p.Arg1751Gln, p.Glu1826Leu and both variants *in cis*. Analysed using HEK293T and MDA-MB-231 cells with 48-hours incubation time and three-four experiments in sextuplicate. Error bars represent standard deviation (n≥18).

4.3 Optimisation and evaluation of TA-assay parameters

4.3.1 Effect of incubation time on sensitivity of the TA-assay

To investigate the effect of incubation time during transfection on the sensitivity of the TA-assay, 8 variants were analysed after 24-hour incubation and compared with the results from 48-hour transfections (4.2.1). The experiments were conducted in HEK293T and MDA-MB-231 cells.

The results comparing 24- and 48-hour incubation times during transfection are illustrated in Figure 25A and B. For variants with TA-activities < 50 %, the prolonged incubation time of 48 hours yielded a significant increase in sensitivity compared to the 24-hour incubation time ($p < 0.001$) in both HEK293T and MDA-MB-231 cell lines. Variants presenting with TA-activity > 50 % displayed no significant effect of increased incubation time was. Variant p.Arg1751Gln was the only variant that displayed differing results between the cell lines, yielding a significant effect in the MDA-MB-231 cells, but not in HEK293T cells.

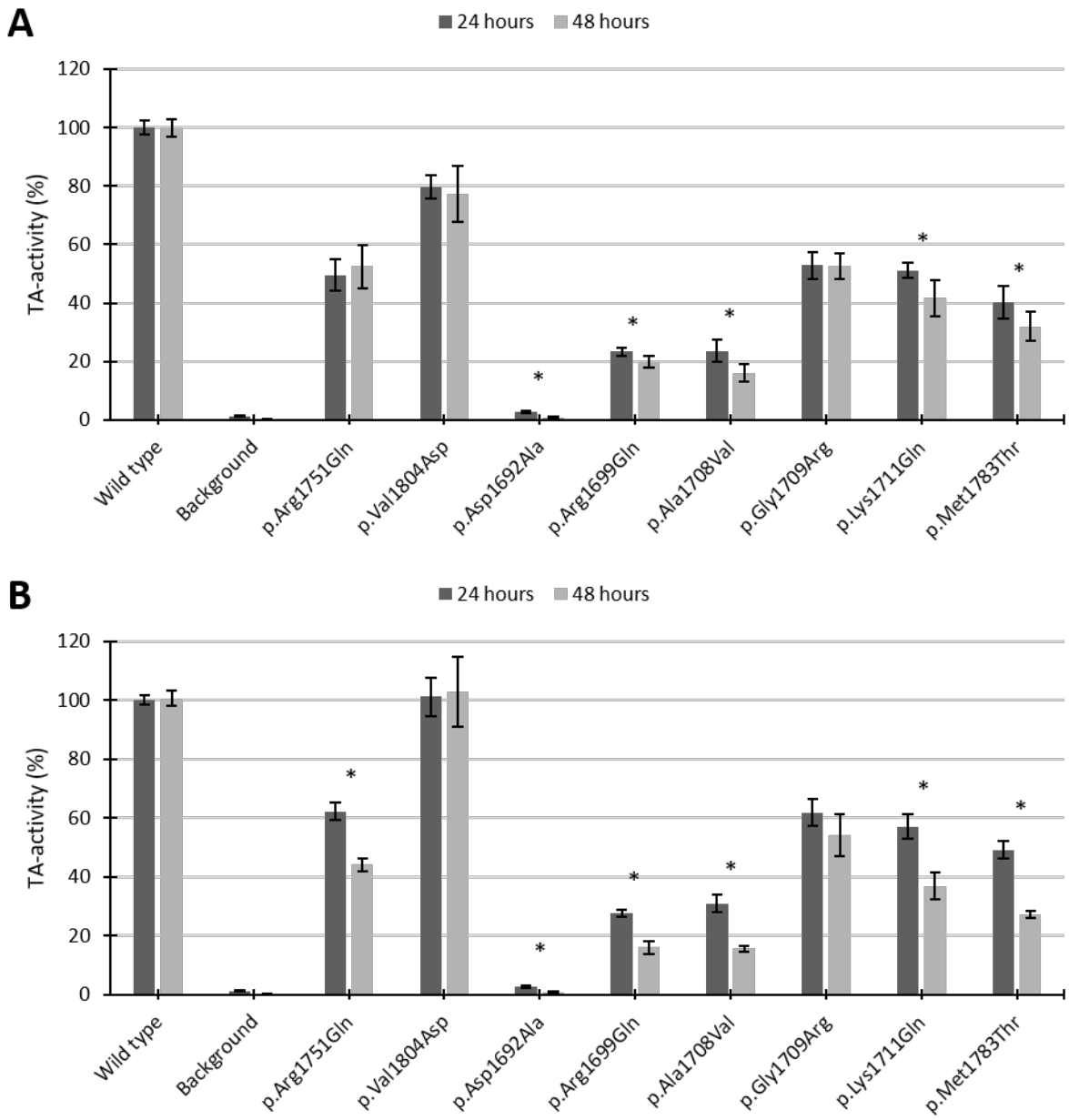

Figure 25. Comparison of TA-activity for selected variants after 24 (dark grey)- and 48 (light grey)-hours incubation time. **A)** HEK293T cells. **B)** MDA-MB-231. TA-activity is displayed as percentage of wild type. Error bars represent standard deviations ($n \geq 18$) for three-four experiments (*P-value < 0.001).

4.3.2 Effect of cell line choice on reproducibility of the TA-assay

The TA-assay was also performed in the MDA-MB-436 cell line, with 48-hours incubation time and the same selection of eight variants as used in the optimisation of incubation times for HEK293T and MDA-MB-231. This was done to see whether choice of cell line affected the results of the assay. Results from the MDA-MB-436 experiments were compared to the results obtained for the same variants obtained with the 48-hour experiments in HEK293T and MDA-MB-231 and are displayed in Figure 26. Measurement of luciferase activity in the MDA-MB-436 cells were much weaker than in the MDA-MB-231 and HEK293T cells, with only 2 of 5 experiments yielding signals strong enough to be distinguishable from empty wells for both firefly and Renilla. TA-activities measured in MDA-MB-436 cells nevertheless reflect largely the same findings as in HEK293T and MDA-MB-231.

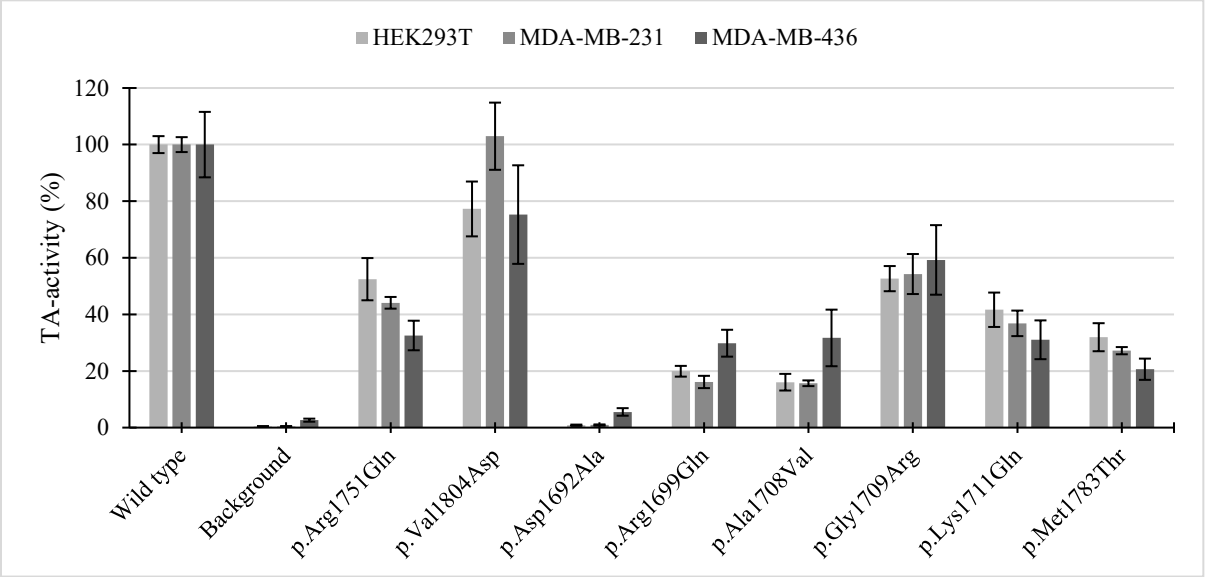

Figure 26. Comparison of TA-activity for variants after 48-hours incubation in HEK293T (light grey), MDA-MB-231 (grey) and MDA-MB-436 (dark grey) cells. TA-activity is shown as mean percentage of wild type. Error bars represent standard deviations for two-four experiments ($n \geq 12$). The background represents cells transfected with reporter plasmids pGAL4-e1b-Luc and phRG-TK only.

4.3.3 Effect of cell line choice on TA-assay transfection efficiency

HEK293T, MDA-MB-231 and MDA-MB-436 were transfected with the firefly and Renilla reporter plasmids (pGAL4-e1b-Luc and phRG-TK, respectively) and a green fluorescent protein (pMaxGFP), as a control of the transfection procedure and to estimate the transfection efficiency. For every cell line, a 48-hour incubation time yielded higher transfection efficiencies. HEK293T provided the highest efficiencies at both 24- and 48-hour incubations, with transfection efficiencies of 55~60 % and 85~90 %, respectively (Figure 27). MDA-MB-231 displayed slightly lower efficiencies compared to HEK293T, with 50~55 % at 24 hours, and 70~75 % at 48-hour incubation (Figure 28). The MDA-MB-436 cells proved difficult to transfect in this assay, yielding low transfection efficiencies (< 5 % at 24 hours and < 10 % at 48 hours, Figure 29). However, transfection for 48 hours yielded a higher efficiency than the 24-hour experiments, with a 25~30 % increase in HEK293T and MDA-MB-231 cells and 5 % increase in MDA-MB-436.

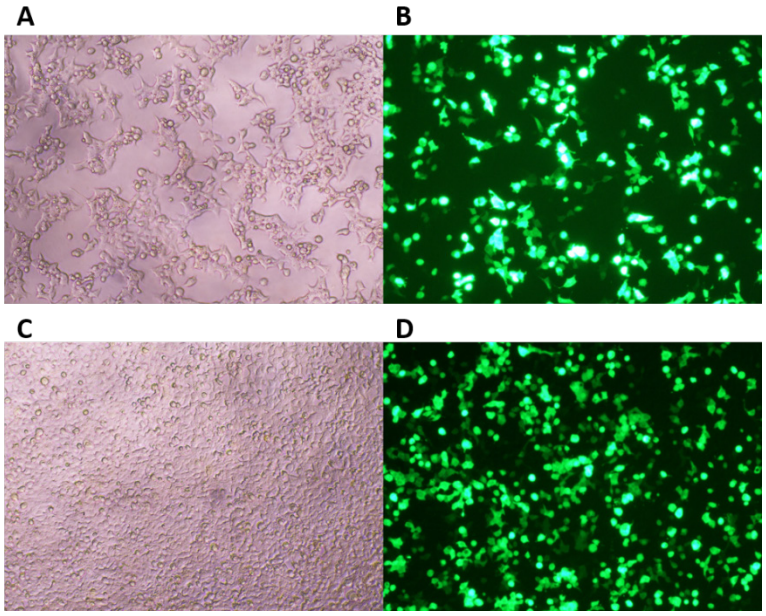

Figure 27. A) 24-hour incubation of TA-assay transfected HEK293T displayed in white light, magnified 100x. **B)** 24-hour incubation of TA-assay transfected HEK293T displayed in ultra violet (UV) light, magnified 100x. Glowing cells were cells successfully transfected with pMaxGFP, yielding a transfection efficiency of 55~60 %. **C)** 48-hour incubation of TA-assay transfected HEK293T displayed in white light, magnified 100x. **D)** 48-hour incubation of TA-assay transfected HEK293T displayed in ultra violet (UV) light, magnified 100x. Glowing cells were cells successfully transfected with pMaxGFP, yielding a transfection efficiency of 85~90 %.

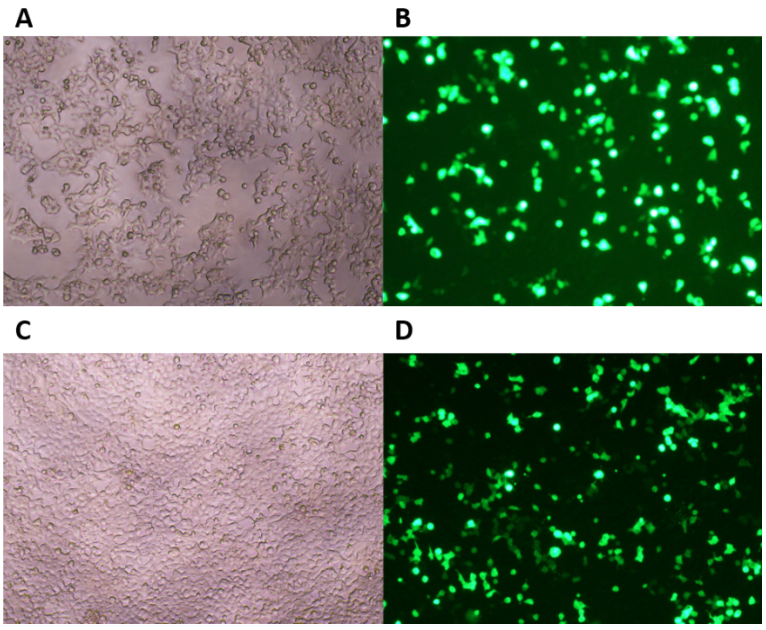

Figure 28. A) 24-hour incubation of TA-assay transfected MDA-MB-231 displayed in white light, magnified 100x. **B)** 24-hour incubation of TA-assay transfected MDA-MB-231 displayed in ultra violet (UV) light, magnified 100x. Glowing cells were cells successfully transfected with pMaxGFP, yielding a transfection efficiency of 50-55 %. **C)** 48-hour incubation of TA-assay transfected MDA-MB-231 displayed in white light, magnified 100x. **D)** 48-hour incubation of TA-assay transfected MDA-MB-231 displayed in ultra violet (UV) light, magnified 100x. Glowing cells were cells successfully transfected with pMaxGFP, yielding a transfection efficiency of 70~75 %.

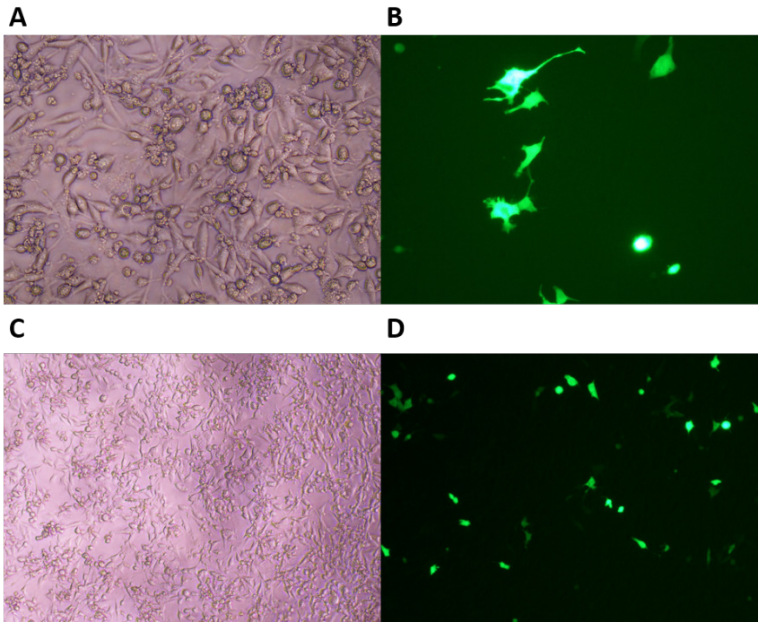

Figure 29. A) 24-hour incubation of TA-assay transfected MDA-MB-436 displayed in white light, magnified 400x. **B)** 24-hour incubation of TA-assay transfected MDA-MB-436 displayed in ultra violet (UV) light, magnified 400x. Glowing cells were cells successfully transfected with pMaxGFP, yielding a transfection efficiency of < 5 %. **C)** 48-hour incubation of TA-assay transfected MDA-MB-436 displayed in white light, magnified 200x. **D)** 48-hour incubation of TA-assay transfected MDA-MB-436 displayed in ultra violet (UV) light, magnified 200x. Glowing cells were cells successfully transfected with pMaxGFP, yielding a transfection efficiency of < 10 %.

4.4 Verification of the TA-assay

4.4.1 Expression of the GAL4 DBD:BRCA1 fusion protein

To confirm that lack of transactivation activity was a result of the variant in question, and not inability to express the variant fusion protein, western blot was performed on lysates from transfected HEK293T and MDA-MB-231 cells. In addition, cells transfected with reporter plasmids only and non-transfected cells were used as controls.

The predicted size of the GAL4 DBD:BRCA1 fusion protein was 69,9 kDa, and a faint band can be observed for some of the samples at this size in the HEK293T samples. However, the intense band above the 75 kDa ladder marker had been confirmed to be specific for the fusion protein as well (personal communication, Jarhelle, E., 2017, Appendix, Section D, page xv). This was illustrated using transfection experiments with the empty vector plasmid pcDNA3 as well as pcDNA3 GAL4 DBD:BRCA1, confirming that the band at ~80 kDa was specific for the GAL4 DBD:BRCA1 insert.

Western blot was performed on RIPA lysates from cell lines HEK293T, to verify the presence of fusion protein GAL4 DBD:BRCA1 (Figure 30A). Bands specific for the GAL4 DBD:BRCA1 fusion protein were detected for all variants. Variants lacking TA-activity (p.Asp1692Ala, p.Gly1706Arg and p.Gly1770Val) displayed weaker bands compared to wild type. Variant p.Ser1655Phe with TA-activity of 3.5 % display band intensity comparable to wild type and variants with high TA-activity, and was stronger than the band observed for p.Met1783Thr with 32 % TA-activity. Loading control β-actin was comparable for all samples, with the exception of p.Ser1655Phe, where the loading control was visibly weaker, likely resulting in an underestimated intensity of the p.Ser1655Phe band. No bands were detected in non-transfected cells, or cells transfected with only reporter plasmids except for loading control.

Western blot analysis on MDA-MB-231 RIPA lysates (Figure 30B) also verified bands specific for fusion protein GAL4 DBD:BRCA1 in all variants tested, with the exception of non-transfected cells and cells transfected with only reporter plasmids. Samples lacking TA-activity that presented weak bands using HEK293T TA-cell lysates (p.Asp1692Ala, p.Val1838Gly, p.Gly1770Val) displayed band intensities comparable to wild type in MDA-MB-231. While variant p.Pro.1776Ser (TA-activity > 100 % in both cell lines) displayed weaker band intensity in MDA-MB-231 lysates than wild type.

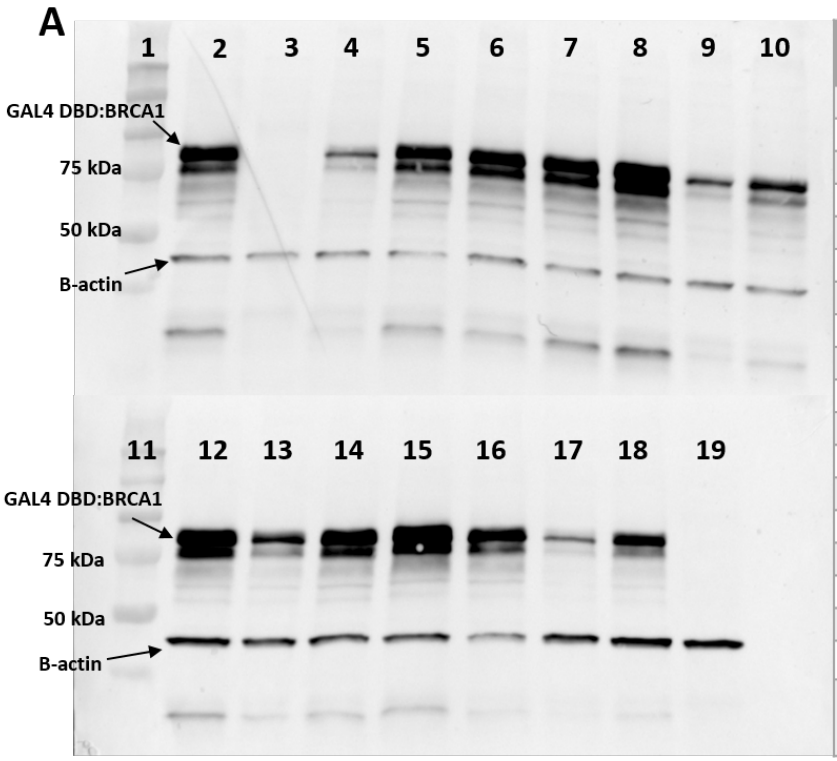

Well	Variant	TA-activity
1	Ladder	-
2	Wild type	100 %
3	Reporter	0.5 %
4	p.Asp1692Ala	0.8 %
5	p.Met1652Ile	74.5 %
6	p.Arg1751Gln	52.4%
7	p.Val1804Asp	77.3 %
8	p.Thr1700Thr	101.6 %
9	p.Gly1706Arg	0.5 %
10	p.Lys1711Gln	41.6 %
11	Ladder	-
12	p.Pro1776Ser	115,4 %
13	p.Met1783Thr	31,9 %
14	p.Gln1826Leu	136,4 %
15	p.Arg1835Gln	109,8 %
16	p.Ser1655Phe	3,5 %
17	p.Gly1770Val	0,5 %
18	p.Arg1699Trp	11,7 %
19	Non-transfected 293T	-

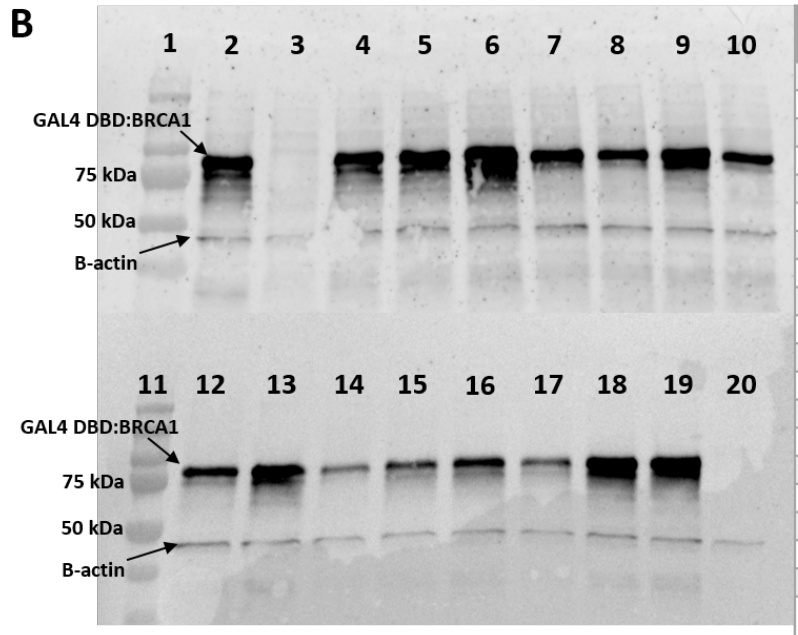

Well	Variant	TA-activity
1	Ladder	-
2	Wild type	100 %
3	Reporter	0,5 %
4	p.Met1652Ile	87,5 %
5	p.Arg1751Gln	44,1 %
6	p.Val1804Asp	103,0 %
7	p.Asp1692Ala	0,9 %
8	p.Val1838Gly	0,5 %
9	p.Ser1655Phe	4,5 %
10	p.Gly1770Val	0,7 %
11	Ladder	-
12	p.Arg1699Trp	14,4 %
13	p.Thr1700Thr	119,7 %
14	p.Gly1706Arg	0,5 %
15	p.Lys1711Gln	36,8 %
16	p.Pro1776Ser	133,7 %
17	p.Met1783Thr	27,2 %
18	p.Gln1826Leu	155,1 %
19	p.Arg1835Gln	122,0 %
20	Non transfected MDA-MB-231	-

Figure 30. Western blot illustrating the presence of GAL4 DBD:BRCA1 fusion protein in transfected cell lines **A)** HEK293T and **B)** MDA-MB-231 protein lysates from TA-assay. Band specific for GAL4 DBD:BRCA1(~80 kDa) and loading control β-actin (42 kDa) are indicated by black arrows. Ladder sizes 50 and 75 kDa are indicated. Tables (right) display well number for each variant/sample and corresponding TA-activity. Blots represent one representative gel for each transfected cell line.

4.4.2 Expression of GAL4 DBD:BRCA1 mRNA in TA-assay transfected cells

To complement the western blots performed on TA-assay cell lysates, qPCR were used to evaluate expression of variant plasmid pcDNA3 GAL4 DBD:BRCA1 in HEK293T and MDA-MB-231, using RNA obtained from TA-assay cell lysates. Expression was calculated utilising the comparative ΔCt method, with GAPDH as reference gene. Amplification of pcDNA3 GAL4 DBD:BRCA1 using SYBR green and *BRCA1* specific primers also targets expression of endogenous *BRCA1*. Non-transfected cells were therefore used as treatment reference to account for this.

Expression of pcDNA3 GAL4 DBD:BRCA1 plasmid in HEK293T cells is illustrated in Figure 31A. Relative expression (RQ) in cells transfected with reporter plasmids pGAL4-e1b-Luc and phRG-TK only, display RQ of *BRCA1* specific transcripts at the same rate as non-transfected cells. Thereby, indicating that transfection does not induce endogenous *BRCA1* expression, and that the non-transfected cells were a satisfactory treatment reference. Variants p.Asp1692Ala, p.Gly1706Arg and p.Gly1770Val all present with complete loss of TA-activity as well as reduced RQ, compared to wild type. Whereas variants p.Arg1751Gln and p.Met1652Ile both displayed RQ levels above that of the wild type, despite having lower TA-activity (52 % and 74 %, respectively).

Expression of variant plasmid pcDNA3 GAL4 DBD:BRCA1 in MDA-MB-231 cells (Figure 31B) revealed RQ levels lower than observed in the HEK293T cells. Similar to its behaviour in HEK293T cells, variant p.Asp1692Ala displayed reduced RQ levels in MDA-MB-231 cells compared to wild type. TA-lacking variants p.Gly1706Arg and p.Gly1770Val presented elevated RQ levels compared to wild type. Variant p.Arg1751Gln with TA-activity of 44 % had an observed RQ level above that of wild type, whereas p.Met1652Ile (87 % TA-activity) showed RQ similar to wild type.

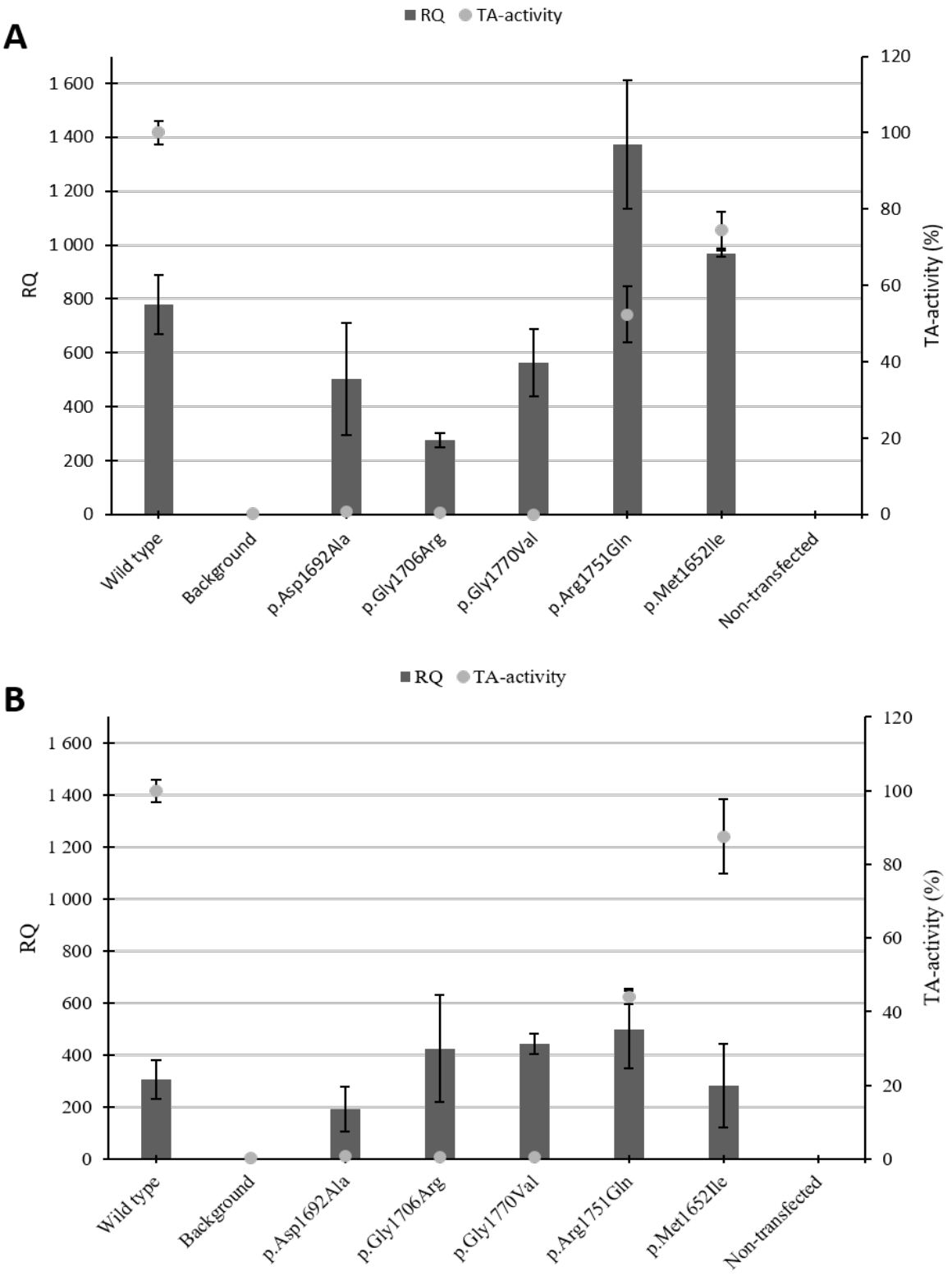

Figure 31. Mean relative expression (RQ) of variant GAL4 DBD:BRCA1 fusion protein in transfected cell lines **A)** HEK293T and **B)** MDA-MB-231 (dark grey bars) with corresponding TA-activities (light grey dots). RQ is displayed as mean relative to expression of endogenous *BRCA1* in non-transfected HEK293T cells. Error bars represent standard deviation ($n_{RQ} = 6$, $n_{TA} \leq 18$). The graph illustrates the independence between RQ and TA-activity, and is based on three qPCR experiments and three-four TA-assay experiments.

4.5 *In silico* assessment of *BRCA1* variants

All variants included in this study were analysed *in silico* using Alamut (described in methods 3.1.1). Table 12 display entries in databases dbSNP, ClinVar, and HGMD as well as allele frequencies reported by ExAC, 1000 Genomes and ESP. Table 13 lists predictions on the variants effect based on reports from SIFT, AlignGVGD and Mutation taster. Allele frequencies are a useful tool in assessing the possible deleterious nature of a variant. The MPAF for *BRCA1* is estimated at 0.1 %, and variant allele frequencies above the MPAF (> 0.1 %) was evidence towards benignity. Common for the VUSs included in this study was the low number of observed alleles in all databases, with only p.Val1804Asp (n = 7) and p.Met1783Thr (n = 21) having n ≥ 7 observed alleles.

Evaluation using predictive software SIFT, AlignGVGD and Mutation taster display some disagreement on class 1-2 and class 4-5 variants. Class 1 variant p.Met1652Ile and class 2 variant p.Val1804Asp, were predicted to be benign by all three software, whereas class 1 variant p.Arg1751Gln was predicted benign by AlignGVGD, but deleterious by SIFT and Mutation taster. Variants p.Ser1655Phe (class 4) and p.Arg1699Trp (class 5) were predicted deleterious by all software. AlignGVGD score p.Ser1655Phe as C25, indicating lower pathogenic impact, and p.Arg1699Trp as C65, suggesting a higher deleterious impact. The class 4 variant p.Gly1770Val was predicted deleterious by SIFT and Mutation taster, but received a C0 score by AlignGVGD, indicating benignity. The discrepancy between the prediction software on these well-characterised variants, illustrated that *in silico* assessment of variants should be used with caution, and as supporting evidence only if they agree. Evaluation of class 3 variants using SIFT, AlignGVGD and Mutation taster generally agree, however, AlignGVGD allow for a more nuanced assessment of variant impact. Variants p.Asp1692Ala, p.Arg1699Gln p.Ala1708Val, p.Gly1709Arg, p.Val1838Gly, p.Gly1706Arg and p.Met1783Thr were predicted to have a deleterious nature by all programs, but with varying AlignGVGD scores. Variants p.Pro1776Ser and p.Glu1826Leu were predicted as benign by all programs. p.Lys1711Gln and p.Arg1835Gln were predicted as benign by SIFT and AlignGVGD, but as disease causing by Mutation taster. Variant p.Thr1700Thr were not eligible for analysis using these software as the variant is synonymous, any deleterious effect must therefore stem from either abnormal splicing or altered expression.

Table 12. Variant entries in databases dbSNP, ClinVar, HGMD and BIC, as well as allele frequencies reported by ExAC, 1000 Genomes and ESP (ALL: All, AFR: African/African American, NFE: Non-Finnish European, AMR: Latino, EAS: East Asian, SAS: South Asian, OTH: Other.)

HGVS variant	HGVS protein	Exon	Type	dbSNP	ClinVar	ExAC	1000 Genomes	ESP	HGMD
c.4956G>A	p.Met1652Ile	16	Missense	rs1799967	-	T = 1.8 %	T = 1.1 %	EA: T = 1.5 % AA: T = 0.2 %	
c.5252G>A	p.Arg1751Gln	20	Missense	rs80357442	RCV000048883.3 RCV000148392.1 RCV000168520.1 RCV000162992.1 RCV000112579.2	NFE: T = 0.0045 %		EA: T = 0.01 %	
c.5411T>A	p.Val1804Asp	23	Missense	rs80356920	RCV000112647.4 RCV000120302.1 RCV000048982.4 RCV000148405.1 RCV000162993.1 RCV000167770.4	ALL: A = 0.0058 % AMR: A = 0.017 % NFE: A = 0.0075 %	T = 0.1 %	-	CM044859
c.4964C>T	p.Ser1655Phe	16	Missense	rs80357390	RCV000223580.1 RCV000112436.1 RCV000048712.2	-	-	-	-
c.5309G>T	p.Gly1770Val	21	Missense	-		-	-	-	-
c.5095C>T	p.Arg1699Trp	18	Missense	rs55770810	RCV000048789.3 RCV000159999.1 RCV000077595.4 RCV000131821.2 RCV000148391.1 RCV000148390.1	ALL: T = 0.0025 % NFE: T = 0.0015 % EAS: T = 0.012 % OTH: T = 0.11 %	-	EA: T = 0.01 %	-
c.5075A>C	p.Asp1692Ala	18	Missense	-	RCV000241473.1	-	-	-	
c.5096G>A	p.Arg1699Gln	18	Missense	rs41293459	RCV000031217.11 RCV000048790.5 RCV000195350.3 RCV000131564.2	ALL: A = 0.0025 % NFE: A = 0.0045 %			CM034007

Table 12 continued. Variant entries in databases dbSNP, ClinVar, HGMD and BIC, as well as allele frequencies reported by ExAC, 1000 Genomes and ESP (ALL: All, AFR: African/African American, NFE: Non-Finnish European, AMR: Latino, EAS: East Asian, SAS: South Asian, OTH: Other.)

HGVS variant	HGVS protein	Exon	Type	dbSNP	ClinVar	ExAC	1000 Genomes	ESP	HGMD
c.5123C>T	p.Ala1708Val	18	Missense	rs28897696	RCV000048803.2 RCV000031221.3 RCV000131166.1	-	-	EA: A = 0.01 % AA: A = 0.05 %	
c.5125G>A	p.Gly1709Arg	18	Missense	-	-	-			-
c.5513T>G	p.Val1838Gly	24	Missense	-	RCV000241502.1	-	-	-	CM169297
c.5100A>G	p.Thr1700Thr	18	Synonymous	rs45519437	RCV000163399.1 RCV000199783.1	ALL: G = 0.0025 % AMR: G = 0.0087 % SAS: G = 0.0061 % NFE: G = 0.0015 %	EA: G = 0.01 %	EA: G = 0.01 %	-
c.5116G>A	p.Gly1706Arg	18	Missense	-	-	-	-	-	-
c.5131A>C	p.Lys1711Gln	18	Missense	-	-	-	-	-	-
c.5326C>T	p.Pro1776Ser	21	Missense	rs1800757	-	-	-	EA: T = 0.01 %	-
c.5348T>C	p.Met1783Thr	22	Missense	rs55808233	RCV000167822.2 RCV000048954.4 RCV000031240.6 RCV000129758.2	ALL: C = 0.017 % AFR: C = 0.19 % AMR: C = 0.0087 %	AFR: 0.1 %	AA: G = 0.18 %	CM041721
c.5477A>T	p.Glu1826Leu	24	Missense	-	-	-	-	-	-
c.5504G>A	p.Arg1835Gln	24	Missense	rs273902776	-	-	-	-	-

Table 13. Variant predictions by SIFT, AlignGVGD and Mutation taster, as well as predicted splicing effects.

Class	HGVS variant	HGVS protein	Exon	Type	SIFT	Align GVGD	Mutation taster	Splice effect
1	**c.4956G>A**	p.Met1652Ile	16	Missense	Tolerated	C0	Polymorphism	none
1	**c.5252G>A**	p.Arg1751Gln	20	Missense	Deleterious	C0	Disease causing (p = 0.999)	none
2	**c.5411T>A**	p.Val1804Asp	23	Missense	Tolerated	C0	Polymorphism (p = 1)	none
4	**c.4964C>T**	p.Ser1655Phe	16	Missense	Deleterious	C25	Disease causing (p = 1)	none
4	**c.5309G>T**	p.Gly1770Val	21	Missense	Deleterious	C0	Disease causing (p = 1)	none
5	**c.5095C>T**	p.Arg1699Trp	18	Missense	Deleterious	C65	Disease causing (p = 1)	none
3	**c.5075A>C**	p.Asp1692Ala	18	Missense	Deleterious	C65	Disease causing (p = 1)	none
3	**c.5096G>A**	p.Arg1699Gln	18	Missense	Deleterious	C35	Disease causing (p = 1)	none
3	**c.5123C>T**	p.Ala1708Val	18	Missense	Deleterious	C65	Disease causing (p = 1)	none
3	**c.5125G>A**	p.Gly1709Arg	18	Missense	Deleterious	C15	Disease causing (p = 1)	none
3	**c.5513T>G**	p.Val1838Gly	24	Missense	Deleterious	C35	Disease causing (p = 1)	none
3	**c.5100A>G**	p.Thr1700Thr	18	Synonymous	-	-	-	none
3	**c.5116G>A**	p.Gly1706Arg	18	Missense	Deleterious	C65	Disease causing (p = 1)	none
3	**c.5131A>C**	p.Lys1711Gln	18	Missense	Tolerated	C0	Disease causing (p = 0.974)	none
3	**c.5326C>T**	p.Pro1776Ser	21	Missense	Tolerated	C0	Polymorphism (p = 0.741)	none
3	**c.5348T>C**	p.Met1783Thr	22	Missense	Deleterious	C45	Disease causing (p = 0.999)	none
3	**c.5477A>T**	p.Glu1826Leu	24	Missense	Tolerated	C0	Polymorphism (p = 0.763)	none
3	**c.5504G>A**	p.Arg1835Gln	24	Missense	Tolerated	C0	Disease causing (p = 0.965)	none

4.6 Characterisation of cell lines

Cell lines HEK293T, MDA-MB-231, MDA-MB-436, SUM102 and MCF-7 was Sanger sequenced to determine the variant status of endogenous *BRCA1* and *TP53*. As well as investigated for expression of endogenous *BRCA1* using qPCR. In addition, the four breast cancer cell lines MDA-MB-231, MDA-MB-436, SUM102 and MCF-7 were studied for response to the cytostatic drugs doxorubicin and carboplatin in relation to *BRCA1* and *TP53* status.

4.6.1 Variant status of endogenous *BRCA1* and *TP53* in cell lines

Sanger sequencing of endogenous *BRCA1* in HEK293T, MDA-MB-231, MDA-MB-436 and SUM102 detected seven homozygous variants; c.2082C>T, c.2311T>C, c.2612C>T, c.3113A>G, c.3548A>G, c.4308T>C and 4837A>G, in all cell lines (Table 14). All seven variants were previously known and classified as benign (class 1). In addition, MDA-MB-436 was homozygous for c.5277+1G>A, a pathogenic class 5 variant that results in aberrant splicing and retention of intron sequence upstream of exon 20, an early stop codon and a non-functional protein (Table 14). Screening of BRCA1 in the MCF-7 cell line detected no variants. All sequenced cell lines, apart from MDA-MB-436 cells, were considered to possess wild type *BRCA1*. Sequencing of endogenous TP53 in HEK293T and MDA-MB-231 were positive for c.840A>T, a pathogenic variant, and MDA-MB-436 and SUM102 were positive for c.215C>G, a benign class 1 variant (Table 14). In addition, MDA-MB-436 was homozygous for the novel variant c.604_610dupCGTGTGG that introduce an early stop codon (Table 14). MCF-7 contained no variants in the *TP53* gene.

Table 14. Variants found in cell lines HEK293T, MDA-MB-231, MDA-MB-436 and SUM102 during sequencing of endogenous *BRCA1* and *TP53*. Nomenclature follows HGVS standards, c.1 corresponds to first nucleotide of ATG. *Novel variant discovered during this work, classification was unknown.

Cell line	Gene	HGVS variant	HGVS protein	Classification
HEK293T MDA-MB-231 MDA-MB-436 SUM102	*BRCA1*	c.2082C>T	p.Ser694Ser	1 – Benign
	BRCA1	c.2311T>C	p.Leu771Leu	1 – Benign
	BRCA1	c.2612C>T	p.Pro871Leu	1 – Benign
	BRCA1	c.3113A>G	p.Glu1038Gly	1 – Benign
	BRCA1	c.3548A>G	p.Lys1183Arg	1 – Benign
	BRCA1	c.4308T>C	p.Ser1436Ser	1 – Benign
	BRCA1	c.4837A>G	p.Ser1613Gly	1 – Benign
MDA-MB-436	*BRCA1*	c.5277+1G>A	- splice donor variant	5 – Pathogenic
	TP53	c.604_610dupCGTGTGG	-	Unclassified*
	TP53	c.215C>G	p.Pro72Arg	1 – Benign
MDA-MB-231	*TP53*	c.840A>T	p.Arg280Ser	5 – Pathogenic
HEK293T	*TP53*	c.840A>T	p.Arg280Ser	5 – Pathogenic
SUM102	*TP53*	c.215C>G	p.Pro72Arg	1 – Benign

4.6.2 Endogenous *BRCA1* mRNA expression in cell lines

Verification of qPCR efficiency and specificity

In order to use the comparative ΔCt method to quantify relative gene expression, the difference between the slopes of target- and reference-gene standard curves must be ≤ 0.1. In addition, both PCR efficiencies should be in the range 90-105 %. Figure 32A and B display the amplification plot for a five-fold *GAPDH* and *BRCA1* cDNA series used in construction of the standard curves. The slope value for *BRCA1* was -3.388, and for *GAPDH* -3.478, resulting in a Δ_{Slope} of 0.09 Figure 32C and D. Placing it below the required value ($\Delta_{Slope} < 0.1$). PCR efficiencies were estimated at 97.3 % and 93.9 % for *BRCA1* and *GAPDH*, respectively.

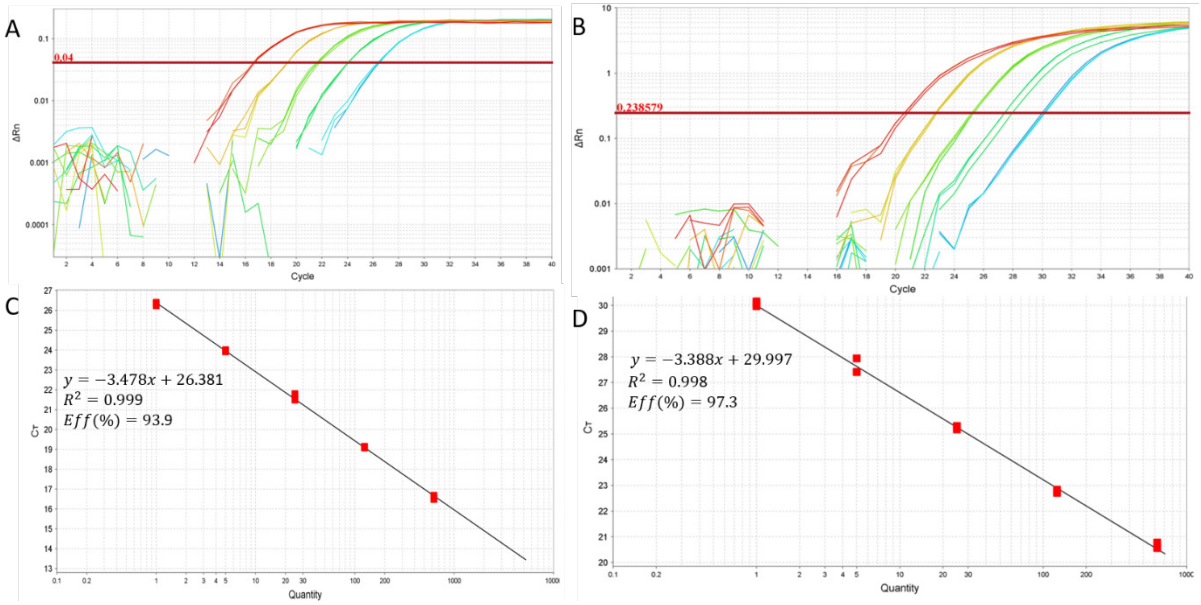

Figure 32. A) Amplification plot of a five-fold cDNA series used in calculation of the *GAPDH* qPCR efficiency. The red line indicates threshold value of 0.04. **B)** Amplification plot of a five-fold cDNA series used in calculation of the *BRCA1* qPCR efficiency. The red line indicates threshold value of 0.24. **C)** Standard curve for *GAPDH* displaying trendline equation, R^2-value and qPCR efficiency (Eff). **D)** Standard curve for *BRCA1* displaying trendline equation, R^2-value and qPCR efficiency (Eff). For all relative concentrations n = 3.

Because SYBR green bound all dsDNA, it was necessary to verify the specificity of the *BRCA1* primers by performing a melting curve analysis. Since DNA denatures at different temperatures depending on sequence, a specific PCR will yield a single peak, while unspecific assays display multiple. Figure 33 display the melting curve for the *BRCA1* qPCR on all cell lines investigated for endogenous *BRCA1* expression, and the single peak illustrate the specific amplification of the *BRCA1* gene.

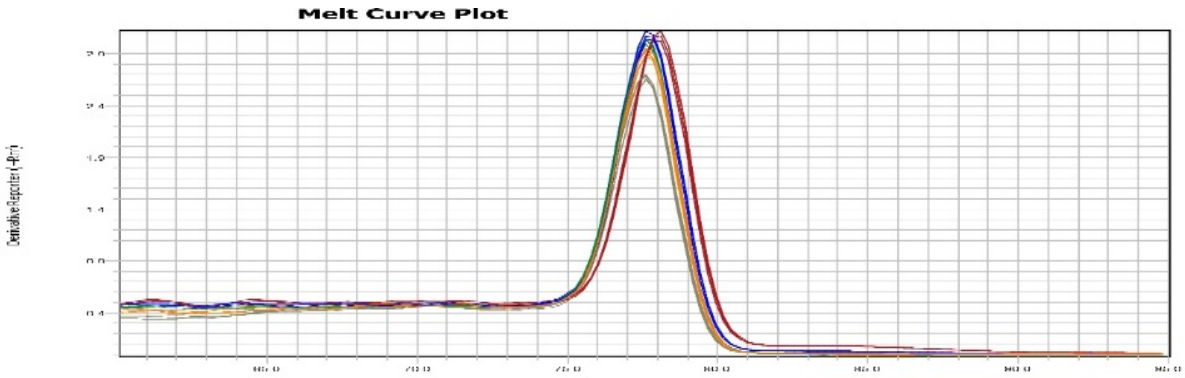

Figure 33. Melting curve used in assessment of *BRCA1* qPCR specificity. The plot display a single peak for cell lines HEK293T, MDA-MB-231, MDA-MB-436, MCF-7 and Sum102, consistent with a specific PCR reaction.

Endogenous *BRCA1* expression in cell lines

Relative expression of endogenous *BRCA1* in breast cancer cell lines HEK293T, MCF-7, SUM102, MDA-MB-436 and MDA-MB-231 were analysed using qPCR. The mean Ct values for *GAPDH* are illustrated in Figure 34, and display an even expression between the cell lines. For the fictive control sample, the mean expression of *GAPDH* in all cell lines were used.

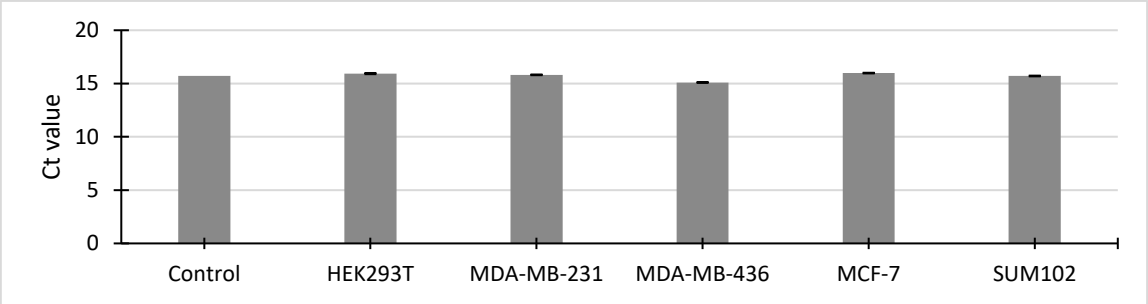

Figure 34. Ct values for reference gene *GAPDH* in cell lines HEK293T, MDA-MB-231, MDA-MB-436, MCF-7, SUM102 and control defined as *BRCA1* null, from one experiment (n=3). Threshold was set to and 0.04.

The relative expression of *BRCA1* in the cell lines investigated, are displayed in Figure 35. The expression of *BRCA1* was highest in the cell lines MDA-MB-231 and MCF-7, both having wild type *BRCA1*. SUM102 presented lower *BRCA1* expression than the other wild type cell lines, while MDA-MB-436 displayed the lowest relative *BRCA1* expression, and was the only cell line to have a deleterious *BRCA1* variant.

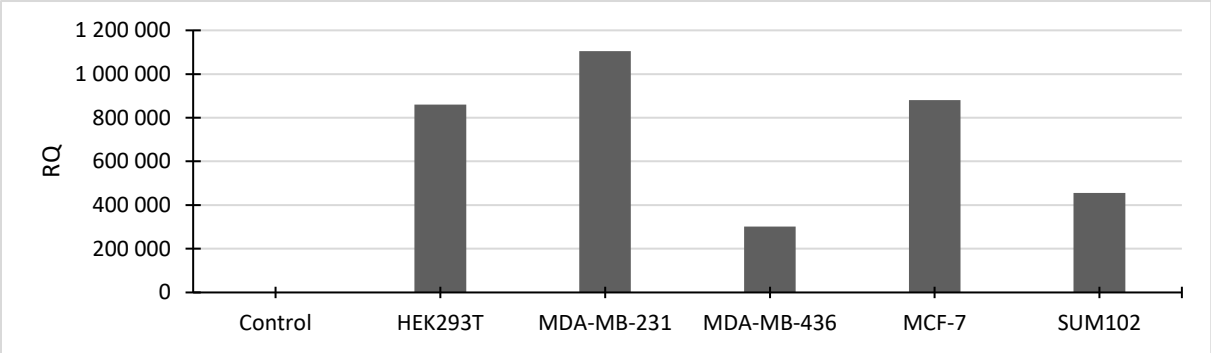

Figure 35. Relative expression (RQ) of *BRCA1*, for one experiment measured using qPCR. Expression is shown relative the reference gene *GAPDH*, a control sample without *BRCA1* expression (set to Ct = 40) that was used as treatment sample.

4.6.3 Response to cytostatic treatment in breast cancer cell lines

A selection of four breast cancer cell lines were tested for response to the cytostatic drugs Doxorubicin and Carboplatin, in relation to their *BRCA1* and *TP53* status.

Effect of Doxorubicin on breast cancer cell viability

The breast cancer cell-lines MDA-MB-231, MDA-MB-436, SUM102 and MCF-7 were treated with increasing doses of Doxorubicin (0-10 μM). Figure 36 display cell viability after 24-hours of treatment. MDA-MB-436 display a high level of resistance to the DNA intercalating effects of Doxorubicin, with little to no effect of the drug on cell viability. MCF-7, like MDA-MB-436, also possess a strong resistance to the effects of the drug. MCF-7 demonstrated an increased viability at all concentrations of Doxorubicin tested, compared to the untreated cells. MDA-MB-231 showed a slightly higher sensitivity to Doxorubicin compared to the afore-mentioned cell-lines, displaying a slight reduction in cell viability at all concentrations. SUM102 presented high sensitivity to the drug, with cell-viability reduced by 80 % at exposure to the lowest level of Doxorubicin tested (0.5 μM), reaching IC_{50} at ~0.3 μM.

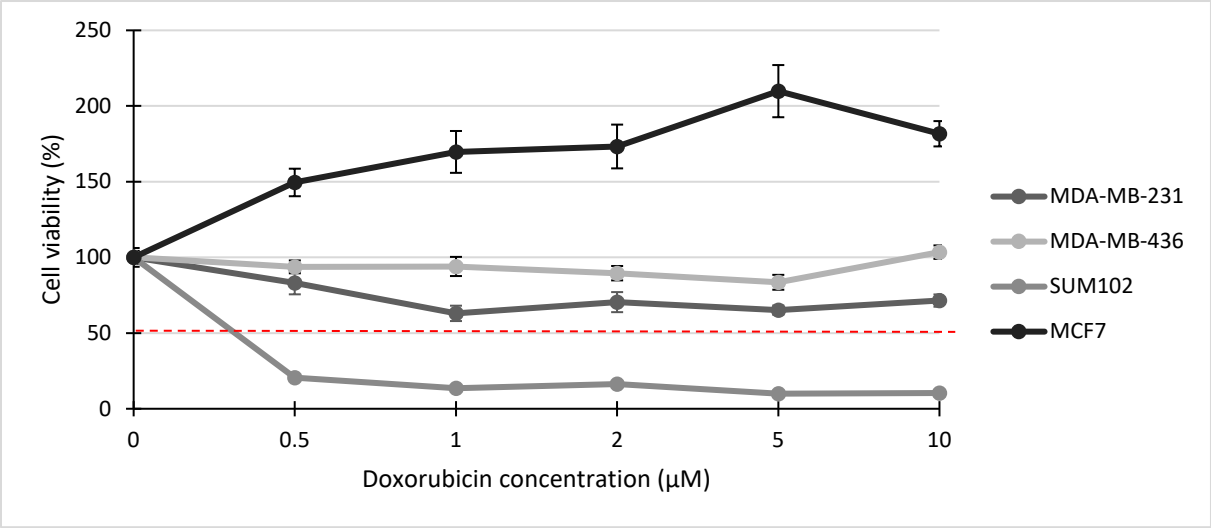

Figure 36. Cell viability measured by Wst-1 at 450 nm, after 24-hours exposure to increasing doses of the cytostatic Doxorubicin. Medians are plotted as percentage ratios of untreated (0 µM) cells for three experiments. The red line indicates IC_{50} and error bars display standard error mean (SEM) (n = 15).

Effect of Carboplatin on breast cancer cell viability

To study the effects of a DNA cross-linking agent on cell viability regarding *BRCA1* and *TP53* status, breast cancer cell lines MDA-MB-231, MDA-MB-436, SUM102 and MCF-7 were treated for 24, 72 and 120 hours with increasing doses of Carboplatin (0-400 µM).

All cell lines displayed a high tolerance to the effects of Carboplatin after 24-hour exposure, never reaching IC_{50}, with the MDA-MB-231 cells being the only cell line to display a slight reduction in cell viability at all concentrations above 20 µM (Figure 37A). The MCF-7, MDA-MB-436 and SUM102 cell lines presented with elevated cell viabilities at concentrations 20-200 µM, with all showing a return to ~100 % viability at 400 µM after 24 hours (Figure 37A). Exposure to Carboplatin for 72 hours resulted in reduced cell viability for the SUM102 and MDA-MB-231 cell lines at concentrations > 20 µM, with the MDA-MB-436 cells displaying a reduction in cell viability at Carboplatin concentrations > 50 µM (Figure 37B). SUM102 reached IC_{50} at ~45 µM, and MDA-MB-231 reached IC_{50} at ~190 µM. The MCF-7 cell line presented a high resilience to the effects of Carboplatin at 72-hour treatments, only displaying a loss in cell viability at 400 µM, but never reaching the IC_{50} limit (Figure 37B). Increasing exposure time to 120 hours resulted in a loss of cell viability for cell lines MCF-7 and MDA-MB436 at concentrations above 20 µM (Figure 37C). Whereas MDA-MB-231 cells revealed no response to Carboplatin concentrations below 50 µM. The SUM102 cell line displayed a dramatic loss in cell viability at 50 µM Carboplatin concentration and above, and the increased viability of SUM102 at 20 µM was deemed an error in the experiment setup. All cell lines

presented severely decreased cell viability to all concentrations above 100 µM, with SUM102 and MCF-7 cells reaching IC_{50} at 45~50 µM, MDA-MB-231 cells reaching IC_{50} at ~80 µM and MDA-MB-436 reaching IC_{50} at 130 µM (Figure 37C).

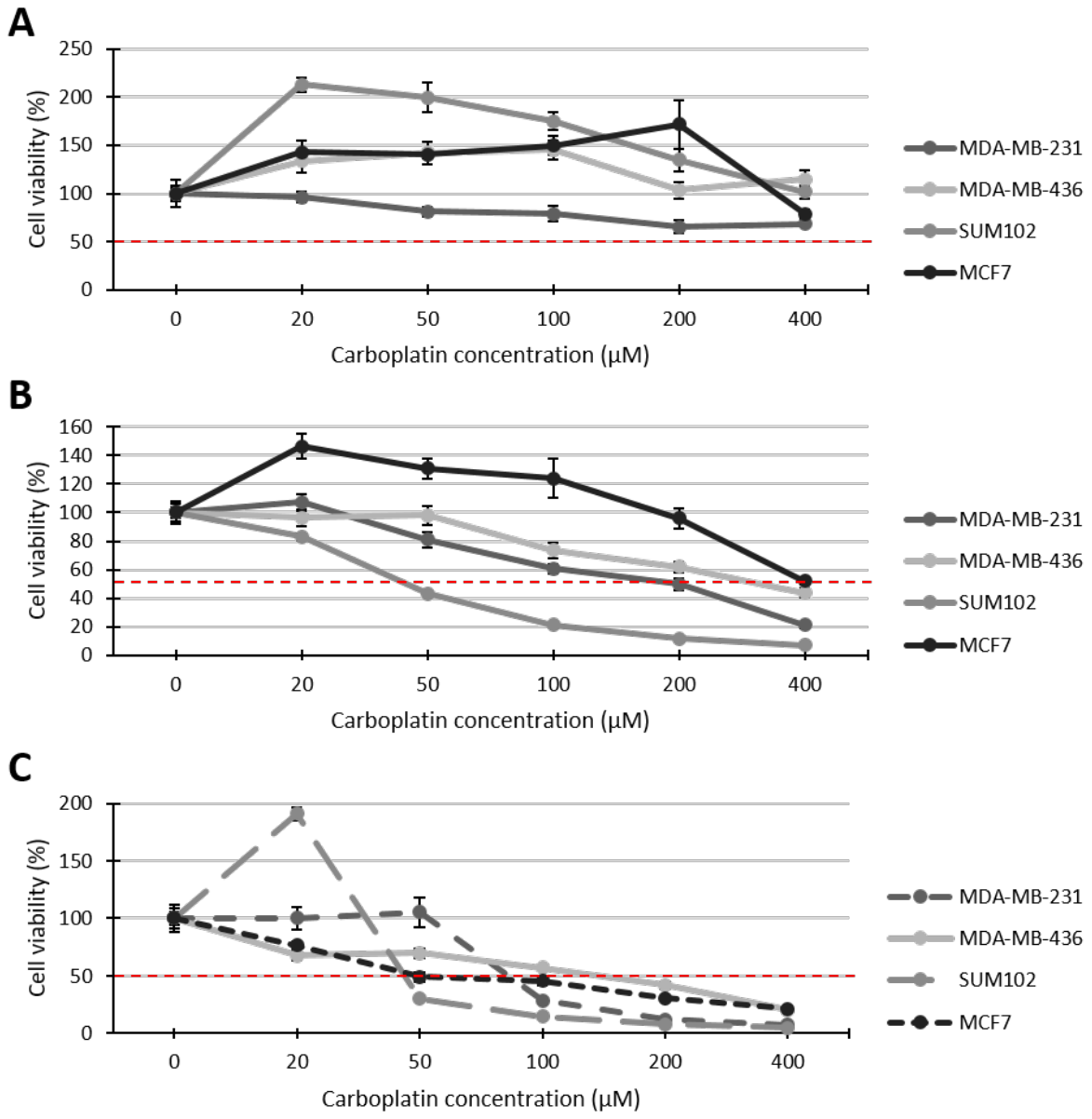

Figure 37. Compared viability of MDA-MB-231, MDA-MB-436, SUM102 and MCF-7 cell lines to increasing doses of the cytostatic Carboplatin (0-400 µM), measured by Wst-1 at 450 nm at different exposure times. **A)** 24-hour exposure time. **B)** 72-hour exposure time. **C)** 120-hour exposure time. Medians are plotted as percentage ratios of untreated (0 µM) cells. The red line indicates IC_{50} and error bars display standard error mean (SEM) (n = 5).

5 Discussion

5.1 BRCA1 variants of unknown significance

Pathogenic variants in *BRCA1* are known to cause HBOC, and 98 % of the deleterious variants located in *BRCA1* are frameshift and/or truncations (Maxwell *et al.* 2016). Missense variants pose a great challenge to clinicians, because they are infrequent, and their impact on protein functionality largely remain unknown. It was therefore necessary to establish an assay that aimed to provide insight into the effect of these variants. The TA-assay measured the TA-activity of the missense variants in the BRCT domain relative to the wild type, and provided an efficient way of assessing the integrity of the BRCT domain that correlated well with the effects of known benign and deleterious variants.

5.1.1 Establishing TA-assay thresholds for determination of *BRCA1* variant risk

In order to use the TA-assay for dividing variants into high- or low-risk categories it was useful to define thresholds of what TA-activities constitute a high or low risk variant. A study suggested a TA-activity threshold of ≤ 45 % for categorising a variant as "high risk", and that any variant displaying TA-activity ≥ 50 % ought to be regarded as "low risk" (Carvalho *et al*. 2007b). Variants displaying TA-activities that fall between these categories could be regarded as intermediate risk. However, the small intermediate interval suggested that the deleterious effect of *BRCA1* variants in the BRCT domain on the TA-assay was of a discrete nature, and that there existed only two classes, high- and low-risk, with no true intermediate class (Carvalho *et al*. 2007b). As the upper boundary for what was considered high risk on the TA-assay the variant (p.Arg1699Trp) that displayed the highest recorded TA-activity (45 %) of a known pathogenic variant in their assay, was chosen (Carvalho *et al*. 2007b). Similarly, they chose the benign variant that displayed the lowest TA-activity (50 %) as the threshold for the low risk group. While the boundaries set likely remain true for the Carvalho *et al.* version of the TA-assay, it is not apparent that this is a universal threshold that can be readily applied to all versions of the assay. Variant p.Arg1699Trp (class 5) was therefore also used as a pathogenic control in our version of the TA-assay, and presented TA-activities of 12 ± 1 % and 14 ± 3 % in HEK293T and MDA-MB-231 cells, respectively. This is a significant reduction in TA-activity compared to the 45 % reported by Carvalho *et al.*, and was likely explained by the increased sensitivity of the assay developed in this thesis, and the differing transfection procedures. The class 4 variants (p.Ser1655Phe and p.Gly1770Val) also included as pathogenic controls in this study displayed TA-activities below p.Arg1699Trp. The benign class 1 and 2

controls (p.Met1652Ile, p.Arg1751Gln and p.Val1804Asp) were used to define the wild type range, with the lowest observed TA-activity in variant p.Arg1751Gln, displaying TA-activities of 52 ± 8 % and 44 ± 3 % in HEK293T and MDA-MB-231 cells, respectively. The two other benign controls presented TA-activities > 70 % in both cell lines. The lower boundary for what ought to be regarded as benign in this version of the TA-assay was set at 44 ± 3 %. As no gain-of-function has been reported to confer with pathogenicity, no upper wild type boundary was set. Using the threshold set by the controls (low-risk > 44 ± 3 %, high-risk < 14 ± 3 %) resulted in placing ~60 % of the class 3 variants investigated in this thesis in either the high- or low-risk group, with the remaining variants placed in the intermediate category.

5.1.2 Risk assessment of *BRCA1* variants

Variants classified as variants of unknown clinical significance (class 3) prior to this work were divided into low, high and intermediate risk groups based on the TA-assay results and the thresholds determined by the controls. Common for all variants in this study was the fact that they were missense variants in *BRCA1*, this was considered as supporting evidence towards a benign interpretation for all variants because only 2 % of deleterious variants in *BRCA1* are missense variations (see Table 4, criterion BP1).

Variants p.Thr1700Thr, p.Gly1709Arg, p.Pro1776Ser, p.Glu1826Leu and p.Arg1835Gln presented with TA-activities in the low risk range defined by the TA-assay controls, and were therefore placed in the low risk category. Four variants (p.Thr1700Thr, p.Pro1776Ser, p.Glu1826Leu and p.Arg1835Gln) presented TA-activities higher than wild type, whereas variant p.Gly1709Arg displayed TA-activity at the lower end of the low risk range. Common for these variants were the lack of enough observations in the ExAC, ESP and 1000 genomes databases for allele frequencies to be used as evidence towards benignity (i.e. they have been found in controls, but not to an extent where they provide sufficient evidence as to be used). However, variant p.Gly1709Arg had failed to be detected in any controls, which could be considered as moderate evidence towards pathogenicity. Variant p.Thr1700Thr was the only variant reported as benign in ClinVar, the other variants were either unknown to the database, or were reported with unknown significance. With the exception of variants p.Arg1835Gln and p.Gly1709Arg, the *in silico* predictions by Alamut Visual agreed on a benign nature for these variants. The prediction software did not reach consensus on variant p.Arg1835Gln, thereby rendering the predictions invalid, whereas variant p.Gly1709Arg were predicted to have a deleterious nature by all software. No functional assays had been performed on any of the variants except for p.Gly1709Arg, that was reported to display TA-activity similar to the wild

type in a study published during the work on this thesis (Jarhelle *et al*. 2016). Our TA-assay results, in combination with the available data, supported a benign interpretation of variants p.Thr1700Thr, p.Pro1776Ser, p.Glu1826Leu and p.Arg1835Gln, and that they were likely benign (class 2). Variant p.Gly1709Arg could likely be considered a benign variant based on the TA-assay results. However, due to *in silico* predictions of a deleterious nature and the lack of alleles in a control population the classification of this variant should be further investigated to rule out any uncertainty, and that the variant, therefore, should retain its status as a VUS (class 3).

Three variants (p.Asp1692Ala, p.Gly1706Arg and p.Val1838Gly) displayed a complete lack of TA-activity on our TA-assay, consistent with pathogenic variant behaviour. The three variants were predicted to have a deleterious nature by all software, and none were reported in the control populations, further supporting a deleterious interpretation. The variants had been reported as disease-causing by HGMD, and were known to ClinVar with variants p.Asp1692Ala and p.Val1838Gly reported as of uncertain significance, while p.Gly1706Arg was reported as disease-causing. No functional assays had been performed on these variants prior to this thesis, however, p.Asp1692Ala and p.Val1838Gly were reported to abolish TA-activity in a study published during the progress of this thesis (Jarhelle *et al*. 2016). Based on these findings and data, it was likely that all three variants were of a pathogenic nature, and represents likely pathogenic (class 4) variants.

Variants p.Arg1699Gln, p.Ala1708Val, p.Lys1711Gln and p.Met1783Thr presented TA-activities in the intermediate range on the TA-assay, and therefore, any risk related to these variants could not be ascertained based on the TA-assay alone. However, variants p.Arg1699Gln and p.Ala1708Val failed to present a significant difference in TA-activity compared to p.Arg1699Trp in the MDA-MB-231 cell line. The intermediate variants also posed the greatest challenge regarding classification, as the available data was either too scarce or ambiguous to conclude with any certainty. The TA-assay results for p.Arg1699Gln presented TA-activities of 20 % and 16 % in HEK293T and MDA-MB-231 cells, respectively. These TA-activities were slightly above the threshold set by the pathogenic control p.Arg1699Trp of 14 %, but as stated above, the lack of a significant difference in TA-activities between pathogenic control and p.Arg1699Gln in MDA-MB-231 cells indicate a deleterious impact. Variant p.Arg1699Gln has been displayed to possess a deleterious effect on BRCA1 in multiple functional assays (Bouwman *et al.* 2013; Lee *et al.* 2010; Spurdle *et al.* 2012; Vallon-Christersson *et al.* 2001), with *in silico* analysis predicting a deleterious effect on the protein.

However, the variant has been shown to result in a lower risk of cancer development than what is typically observed in *BRCA1* (Spurdle *et al*. 2012). While pathogenic variants in *BRCA1* usually confer high penetrance, p.Arg1699Gln displayed penetrance at a moderate level. Interestingly, the variant was shown to display similar behaviour on multiple functional assays compared to the pathogenic variant p.Arg1699Trp, with the exception of the effect on homology directed repair (Bouwman *et al*. 2013; Lee *et al*. 2010; Vallon-Christersson *et al*. 2001). A study revealed that while p.Arg1699Trp had defective HR, the HR capabilities of p.Arg1699Gln were intermediate, but not significantly decreased compared to wild type (Bouwman *et al*. 2013). Similar to variant p.Arg1699Gln, our TA-assay results for variant p.Ala1708Val of 16 % in HEK293T and MDA-MB-231 cells were slightly above the 14 % threshold suggested by the pathogenic controls, placing it in the intermediate range. However, the fact that p.Ala1708Val presented no significantly different TA-activity compared to the pathogenic control in MDA-MB-231 cells, indicate that the variant likely possess a deleterious nature. *In silico* analysis of p.Ala1708Val predicted a deleterious nature in Alamut Visual, supporting pathogenicity. Variant p.Ala1708Val had been reported to be functionally compromised on multiple functional assays (Lee *et al*. 2010) and was suggested to be a moderately penetrant variant in a study using multifactorial likelihood analysis and multiple functional assays, proving that p.Ala1708Val had intermediate TA-activity, normal foci formation during DNA damage, but induced centrosome amplification (Lovelock *et al*. 2007). Interestingly, p.Arg1699Gln and p.Ala1708Val were the only two variants that had been suggested to have moderate penetrance, which was unusual in *BRCA1* variants. It is a possibility that some variants in the lower intermediate/high end of the high-risk TA-activity range represent deleterious variants with moderate penetrance and intermediate risk. This is contrary to the hypothesis stating that there was unlikely to exist an intermediate risk group. Our findings indicate that variants p.Arg1699Gln and p.Ala1708Val indeed represent an intermediate risk group, and that they could be regarded as likely pathogenic (class 4) variants, and treated in a similar manner as deleterious variants found in genes with moderate penetrance such as PALB2 and CHEK2 (Spurdle *et al*. 2012). It would be of interest to study the performance of p.Ala1708Val on the homology directed repair assay (Bouwman *et al.* 2013), as this was the only assay in which p.Arg1699Gln was reported to display differing results compared to the pathogenic variant p.Arg1699Trp. Unlike the aforementioned intermediate variants, p.Lys1711Gln displayed TA-activities closer to the low risk threshold (41 % and 37 % in HEK293T and MDA-MB-231 cells, respectively) Analysis using *in silico* prediction software failed to agree on the nature of the variant, and the predictions could therefore not be used as

evidence. The detection failure of variant p.Lys1711Gln in ExAC, ESP or 1000 genomes controls support a deleterious interpretation. However, it could be that p.Lys1711Gln represents a low risk variant at the lower end of the TA-activity spectrum, but a better definition of the thresholds for categorising variants would need to be established, using a larger selection of known pathogenic (class 5) and benign (class 1) variants. Until a better assessment of p.Lys1711Gln can be performed, it should likely retain its status as a VUS (class 3).

The last of the intermediate variants, p.Met1783Thr, presented TA-activities of 32 % and 28 % in HEK293T and MDA-MB-231 cells, respectively, in our TA-assay. These observations place the variant in the middle of the intermediate range established by the TA-assay controls. *In silico* analysis of the variant predicted a deleterious effect on protein, in all software. p.Met1783Thr had also been previously investigated using multiple functional assays (TA-assay, protease sensitivity (PS), phosphopeptide binding activity/specificity (PBA/S) (Lee *et al.* 2010) and small colony phenotype (SCP) (Coyne *et al.* 2004)). Functional impact of the variant was reported in the SCP assay, while no effect was reported in the PS and PBS assays, and no concluding results reported on the TA-assay and PBA assay. Additionally, the variant was shown to have a mild destabilising effect on protein, however, no effect on binding affinity was reported (Drikos *et al*. 2009; Gaboriau *et al*. 2015). The variant was known to ClinVar, with three reports of a benign nature, three reports of a likely benign nature and one report of unknown significance. The allele frequencies reported for the p.Met1783Thr variant were almost double what could be expected for the disease, and with a higher number of observed alleles than for any other variant included in this thesis (ExAC: MAF = 20/10368 = 0.19 %, ESP: MAF = 8/4406 = 0.18 % vs. MPAF: 0.1 %). The probability of this variant possessing a deleterious nature seemed unlikely, given the high allele frequencies and high number of observations. It could be that p.Met1783Thr represented a benign variant at the low-end threshold of wild type TA-activity, and that benign control variant p.Arg1751Gln did not represent a true lower limit for low risk variants. The fact that p.Met1783Thr has largely been detected in African and Afro-American populations (McKean-Cowdin *et al*. 2005), provide some uncertainty to the notion of the variant being completely benign, as it is unknown how this variant would behave in other populations. Nevertheless, given the amount of evidence indicating a benign nature, p.Met1783Thr could be regarded as a likely benign, class 2, variant.

5.1.3 Reclassification of *BRCA1* variants during this study

Some of the variants classified as variants of unknown clinical significance (class 3) had recently been re-evaluated and reclassified by the Oslo University hospital, Department of Medical Genetics, as part of the standard procedure regarding variant risk assessment.

Of the variants used as controls only p.Val1804Asp was reclassified, from likely benign (class 2) to benign (class 1). Our TA-assay results for p.Val1804Asp were 77 % in HEK293T cells, 102 % in MDA-MB-231 cells, and were consistent with the evaluation that the variant was benign. Reclassification of p.Val1804Asp was largely based on TA-assay results showing the variant to be low-risk (Carvalho *et al*. 2007b) and multifactorial probability analysis suggesting the variant to be benign (Easton *et al*. 2007). High allele frequencies with more than five alleles in ExAC, as well as all prediction software predicted the variant to be benign were considered supporting evidence in favour of benignity. Additionally, it had recently been reported as benign by the Evidence-based Network for the Interpretation of Germline Mutant Alleles (ENIGMA) consortium. p.Val1804Asp was reported to have no functional impact on a panel of functional assays (TA, PS PBA/S (Lee *et al*. 2010)), and no impact on the SCP-assay (Coyne *et al.* 2004). Using a version of the TA-assay investigating the BRCA1 ability to transactivate p53 response elements using full length variant *BRCA1*, p.Val1804Asp was found to be functionally compromised (Ostrow *et al*. 2004). However, the TA-assay utilised by Ostrow *et al*., specifically measure the ability of the BRCT domain to recognise and mediate transactivation of p53 responsive elements. While it could be that p.Val1804Asp causes a loss in recognition of p53 responsive elements, it does not necessarily mean that the transactivation ability of the BRCT domain is completely compromised. By fusing the BRCT domain to a GAL4 DBD, as done in this thesis and in the studies by Carvalho *et al*. and Lee *et al.*, the measured TA-activity was independent of gene specific elements, and therefore provided a general view of the p.Val1804Asp variants impact on transactivation and domain integrity. Given the amount of evidence against p.Val1804Asp being a pathogenic variant, it could be that loss of the ability of BRCA1 to recognise p53 specific elements alone, do not contribute to a significantly increased risk of tumourigenesis.

Reclassification of the VUSs (class 3) included in this study, largely agree with the results presented in this thesis. Variants displaying low risk in our TA-assay (p.Thr1700Thr, p.Gly1709Arg, p.Pro1776Ser, p.Glu1826Leu and p.Arg1835Gln) had all been reclassified to likely benign (class 2), with the exception of p.Gly1709Arg and p.Arg1835Gln, who remained class 3 variants. Variants classified as high risk on our TA-assay (p.Asp1692Ala, p.Gly1706Arg

and p.Val1838Gly) had been reclassified as likely pathogenic (class 4). Of the intermediate risk variants one had been reclassified as likely pathogenic (p.Arg1699Gln), and one as a benign class 1 variant (p.Met1783Thr). The two remaining variants (p.Ala1708Val and p.Lys1711Gln) retained their class 3 status.

While we agreed with most of the recent reclassifications, we believe that variant p.Ala1708Val likely represented a deleterious intermediate risk variant, similar to the reclassified variant p.Arg1699Gln, and that p.Ala1708Val could be reclassified as likely pathogenic (class 4) with moderate penetrance. The reclassification of p.Met1783Thr to class 1 did not seem as obvious as a class 1 category would imply. Despite high allele frequencies and reports of a benign impact, the variant had mainly been found in African and Afro-American populations, with no data concerning how the variant behave in other populations. Combined with the predictions of a deleterious nature, and with multiple functional assays that indicated a slightly deleterious effect on the protein, we concluded that the variant would better be defined as a likely benign, class 2 variant. As for variant p.Arg1835Gln, our results agree with a benign interpretation, and that the variant could likely be reclassified from class 3 to likely benign (class 2).

5.1.4 Additional effect of BRCA1 variants *in cis*

While little work had been performed on *BRCA1* variants *in cis* in the past, an investigation into the possible effects of including a polymorphism in combination with deleterious variants and VUSs, were unable to find any significant impact on TA-activities (Carvalho *et al.* 2007b). It was, therefore, surprising to find that examination of possible additive effects of double *cis* variants revealed a significant impact in both variant combinations tested in this thesis (p.Asp1692Ala/p.Val1804Asp and p.Arg1751Gln/p.Glu1826Leu). The fact that p.Asp1692Ala/p.Val1804Asp displayed an additional reduction in the TA-activities compared to p.Asp1692Ala alone, could be an indication that neutral variants can affect the performance of deleterious variants on the TA-assay. Interestingly, the combination of p.Arg1751Gln/p.Glu1826Leu displayed TA-activities intermediate to p.Arg1751Gln and p.Glu1826Leu alone. This implied that the elevated TA-activity of p.Glu1826Leu was able to rescue some of the loss in the TA-activity displayed by p.Arg1751Gln. It would be interesting to see if variants with TA-activities above wild type, such as p.Glu1826Leu, are capable of affecting the TA-activities of known deleterious and intermediate variants when combined. If no additive effect of high TA-activity variants can be observed in combination with known deleterious variants, but affects some variants in the intermediate range, this might provide a

new way of identifying the truly deleterious variants that have a strong impact on protein functionality.

5.1.5 Verification of the TA-assay

Analysis of fusion protein GAL4 DBD:BRCA1 expression in TA-cell lysates from HEK293T and MDA-MB-231 cells by western blot, indicated that the observed intensity of the bands not entirely reflected the TA-activity of the variants. The fact that some variants displayed weak bands as well as a severe lack of TA-activity, could be explained by the variant having a destabilising effect on the protein, as has been reported to be the case for several *BRCA1* missense variants (Gaboriau *et al.* 2015). Investigation of *BRCA1* missense variants via the TA-assay have often been conducted in both yeast and mammalian cells, and these studies illustrated that protein instability due to specific variants readily occur in mammalian cells, but not in yeast (Carvalho *et al*. 2007a). It has been suggested that this instability may represent the true deleterious effect of certain variants, and that the lack of TA-activity is caused by increased degradation of BRCA1 rather than loss of its inherent transactivation abilities.

As illustrated by variants p.Arg1751Gln and p.Pro1776Ser on western blot of MDA-MB-231 lysates (Figure 30B), the lack of correlation between TA-activity and band intensity is apparent. p.Arg1751Gln displayed stronger bands compared to p.Pro1776Ser, despite having lower TA-activity. This has also been illustrated in a study where variants displaying wild type TA-activity had markedly weaker bands than wild type (Carvalho *et al.* 2007b). These findings indicate that the usefulness of western blot analysis on this assay was limited to verifying successful expression of the fusion protein, and that any variance in band intensity because of protein instability, must be considered independently for each variant, preferably using functional assays on full-length *BRCA1*.

Analysis of *BRCA1* variant mRNA revealed some differences in the expression levels of the GAL4 DBD:BRCA1 fusion protein, both between individual variants and cell lines. Expression of the fusion protein were lower in the MDA-MB-231 cells than in HEK293T cells for all variants tested, including wild type. A possible explanation for the reduced expression levels in MDA-MB-231 compared to HEK293T cells can in part be attributed to the lower transfection efficiencies observed in the cell line. It could be that since MDA-MB-231 was a cancerous cell line, whereas HEK293T cells were not, that the reduced transfection efficiencies and expression levels reflected more complex mechanisms related to the cells state (cancerous/normal).

However, this is beyond the scope of this thesis and the data obtained in this study, and further inquiry needs to be undertaken to answer this in more detail. Nevertheless, variants that presented with loss of TA-activity displayed lower relative expression in HEK293T cells compared to wild type. Whereas variant p.Arg1751Gln presented elevated relative expression in HEK293T cells compared to wild type, despite having reduced TA-activity (~50 %). These results indicated that TA-activity was not exclusively dependent on expression levels.

5.1.6 Evaluation of TA-assay parameters

The effect of increased incubation time on the sensitivity of the TA-assay revealed a significant benefit using 48-hour incubation instead of 24 hours, on variants with TA-activity < 50 %. This increase in sensitivity is consistent with observations by the Iversen, N. research group (personal communication, Iversen, N., 2017) using similar dual luciferase based assays. Other attempts at investigating *BRCA1* variants utilising TA-assays have usually been conducted with an incubation period of 24 hours (Jarhelle *et al*. 2016; Kaufman *et al*. 2006; Lee *et al*. 2010; Phelan *et al*. 2005; Tischkowitz *et al*. 2008; Vallon-Christersson *et al*. 2001). The increased sensitivity of the assay, obtained by increasing the incubation time to 48 hours, should enable a more precise distinction of intermediate variants. Given that variants p.Arg1699Gln and p.Ala1708Val suggest the existence of an intermediate risk group with moderate penetrance, the ability to better recognize this group could be of clinical importance, especially in regard to prophylactic treatments.

The TA-assays were performed utilising the HEK293T and MDA-MB-231 cell lines, and data obtained from the TA-assays revealed little variability in the results between cell lines, especially at low TA-activities. The larger discrepancies between the cell lines were confined well within the wild type TA-activity range, and therefore posed no challenges towards assignment of variants to the low- or high-risk categories. MDA-MB-231 cells generally displayed larger variability in the data than the HEK293T cells, especially in variants with TA-activity > 70 %. To investigate the seemingly independent relationship between TA-assay performance and choice of cell line, the TA-assay experiments were repeated using MDA-MB-436 cells on a selection of variants. Variants were chosen as they represented variants with a broad range of TA-activities, mainly around TA-activities of 20~60 %, the area thought to yield the highest probability of observing variability. In the MDA-MB-436 cells we achieved low transfection efficiencies, and very low luciferase signals. Comparing the results from MDA-MB-436 to HEK293T and to the MDA-MB-231 cells, the results revealed relatively high

agreement between the cell lines. However, in MDA-MB-436 cells TA-activities for variants p.Asp1692Ala, p.Arg1699Gln and p.Ala1708Val, were slightly elevated while the TA-activity for variant p.Met1783Thr was reduced. The reason for the difficulties in repeating the TA-assay with MDA-MB-436 cells was unclear, and similar assays performed using this cell line with other genes by the Iversen, N. research group prior to this study, also resulted in low luciferase signals (personal communication, Iversen, N., 2017). This study has shown that the MDA-MB-436 cell line contain variants that result in loss of both *BRCA1* and *TP53*, in addition, the cell line was highly sensitive to confluency levels during growth, requiring a high degree of cell-cell contact. These observations may be part of the reason why the MDA-MB-436 cell line proved difficult to use on the TA-assay. A more thorough testing and optimisation of MDA-MB-436 on the TA-assay was not performed due to time constraints, and it could be that further optimisation would yield better results in using the MDA-MB-436 cell line. Nevertheless, the general agreement between the three cell lines indicated that the assays were relatively independent of the cell lines chosen and endogenous *BRCA1*/*TP53* status.

5.1.7 Limitations of the TA-assay

There are several limitations to the TA-assay, mainly that investigation of *BRCA1* variants on the TA-assay are limited to variants in or near the BRCT-domain. Secondly, the assay is performed only on a subsection of the gene, and how well the TA-assay reflects variant effect on full length BRCA1 is largely unknown. Additionally, a wild type like result on the TA-assay cannot be regarded as conclusive evidence towards benignity, as the biological effect of the missense variant can escape detection on this assay (e.g. variants resulting in aberrant splicing). Despite this, the TA-assay provides a reliable assessment of the BRCT-domains integrity, and the reported correlation between cancer predisposing variants and TA-results are high (Carvalho *et al.* 2007a). The ability of the TA-assay to assess the integrity of the BRCT-domain makes it well suited for efficiently dividing BRCA1 BRCT-variants into high and low risk groups, but provides little or no explanation to the biological mechanism of how the variant triggers tumourigenesis.

It is also difficult to directly compare results between studies, as different setups and assay parameters have differing results. Traditionally, evaluation of a variant on a TA-assay have been done without defining thresholds. It seems, however, likely that these thresholds exist and that defining these would be beneficial, particularly for variants where little or no other data are available. The thresholds used for dividing a variant to the high/low or intermediate groups,

should only be applied for determination of a variant if the TA-assay follow the exact same setup as was utilised during construction of defined boundaries.

5.1.8 A note on aberrant splicing

Since the TA-assay results are largely irrelevant if the variant in question results in aberrant splicing, it was of interest to investigate the variants with respect to this. For the 12 variants classified as VUSs prior to this study, six had been included in studies on splicing and all presented normal splicing (p.Asp1692Ala, p.Ala1708Val, p.Gly1709Arg, p.Pro1776Ser, p.Arg1699Gln and p.Val1838Gly) (Jarhelle *et al*. 2016; Nangota 2014). The remaining six variants (p.Thr1700Thr, p.Gly1706Arg, p.Lys1711Gln, p.Met1783Thr, p.Glu1826Leu and p.Arg1835Gln) were intended to be investigated for aberrant splicing using PAXgene blood from patients. Unfortunately, these samples could not be obtained in time, and despite that *in silico* assessments predicted no effect on splicing for any of the variants included, the possibility of aberrant splicing in these six variants, while deemed low, cannot be categorically dismissed.

5.2 Characterisation of breast cancer cell lines

The effect of cytostatic treatment differs between individual patients, and acquired drug resistance poses a serious problem for treatment of breast cancer patients. The understanding of the molecular basis of cytostatic treatment and development of resistance is incomplete. Therefore, it was of interest to investigate a possible relation between drug effect and the status of *BRCA1* and *TP53* in breast cancer cell lines.

5.2.1 *BRCA1* and *TP53* related response to cytostatic treatment in breast cancer cells

Investigation of breast cancer cell line response to the cytostatic drug Doxorubicin revealed a high degree of resistance in the triple negative basal cell lines MDA-MB-231 and MDA-MB-436, displaying little effect from the drug at any concentration. Both MDA-MB-231 and MDA-MB-436 cells had compromised p53 functionality, while only MDA-MB-436 had non-functioning BRCA1. Surprisingly, the luminal hormone receptor positive MCF-7 cell line presented elevated cell viability at all concentrations. The triple negative basal cell line SUM102 displayed high sensitivity to Doxorubicin at all concentrations. Contrary to the MDA-MB-436 cell line, both SUM102 and MCF-7 possessed wild type *BRCA1* and *TP53*, however, relative expression of *BRCA1* in SUM102 was half of the expression in MCF-7 cells. When compared, the triple negative basal cell lines (SUM102, MDA-MB-231 and MDA-MB-436) indicated that loss of p53 functionality might contribute to increased resistance to Doxorubicin. It was somewhat surprising that the *BRCA1* lacking cell line MDA-MB-436 display virtually no effect of the treatment, since it has been illustrated that Doxorubicin has an increased effect on HR and NER deficient cells (Spencer *et al.* 2008). It could be that *BRCA1* mediated HR is a secondary cellular approach of dealing with DNA intercalations, and that the repair mechanism for this type of damage is mainly facilitated through NER. This could explain why the loss of *BRCA1* and subsequent impairment of HR does not impact proliferation in the MDA-MB-436 cell line, given that the cell line possesses a fully functional NER pathway.

Favourable results in treatment of metastatic breast cancer patients with Carboplatin have been reported, but the effects of the drug were much slower and required higher doses than the sister drug Cisplatin (Perez 2004). All cell lines exposed to increasing concentrations of Carboplatin displayed high cell viability at all concentrations during a 24-hour exposure, and this was likely due to the slow metabolic rate of Carboplatin. The MDA-MB-231 cell line displayed a high cell viability during treatment with Carboplatin up to a concentration of 50 µM, before dropping below IC_{50} at 100 µM, whereas MDA-MB-436 displayed reduced viability at all concentrations. The response of MDA-MB-436 cells to even low concentrations of Carboplatin could likely be

explained by its lack of *BRCA1*, and subsequent loss of HR capabilities. The MDA-MB-436 cell line, despite having a higher sensitivity to low doses of Carboplatin, revealed a better tolerance to the drug at high concentrations compared to the MDA-MB-231 cells. Suggesting that the *BRCA1* mediated HR function of MDA-MB-231 was outcompeted by the drugs effect at elevated concentrations. MCF-7 displayed tolerance to the drug comparable to MDA-MB-436 cells. It is of interest that SUM102 cells displayed low cellular viability during exposure to both Doxorubicin and Carboplatin, implying that it may have had a compromised repair pathway that was vital for repairing both DNA intercalations and crosslinks. It has been reported that mismatch repair (MMR) is an important mechanism in resistance to platin based cytostatic (Rabik & Dolan 2007), such as Carboplatin. Therefore, it would be interesting to see if any genes involved in the MMR or other repair pathways were compromised in the SUM102 cells. It could also be that due to the low expression of *BRCA1* in SUM102, that it was more sensitive to the effects of Carboplatin.

6 Concluding remarks

We have demonstrated that the optimised TA-assay developed in this thesis efficiently provide useful data regarding risk assessment and classification of *BRCA1* BRCT missense variants. However, there is still a demand for a better definition of the intermediate risk-thresholds, and an analysis of a larger selection of well-defined class 1 and 5 variants in the assay would help remedy this. While displaying a high correlation between TA-activity results and risk level, the assay provides little explanation of the underlying mechanism of the potential tumourigenic behaviour of the variants. It would be useful to study the variants in full length *BRCA1*, with a panel of functional tests e.g. foci formation, protein stability and binding affinity, to better ascertain the nature of their impact. This would likely prove necessary for variants that inevitably end up with intermediate TA-activities regardless of any improvement in threshold definitions, as well as for variants were the available data are conflicting. Likewise, it is necessary to confirm that the variants p.Thr1700Thr, p.Gly1706Arg, p.Lys1711Gln, p.Met1783Thr, p.Glu1826Leu and p.Arg1835Gln did not result in aberrant splicing. This can be investigated either by mRNA analysis on patient blood samples, or with a functional assay such as the minigene assay.

To summarise, we proposed the following classifications for the 12 *BRCA1* BRCT missense variants included in this thesis: p.Thr1700Thr, p.Pro1776ser, p.Met1783Thr, p.Glu1826Leu and p.Arg1835Gln as likely benign (class 2) variants. p.Asp1692Ala, p.Arg1699Gln, p.Gly1706Arg, p.Ala1708Val and p.Val1838Gly are likely pathogenic (class 4) variants, where p.Arg1699Gln and p.Ala1708Val probably represents pathogenic variants with moderate penetrance. The last two variants p.Gly1709Arg and p.Lys1711Gln, remained classified as VUSs (class 3) due to insufficient and contradictory data. We also found that the triple negative breast cancer cell lines displayed a lower sensitivity to treatment with the DNA intercalating cytostatic Doxorubicin, whereas treatment with the DNA cross-linking agent Carboplatin resulted in higher sensitivity and reduced cell viability. We also found a novel *TP53* variant (c.604_610dupCGTGTGG) in cell line MDA-MB-436 that likely resulted in loss of p53 functionality. Breast cancer cell lines with deleterious p53 variants also displayed a lower sensitivity to Doxorubicin, suggesting a role for p53 in acquired drug resistance.

7 References

Amin, M. B., Greene, F. L., Edge, S. B., Compton, C. C., Gershenwald, J. E., Brookland, R. K., Meyer, L., Gress, D. M., Byrd, D. R. & Winchester, D. P. (2017). The Eighth Edition AJCC Cancer Staging Manual: Continuing to build a bridge from a population-based to a more "personalized" approach to cancer staging. *CA Cancer J Clin*, 67 (2): 93-99.

Anderson, S. F., Schlegel, B. P., Nakajima, T., Wolpin, E. S. & Parvin, J. D. (1998). BRCA1 protein is linked to the RNA polymerase II holoenzyme complex via RNA helicase A. *Nat Genet*, 19 (3): 254-6.

Atchley, D. P., Albarracin, C. T., Lopez, A., Valero, V., Amos, C. I., Gonzalez-Angulo, A. M., Hortobagyi, G. N. & Arun, B. K. (2008). Clinical and pathologic characteristics of patients with BRCA-positive and BRCA-negative breast cancer. *J Clin Oncol*, 26 (26): 4282-8.

Bouwman, P., van der Gulden, H., van der Heijden, I., Drost, R., Klijn, C. N., Prasetyanti, P., Pieterse, M., Wientjens, E., Seibler, J., Hogervorst, F. B., et al. (2013). A high-throughput functional complementation assay for classification of BRCA1 missense variants. *Cancer Discov*, 3 (10): 1142-55.

Brown, J. S., Kaye, S. B. & Yap, T. A. (2016). PARP inhibitors: the race is on. *Br J Cancer*, 114 (7): 713-5.

Cancer Registry of Norway. (2016). *Brystkreft*. kreftregisteret.no. Available at: https://www.kreftregisteret.no/Generelt/Fakta-om-kreft/Brystkreft-Alt2/ (accessed: 14.02).

Carvalho, M. A., Couch, F. J. & Monteiro, A. N. (2007a). Functional assays for BRCA1 and BRCA2. *Int J Biochem Cell Biol*, 39 (2): 298-310.

Carvalho, M. A., Marsillac, S. M., Karchin, R., Manoukian, S., Grist, S., Swaby, R. F., Urmenyi, T. P., Rondinelli, E., Silva, R., Gayol, L., et al. (2007b). Determination of cancer risk associated with germ line BRCA1 missense variants by functional analysis. *Cancer Res*, 67 (4): 1494-501.

Clark, S. L., Rodriguez, A. M., Snyder, R. R., Hankins, G. D. & Boehning, D. (2012). Structure-Function Of The Tumor Suppressor BRCA1. *Comput Struct Biotechnol J*, 1 (1).

Couch, F. J. & Weber, B. L. (1996). Mutations and polymorphisms in the familial early-onset breast cancer (BRCA1) gene. Breast Cancer Information Core. *Hum Mutat*, 8 (1): 8-18.

Couch, F. J., Hart, S. N., Sharma, P., Toland, A. E., Wang, X., Miron, P., Olson, J. E., Godwin, A. K., Pankratz, V. S., Olswold, C., et al. (2015). Inherited mutations in 17 breast cancer susceptibility genes among a large triple-negative breast cancer cohort unselected for family history of breast cancer. *J Clin Oncol*, 33 (4): 304-11.

Coyne, R. S., McDonald, H. B., Edgemon, K. & Brody, L. C. (2004). Functional characterization of BRCA1 sequence variants using a yeast small colony phenotype assay. *Cancer Biol Ther*, 3 (5): 453-7.

Cressman, V. L., Backlund, D. C., Hicks, E. M., Gowen, L. C., Godfrey, V. & Koller, B. H. (1999). Mammary tumor formation in p53- and BRCA1-deficient mice. *Cell Growth Differ*, 10 (1): 1-10.

Crown, J., O'Shaughnessy, J. & Gullo, G. (2012). Emerging targeted therapies in triple-negative breast cancer. *Ann Oncol*, 23 Suppl 6: vi56-65.

Domchek, S. M., Tang, J., Stopfer, J., Lilli, D. R., Hamel, N., Tischkowitz, M., Monteiro, A. N., Messick, T. E., Powers, J., Yonker, A., et al. (2013). Biallelic deleterious BRCA1 mutations in a woman with early-onset ovarian cancer. *Cancer Discov*, 3 (4): 399-405.

Drikos, I., Nounesis, G. & Vorgias, C. E. (2009). Characterization of cancer-linked BRCA1-BRCT missense variants and their interaction with phosphoprotein targets. *Proteins*, 77 (2): 464-76.

Easton, D. F., Deffenbaugh, A. M., Pruss, D., Frye, C., Wenstrup, R. J., Allen-Brady, K., Tavtigian, S. V., Monteiro, A. N., Iversen, E. S., Couch, F. J., et al. (2007). A systematic genetic assessment of 1,433 sequence variants of unknown clinical significance in the BRCA1 and BRCA2 breast cancer-predisposition genes. *Am J Hum Genet*, 81 (5): 873-83.

Fan, S., Ma, Y. X., Wang, C., Yuan, R. Q., Meng, Q., Wang, J. A., Erdos, M., Goldberg, I. D., Webb, P., Kushner, P. J., et al. (2001). Role of direct interaction in BRCA1 inhibition of estrogen receptor activity. *Oncogene*, 20 (1): 77-87.

Friedman, L. S., Ostermeyer, E. A., Szabo, C. I., Dowd, P., Lynch, E. D., Rowell, S. E. & King, M. C. (1994). Confirmation of BRCA1 by analysis of germline mutations linked to breast and ovarian cancer in ten families. *Nat Genet*, 8 (4): 399-404.

Gaboriau, D. C., Rowling, P. J., Morrison, C. G. & Itzhaki, L. S. (2015). Protein stability versus function: effects of destabilizing missense mutations on BRCA1 DNA repair activity. *Biochem J*, 466 (3): 613-24.

Gartel, A. L. & Radhakrishnan, S. K. (2005). Lost in transcription: p21 repression, mechanisms, and consequences. *Cancer Res*, 65 (10): 3980-5.

Go, R. S. & Adjei, A. A. (1999). Review of the comparative pharmacology and clinical activity of cisplatin and carboplatin. *J Clin Oncol*, 17 (1): 409-22.

Gowen, L. C., Johnson, B. L., Latour, A. M., Sulik, K. K. & Koller, B. H. (1996). Brca1 deficiency results in early embryonic lethality characterized by neuroepithelial abnormalities. *Nat Genet*, 12 (2): 191-4.

Hall, J. M., Lee, M. K., Newman, B., Morrow, J. E., Anderson, L. A., Huey, B. & King, M. C. (1990). Linkage of early-onset familial breast cancer to chromosome 17q21. *Science*, 250 (4988): 1684-9.

Hohenstein, P., Kielman, M. F., Breukel, C., Bennett, L. M., Wiseman, R., Krimpenfort, P., Cornelisse, C., van Ommen, G. J., Devilee, P. & Fodde, R. (2001). A targeted mouse Brca1 mutation removing the last BRCT repeat results in apoptosis and embryonic lethality at the headfold stage. *Oncogene*, 20 (20): 2544-50.

Houdayer, C. (2011). In silico prediction of splice-affecting nucleotide variants. *Methods Mol Biol*, 760: 269-81.

Hulka, B. S. & Moorman, P. G. (2008). Breast cancer: hormones and other risk factors. *Maturitas*, 61 (1-2): 203-13; discussion 213.

Janavicius, R. (2010). Founder BRCA1/2 mutations in the Europe: implications for hereditary breast-ovarian cancer prevention and control. *EPMA J*, 1 (3): 397-412.

Jarhelle, E., Riise Stensland, H. M., Maehle, L. & Van Ghelue, M. (2016). Characterization of BRCA1 and BRCA2 variants found in a Norwegian breast or ovarian cancer cohort. *Fam Cancer*.

Johnson, N., Johnson, S. F., Yao, W., Li, Y. C., Choi, Y. E., Bernhardy, A. J., Wang, Y., Capelletti, M., Sarosiek, K. A., Moreau, L. A., et al. (2013). Stabilization of mutant BRCA1 protein confers PARP inhibitor and platinum resistance. *Proc Natl Acad Sci U S A*, 110 (42): 17041-6.

Kang, H. J., Hong, Y. B., Kim, H. J., Rodriguez, O. C., Nath, R. G., Tilli, E. M., Albanese, C., Chung, F. L., Kwon, S. H. & Bae, I. (2011). Detoxification: a novel function of BRCA1 in tumor suppression? *Toxicol Sci*, 122 (1): 26-37.

Kao, J., Salari, K., Bocanegra, M., Choi, Y. L., Girard, L., Gandhi, J., Kwei, K. A., Hernandez-Boussard, T., Wang, P., Gazdar, A. F., et al. (2009). Molecular profiling of breast cancer cell lines defines relevant tumor models and provides a resource for cancer gene discovery. *PLoS One*, 4 (7): e6146.

Karami, F. & Mehdipour, P. (2013). A comprehensive focus on global spectrum of BRCA1 and BRCA2 mutations in breast cancer. *Biomed Res Int*, 2013: 928562.

Katsuki, Y. & Takata, M. (2016). Defects in homologous recombination repair behind the human diseases: FA and HBOC. *Endocr Relat Cancer*, 23 (10): T19-37.

Kaufman, B., Laitman, Y., Carvalho, M. A., Edelman, L., Menachem, T. D., Zidan, J., Monteiro, A. N. & Friedman, E. (2006). The P1812A and P25T BRCA1 and the 5164del4 BRCA2 mutations: occurrence in high-risk non-Ashkenazi Jews. *Genet Test*, 10 (3): 200-7.

Lee, M. S., Green, R., Marsillac, S. M., Coquelle, N., Williams, R. S., Yeung, T., Foo, D., Hau, D. D., Hui, B., Monteiro, A. N., et al. (2010). Comprehensive analysis of missense variations in the BRCT domain of BRCA1 by structural and functional assays. *Cancer Res*, 70 (12): 4880-90.

Leung, C. C. & Glover, J. N. (2011). BRCT domains: easy as one, two, three. *Cell Cycle*, 10 (15): 2461-70.

Liang, H. & Tan, A. R. (2010). Iniparib, a PARP1 inhibitor for the potential treatment of cancer, including triple-negative breast cancer. *IDrugs*, 13 (9): 646-56.

Lovelock, P. K., Spurdle, A. B., Mok, M. T., Farrugia, D. J., Lakhani, S. R., Healey, S., Arnold, S., Buchanan, D., kConFab, I., Couch, F. J., et al. (2007). Identification of BRCA1 missense substitutions that confer partial functional activity: potential moderate risk variants? *Breast Cancer Res*, 9 (6): R82.

Lukong, K. E. (2017). Understanding breast cancer - The long and winding road. *BBA Clin*, 7: 64-77.

MacLachlan, T. K., Somasundaram, K., Sgagias, M., Shifman, Y., Muschel, R. J., Cowan, K. H. & El-Deiry, W. S. (2000). BRCA1 effects on the cell cycle and the DNA damage response are linked to altered gene expression. *J Biol Chem*, 275 (4): 2777-85.

MacLachlan, T. K., Takimoto, R. & El-Deiry, W. S. (2002). BRCA1 directs a selective p53-dependent transcriptional response towards growth arrest and DNA repair targets. *Mol Cell Biol*, 22 (12): 4280-92.

Maxwell, K. N., Hart, S. N., Vijai, J., Schrader, K. A., Slavin, T. P., Thomas, T., Wubbenhorst, B., Ravichandran, V., Moore, R. M., Hu, C., et al. (2016). Evaluation of ACMG-Guideline-Based Variant Classification of Cancer Susceptibility and Non-Cancer-Associated Genes in Families Affected by Breast Cancer. *Am J Hum Genet*, 98 (5): 801-17.

McKean-Cowdin, R., Spencer Feigelson, H., Xia, L. Y., Pearce, C. L., Thomas, D. C., Stram, D. O. & Henderson, B. E. (2005). BRCA1 variants in a family study of African-American and Latina women. *Hum Genet*, 116 (6): 497-506.

Miki, Y., Swensen, J., Shattuck-Eidens, D., Futreal, P. A., Harshman, K., Tavtigian, S., Liu, Q., Cochran, C., Bennett, L. M., Ding, W., et al. (1994). A strong candidate for the breast and ovarian cancer susceptibility gene BRCA1. *Science*, 266 (5182): 66-71.

Millot, G. A., Carvalho, M. A., Caputo, S. M., Vreeswijk, M. P., Brown, M. A., Webb, M., Rouleau, E., Neuhausen, S. L., Hansen, T., Galli, A., et al. (2012). A guide for functional analysis of BRCA1 variants of uncertain significance. *Hum Mutat*, 33 (11): 1526-37.

Moisan, A., Larochelle, C., Guillemette, B. & Gaudreau, L. (2004). BRCA1 can modulate RNA polymerase II carboxy-terminal domain phosphorylation levels. *Mol Cell Biol*, 24 (16): 6947-56.

Monteiro, A. N., August, A. & Hanafusa, H. (1996). Evidence for a transcriptional activation function of BRCA1 C-terminal region. *Proc Natl Acad Sci U S A*, 93 (24): 13595-9.
Monteiro, A. N. (2000). BRCA1: exploring the links to transcription. *Trends Biochem Sci*, 25 (10): 469-74.
Mukherjee, S. (2010). *The emperor of all maladies : a biography of cancer*. 1st Scribner hardcover ed. New York: Scribner. xiv, 571 p., 8 p. of plates pp.
Mullan, P. B., Quinn, J. E. & Harkin, D. P. (2006). The role of BRCA1 in transcriptional regulation and cell cycle control. *Oncogene*, 25 (43): 5854-63.
Møller, P., Hagen, A. I., Apold, J., Maehle, L., Clark, N., Fiane, B., Lovslett, K., Hovig, E. & Vabo, A. (2007). Genetic epidemiology of BRCA mutations--family history detects less than 50% of the mutation carriers. *Eur J Cancer*, 43 (11): 1713-7.
Nangota, C. (2014). *mRNA analysis of BRCA1 and BRCA2 sequence variants*. Master thesis. Oslo: Oslo and Akershus university college of applied sciences
Neish, A. S., Anderson, S. F., Schlegel, B. P., Wei, W. & Parvin, J. D. (1998). Factors associated with the mammalian RNA polymerase II holoenzyme. *Nucleic Acids Res*, 26 (3): 847-53.
Ng, P. C. & Henikoff, S. (2001). Predicting deleterious amino acid substitutions. *Genome Res*, 11 (5): 863-74.
Norwegian Directorate of Health. (2014). *Pakkeforløp for brystkreft*: Norwegian Directorate of Health.
Norwegian directorate of Health. (2016). *Nasjonalt handlingsprogram med retningslinjer for diagnostikk, behandling og oppfølging av pasienter med brystkreft*. 183 pp.
Ostrow, K. L., McGuire, V., Whittemore, A. S. & DiCioccio, R. A. (2004). The effects of BRCA1 missense variants V1804D and M1628T on transcriptional activity. *Cancer Genet Cytogenet*, 153 (2): 177-80.
Ouchi, T., Monteiro, A. N., August, A., Aaronson, S. A. & Hanafusa, H. (1998). BRCA1 regulates p53-dependent gene expression. *Proc Natl Acad Sci U S A*, 95 (5): 2302-6.
Perez, E. A. (2004). Carboplatin in combination therapy for metastatic breast cancer. *Oncologist*, 9 (5): 518-27.
Perou, C. M., Sorlie, T., Eisen, M. B., van de Rijn, M., Jeffrey, S. S., Rees, C. A., Pollack, J. R., Ross, D. T., Johnsen, H., Akslen, L. A., et al. (2000). Molecular portraits of human breast tumours. *Nature*, 406 (6797): 747-52.
Phelan, C. M., Dapic, V., Tice, B., Favis, R., Kwan, E., Barany, F., Manoukian, S., Radice, P., van der Luijt, R. B., van Nesselrooij, B. P., et al. (2005). Classification of BRCA1 missense variants of unknown clinical significance. *J Med Genet*, 42 (2): 138-46.
Prakash, R., Zhang, Y., Feng, W. & Jasin, M. (2015). Homologous recombination and human health: the roles of BRCA1, BRCA2, and associated proteins. *Cold Spring Harb Perspect Biol*, 7 (4): a016600.
Rabik, C. A. & Dolan, M. E. (2007). Molecular mechanisms of resistance and toxicity associated with platinating agents. *Cancer Treat Rev*, 33 (1): 9-23.
Rakha, E. A. & Ellis, I. O. (2009). Triple-negative/basal-like breast cancer: review. *Pathology*, 41 (1): 40-47.
Richards, S., Aziz, N., Bale, S., Bick, D., Das, S., Gastier-Foster, J., Grody, W. W., Hegde, M., Lyon, E., Spector, E., et al. (2015). Standards and guidelines for the interpretation of sequence variants: a joint consensus recommendation of the American College of Medical Genetics and Genomics and the Association for Molecular Pathology. *Genet Med*, 17 (5): 405-24.
Roy, R., Chun, J. & Powell, S. N. (2011). BRCA1 and BRCA2: different roles in a common pathway of genome protection. *Nat Rev Cancer*, 12 (1): 68-78.

Sawyer, S. L., Tian, L., Kahkonen, M., Schwartzentruber, J., Kircher, M., University of Washington Centre for Mendelian, G., Consortium, F. C., Majewski, J., Dyment, D. A., Innes, A. M., et al. (2015). Biallelic mutations in BRCA1 cause a new Fanconi anemia subtype. *Cancer Discov*, 5 (2): 135-42.

Schuyer, M. & Berns, E. M. (1999). Is TP53 dysfunction required for BRCA1-associated carcinogenesis? *Mol Cell Endocrinol*, 155 (1-2): 143-52.

Scully, R., Anderson, S. F., Chao, D. M., Wei, W., Ye, L., Young, R. A., Livingston, D. M. & Parvin, J. D. (1997). BRCA1 is a component of the RNA polymerase II holoenzyme. *Proc Natl Acad Sci U S A*, 94 (11): 5605-10.

Shakya, R., Reid, L. J., Reczek, C. R., Cole, F., Egli, D., Lin, C. S., deRooij, D. G., Hirsch, S., Ravi, K., Hicks, J. B., et al. (2011). BRCA1 tumor suppression depends on BRCT phosphoprotein binding, but not its E3 ligase activity. *Science*, 334 (6055): 525-8.

Siegel, R., Naishadham, D. & Jemal, A. (2013). Cancer statistics, 2013. *CA Cancer J Clin*, 63 (1): 11-30.

Simoes, B. M., Piva, M., Iriondo, O., Comaills, V., Lopez-Ruiz, J. A., Zabalza, I., Mieza, J. A., Acinas, O. & Vivanco, M. D. (2011). Effects of estrogen on the proportion of stem cells in the breast. *Breast Cancer Res Treat*, 129 (1): 23-35.

Somasundaram, K., Zhang, H., Zeng, Y. X., Houvras, Y., Peng, Y., Zhang, H., Wu, G. S., Licht, J. D., Weber, B. L. & El-Deiry, W. S. (1997). Arrest of the cell cycle by the tumour-suppressor BRCA1 requires the CDK-inhibitor p21WAF1/CiP1. *Nature*, 389 (6647): 187-90.

Song, W., Gardner, S. A., Hovhannisyan, H., Natalizio, A., Weymouth, K. S., Chen, W., Thibodeau, I., Bogdanova, E., Letovsky, S., Willis, A., et al. (2016). Exploring the landscape of pathogenic genetic variation in the ExAC population database: insights of relevance to variant classification. *Genet Med*, 18 (8): 850-4.

Spencer, D. M., Bilardi, R. A., Koch, T. H., Post, G. C., Nafie, J. W., Kimura, K., Cutts, S. M. & Phillips, D. R. (2008). DNA repair in response to anthracycline-DNA adducts: a role for both homologous recombination and nucleotide excision repair. *Mutat Res*, 638 (1-2): 110-21.

Spurdle, A. B., Whiley, P. J., Thompson, B., Feng, B., Healey, S., Brown, M. A., Pettigrew, C., kConFab, Van Asperen, C. J., Ausems, M. G., et al. (2012). BRCA1 R1699Q variant displaying ambiguous functional abrogation confers intermediate breast and ovarian cancer risk. *J Med Genet*, 49 (8): 525-32.

Sy, S. M., Huen, M. S. & Chen, J. (2009). PALB2 is an integral component of the BRCA complex required for homologous recombination repair. *Proc Natl Acad Sci U S A*, 106 (17): 7155-60.

Szabo, C. I., Worley, T. & Monteiro, A. N. (2004). Understanding germ-line mutations in BRCA1. *Cancer Biol Ther*, 3 (6): 515-20.

Tavtigian, S. V., Deffenbaugh, A. M., Yin, L., Judkins, T., Scholl, T., Samollow, P. B., de Silva, D., Zharkikh, A. & Thomas, A. (2006). Comprehensive statistical study of 452 BRCA1 missense substitutions with classification of eight recurrent substitutions as neutral. *J Med Genet*, 43 (4): 295-305.

Thermo Fischer Scientific. *How cationic lipid mediated transfection works*. Online. Available at: https://www.thermofisher.com/no/en/home/references/gibco-cell-culture-basics/transfection-basics/gene-delivery-technologies/cationic-lipid-mediated-delivery/how-cationic-lipid-mediated-transfection-works.html (accessed: 02.05.2017).

Tischkowitz, M., Hamel, N., Carvalho, M. A., Birrane, G., Soni, A., van Beers, E. H., Joosse, S. A., Wong, N., Novak, D., Quenneville, L. A., et al. (2008). Pathogenicity of the BRCA1 missense variant M1775K is determined by the disruption of the BRCT

phosphopeptide-binding pocket: a multi-modal approach. *Eur J Hum Genet*, 16 (7): 820-32.
Vallon-Christersson, J., Cayanan, C., Haraldsson, K., Loman, N., Bergthorsson, J. T., Brondum-Nielsen, K., Gerdes, A. M., Moller, P., Kristoffersson, U., Olsson, H., et al. (2001). Functional analysis of BRCA1 C-terminal missense mutations identified in breast and ovarian cancer families. *Hum Mol Genet*, 10 (4): 353-60.
van Marcke, C., De Leener, A., Berliere, M., Vikkula, M. & Duhoux, F. P. (2016). Routine use of gene panel testing in hereditary breast cancer should be performed with caution. *Crit Rev Oncol Hematol*, 108: 33-39.
Vuong, D., Simpson, P. T., Green, B., Cummings, M. C. & Lakhani, S. R. (2014). Molecular classification of breast cancer. *Virchows Arch*, 465 (1): 1-14.
Wang, L. & Di, L. J. (2014). BRCA1 and estrogen/estrogen receptor in breast cancer: where they interact? *Int J Biol Sci*, 10 (5): 566-75.
Wang, X. W., Zhan, Q., Coursen, J. D., Khan, M. A., Kontny, H. U., Yu, L., Hollander, M. C., O'Connor, P. M., Fornace, A. J., Jr. & Harris, C. C. (1999). GADD45 induction of a G2/M cell cycle checkpoint. *Proc Natl Acad Sci U S A*, 96 (7): 3706-11.
Williams, R. S., Chasman, D. I., Hau, D. D., Hui, B., Lau, A. Y. & Glover, J. N. (2003). Detection of protein folding defects caused by BRCA1-BRCT truncation and missense mutations. *J Biol Chem*, 278 (52): 53007-16.
Wu, Q., Jubb, H. & Blundell, T. L. (2015). Phosphopeptide interactions with BRCA1 BRCT domains: More than just a motif. *Prog Biophys Mol Biol*, 117 (2-3): 143-8.
Yarden, R. I., Pardo-Reoyo, S., Sgagias, M., Cowan, K. H. & Brody, L. C. (2002). BRCA1 regulates the G2/M checkpoint by activating Chk1 kinase upon DNA damage. *Nat Genet*, 30 (3): 285-9.
Zhang, F., Ma, J., Wu, J., Ye, L., Cai, H., Xia, B. & Yu, X. (2009). PALB2 links BRCA1 and BRCA2 in the DNA-damage response. *Curr Biol*, 19 (6): 524-9.

8 Appendix

Section A

Appendix A contains tables of instruments, software, kits, reagents and disposables used in this study.

Table S1. Instruments and suppliers.

Instrument	Supplier
ABI 3730 DNA Analyser	Applied Biosystems®
BioMek FX	Beckman Coulter
ImageQuant™ LAS 4000	GE Healthcare Life Sciences
TS8024 Lab Drying Convection Oven	Termaks
NanoDrop® ND-1000	Thermo Scientific
Nikon Eclipse TE 300	Nikon
Nikon Eclipse Ts2-FL	Nikon
NucleoCounter® NC-100™	ChemoMetec A/S
Forma™ 370 Steri-Cycle™ CO2 Incubator	Thermo Scientific
Applied Biosystems™ QuantStudio™ 12K Flex Real-Time System	Thermo Scientific
Synergy™ H1	BioTek
Veriti™ 96 well Thermal Cycler	Applied Biosystems®
VersaMax microplate reader	Molecular Devices

Table S2. Software and suppliers.

Software	Supplier
Alamut® Visual	Interactive Biosoftware
CleanSEQ® for BioMek® FX v. 2.74	Agencourt®
Gen5™ Microplate Reader and Imager Software	BioTek
SeqPilot v.4.3.1	JSI medical systems
SnapGene® 3.3.2	GSL Biotech
SoftMax® Pro 6.4	Molecular Devices
ImageQuant™ TL 1D v8.1	GE Healthcare Life Sciences

Table S3. Disposables and suppliers.

Disposables	Supplier
Nunc™ Cell Culture Treated Multidishes (96-well and 12-well)	Thermo Scientific
NucleoCassette™	ChemoMetec A/S
Microcellulose Membranes, 0,2 µm	Bio-Rad
Microplate, 96 well, ps, half area, µclear®, white, med. Binding.	Greiner bio-one GmbH
Mini-PROTEAN® TGX™ Gels, 10 %, 10-well comb, 30 µL	Bio-Rad

Table S4. Kits, suppliers and catalogue numbers.

Kit	Supplier	Catalog number
Agencourt® CleanSEQ®	Beckman Coulter, CA, USA	A2915 4
BigDye® Terminator v3.1 Cycle Sequencing Kit	Thermo Fisher Scientific, Waltham, MA, USA	4337455
Dual-Luciferase® Reporter Assay System	Promega, Madison, Wi, USA	E1960
ECL™ Prime Western Blotting Detection Reagent	GE Healthcare, Buckinghamshire, UK	RPN2232
High Capacity cDNA Reverse Transcription Kit, 1000 reactions	Applied Biosystems®	4368813
Lipofectamine® 3000 Transfection Reagent	Invitrogen, Carlsbad, CA, USA	L3000008
Pierce™ BCA Protein Assay Kit	Thermo Fisher Scientific, Waltham, MA, USA	23225
QIAamp DNA Mini Kit	Qiagen GmbH, Hilden, Germany	51304
QuikChange XL II Site-Directed Mutagenesis Kit	Agilent Technologies	200517-4
RNAqueous® Total RNA Isolation Kit	Thermo Fisher Scientific, Waltham, MA, USA	AM1912
ZymoPURE™ Plasmid Maxiprep Kit	Zymo Research, Irvine, CA, USA	D4202 & D4203
Zyppy™ Plasmid Miniprep Kit	Zymo Research, Irvine, CA, USA	D4036, D4019 & D4037

Table S5. Chemicals, suppliers and catalogue numbers.

Chemicals	Supplier	
10x TBS	Bio-Rad	170-6435
10x TGS Buffer	Bio-Rad	161-0732
100x Halt™ Protease & Phosphatase inhibitor cocktail	Thermo Fisher Scientific	78440
Adriamycin®, 2 mg/mL	Pfizer	505875
Ampicillin, Sodium Salt	Calbiochem®	171254
Bovine Serum Albumin	Sigma-Aldrich®	A7906-100G
Carboplatin Hospira, 10 mg/mL	Hospira	564931
Cell proliferation reagent WST-1	Sigma-Aldrich®	11644807001
Dulbecco's Modified Eagle Medium (DMEM)	Thermo Fisher Scientific	
Dulbecco's phosphate-buffered saline (DPBS)	Thermo Fisher Scientific	14190250
Glycine	Bio-Rad	161-0718
Glycerol	VWR Chemicals	101184K
Halt™ Protease & Phosphatase Inhibitor cocktail (100x)	Thermo Fisher Scientific	1861281
HuMEC Basal Serum-Free Medium	Thermo Fisher Scientific	12753018
HuMEC Supplement Kit	Thermo Fisher Scientific	12755013
Methanol	Emsure®	1.06009.2511
Peptone from casein	Merck, Darmstadt, Germany	1.11931.1000
Ponceau S solution	Sigma-Aldrich	P7171-1L
Roswell Park Memorial Institute (RPMI) 1640	Thermo Fisher Scientific	11875093
S.O.C. Medium	Invitrogen™	1749148
Sodium chloride	Merck, Darmstadt, Germany	1.06404.5000
Trizma® base	Sigma-Aldrich®	T1503-1KG

Trypsin-EDTA (0.05 %)	Thermo Fisher Scientific	25300054
Tween® 20 viscous liquid	Sigma-Aldrich®	P1379
Yeast Extract	Sigma-Aldrich®	Y1625-250G

Table S6. Antibodies and protein ladder

Name	Supplier
Precision Plus Protein™ Dual Xtra Standards (161-0377)	BioRad
BRCA1 Antibody (C-20): sc-642	Santa Cruz Biotechnology
BRCA1 Antibody (D-9): sc-6954	Santa Cruz Biotechnology
m-IgGκ BP-HRP: sc-516102	Santa Cruz Biotechnology

Section B

This appendix contains primers, reaction mixes and PCR cycling parameters used in this study.

Table S7. Primers used for incorporation of BRCA1 variants in plasmid pcDNA3 GAL4 DBD:BRCA1 by in vitro mutagenesis. Variant nucleotides are given in bold capitals.

Variant	Direction	Sequence 5'-3'
p.Met1652Ile	fwd	ggggtcaggccagacaccac**T**atggacattcttttgttg
	rev	caacaaaagaatgtccat**A**gtggtgtctggcctgacccc
p.Ser1655Phe	fwd	ctggggtcaggcca**A**acaccaccatggacattc
	rev	gaatgtccatggtggtgt**T**tggcctgaccccag
p.Asp1692Ala	fwd	ccgttcacacacaaactcagca**G**ctgttttcataacaacatg
	rev	catgttgttatgaaaacag**C**tgctgagtttgtgtgtgaacgg
p.Arg1699Trp	fwd	cctagaaaatatttcagtgtcc**A**ttcacacacaaactcagc
	rev	gctgagtttgtgtgtgaa**T**ggacactgaaatattttctagg
p.Arg1699Gln	fwd	cctagaaaatatttcagtgtc**T**gttcacacacaaactcagc
	rev	gctgagtttgtgtgtgaac**A**gacactgaaatattttctagg
p.Thr1700Thr	fwd	cccgcaattcctagaaaatatttcag**C**gtccgttcacacacaaac
	rev	gtttgtgtgtgaacggac**G**ctgaaatattttctaggaattgcggg
p.Gly1706Arg	fwd	cccattttcctcccgcaattc**T**tagaaaatatttcagtg
	rev	cactgaaatattttcta**A**gaattgcgggaggaaaatggg
p.Ala1708Val	fwd	ctacccattttcctccc**A**caattcctagaaaatatttcagtg
	rev	cactgaaatattttctaggaattg**T**gggaggaaaatgggtag
p.Gly1709Arg	fwd	ctacccattttcctc**T**cgcaattcctagaaaatatttcagtg
	rev	cactgaaatattttctaggaattgcg**A**gaggaaaatgggtag
p.Lys1711Gln	fwd	cccagaaatagctaactacccatt**G**tcctcccgcaattcctag
	rev	ctaggaattgcgggagga**C**aatgggtagttagctatttctggg
p.Arg1751Gln	fwd	ctgtcctgggattctcttgct**T**gctttggaccttggtggtttc
	rev	gaaaccaccaaggtccaaagc**A**agcaagagaatcccaggacag
p.Gly1770Val	fwd	gtgggcatgttggtgaagggc**A**catagcaacagatttctag
	rev	ctagaaatctgttgctatg**T**gcccttcaccaacatgcccac
p.Pro1776Ser	fwd	ccattccagttgatctgtgg**A**catgttggtgaagggcccatagc
	rev	gctatgggcccttcaccaacatg**T**ccacagatcaactggaatgg
p.Met1783Thr	fwd	gcaccacacagctgtacc**G**tccattccagttgatctgtgggc
	rev	gcccacagatcaactggaatgga**C**ggtacagctgtgtggtgc
p.Val1804Asp	fwd	gcacaaccacaattgggtgg**T**cacctgtgccaagggtgaatg
	rev	cattcacccttggcacaggtg**A**ccacccaattgtggttgtgc
p.Glu1826Leu	fwd	caggtgcctcacacatc**A**gcccaattgcatggaagccattgtc
	rev	gacaatggcttccatgcaattgggc**T**gatgtgtgaggcacctg
p.Arg1835Gln	fwd	gctacactgtccaacacccactct**T**gggtcaccacaggtgcctc
	rev	gaggcacctgtggtgaccc**A**agagtgggtgttggacagtgtagc
p.Val1838Gly	fwd	gtgctacactgtccaac**C**cccactctcgggtcaccac
	rev	gtggtgacccgagagtggg**G**gttggacagtgtagcac

Table S8. *In vitro* mutagenesis reaction-mix per sample utilised for incorporation of *BRCA1* BRCT missense variants.

Reagent	Volume	Concentration
10x reaction buffer	5 µL	-
dsDNA template	1 µL	10 ng
Forward primer	1 µL	125 ng
Reverse primer	1 µL	125 ng
dNTP mix	1 µL	-
QuikSolution	3 µL	-
ddH_2O	38 µL	-
PfuUltra HF DNA polymerase	1 µL	2.5 U/µL

Table S9. *In vitro* mutagenesis cycling parameters utilised for incorporation of *BRCA1* BRCT missense variants.

Segment	Temperature	Time	
Denature	95 °C	1'	
Denature	95 °C	50"	
Annealing	60 °C	50"	x 18
Extension	68 °C	8'	
Extension	68 °C	7'	
Hold	4 °C	∞	

Table S10. Sequencing primers used in verification of plasmid DNA sequence.

Name	Location	Direction	Exon	Sequence 5'-3'
T7for.	pcDNA3	Fwd	-	TAATACGACTCACTATAGGG
BRCA1_c.3548AG_SNP	*BRCA1*	Rev	13	CTAACACAGCTTCTAGTTCAGCC
13F_BRCA1_mRNA	*BRCA1*	Fwd	13	GACTCTTCTGCCCTTGAGGA
BRCA1_c.4308TC_SNP	*BRCA1*	Rev	15	TGATGGGCATTTAGAAGGGG
15F_BRCA1_mRNA	*BRCA1*	Fwd	15	GATGTGGAGGAGCAACAGCT
17F_BRCA1_mRNA	*BRCA1*	Fwd	17	GTTTGCCAGAAAACACCACA
20F_BRCA1_mRNA	*BRCA1*	Fwd	20	GGAGATGTGGTCAATGGAAGAAAC
BGHrev.	pcDNA3	Rev	-	TAGAAGGCACAGTCGAGG

Table S11. Sanger sequencing reaction-mix per sample used in verification of plasmid DNA sequence.

Reagent	Volume	Concentration
5x Sequencing Buffer	1.88 µL	-
Primer	1.00 µL	3.2 pmol
BigDye v3.1	0.25 µL	-
Template	1.00 µL	200 ng
ddH_2O	5.88 µL	-

Table S12. Sanger sequencing cycling parameters used in verification of plasmid DNA sequence..

Segment	Temperature	Time	
Denature	96 °C	1'	
Denature	96 °C	10"	
Annealing	50 °C	5"	x 25
Extension	60 °C	4'	
Soak	10 °C	∞	

Table S13. *BRCA1* primers used in Sanger sequencing of cell lines. Uppercase letters are *BRCA1* specific sequence, lowercase letters are M13 tails.

Name	Exon	Direction	Sequence 5'-3'
BRCA1_2v2F	2	Fwd	tgtaaaacgacggccagtGGACGTTGTCATTAGTTCTTTGGTTTG
BRCA1_2v2R	2	Rev	caggaaacagctatgaccCGGACCACAGGATTTGTGTTGA
BRCA1_2v3R	2	Rev	caggaaacagctatgaccGACCACAGGATTTGTGTTGAAAA
BRCA1_3F	3	Fwd	tgtaaaacgacggccagtTGCACCCACAGTGATAGTGCAGA
BRCA1_3R	3	Rev	caggaaacagctatgaccTCTGAGAAAGAATGAAATGGAGTTGGA
BRCA1_5F	5	Fwd	tgtaaaacgacggccagtGGCTCTTAAGGGCAGTTGTG
BRCA1_5R	5	Rev	caggaaacagctatgaccAAGGCAGATGTCCCATAAAACTT
BRCA1_6F	6	Fwd	tgtaaaacgacggccagtTGCAATGCATTATATCTGCTGTGGAT
BRCA1_6R	6	Rev	caggaaacagctatgaccAAGGTGTGAGACCAGTGGGAGTAATTT
BRCA1_7.1F	7	Fwd	tgtaaaacgacggccagtGGTGTGTCATTTGTTTAATTTGTGTGC
BRCA1_7.1R	7	Rev	caggaaacagctatgaccTTCGGGTTCACTCTGTAGAAGTCTTT
BRCA1_7.2F	7	Fwd	tgtaaaacgacggccagtCATAGGGTTTCTCTTGGTTTCTTTGA
BRCA1_7.2R	7	Rev	caggaaacagctatgaccCAATGCTCAATAAAGAGATGTTGCCA
BRCA1_8F	8	Fwd	tgtaaaacgacggccagtGGTCTCACTCTGTTGCTTATGCTGG
BRCA1_8R	8	Rev	caggaaacagctatgaccTCTTCAAGGTGGGAACTGCGTC
BRCA1_9F	9	Fwd	tgtaaaacgacggccagtCGAAGCCCATGCCTTTAACCA
BRCA1_9R	9	Rev	caggaaacagctatgaccCACCAAATCCCAAGTCGTGTG
BRCA1_10F	10	Fwd	tgtaaaacgacggccagtCTGCCTCCCAGGTTGAAGCC
BRCA1_10R	10	Rev	caggaaacagctatgaccTGGGTTGTAAAGGTCCCAAATGGT
BRCA1_11.1F	11	Fwd	tgtaaaacgacggccagtTGGTTGATTTCCACCTCCAAGG
BRCA1_11.1R	11	Rev	caggaaacagctatgaccTCTCTAGGATTCTCTGAGCATGGCA

BRCA1_11.2F	11	Fwd	tgtaaaacgacggccagtCATGCCAGCTCATTACAGCATGA
BRCA1_11.2R	11	Rev	caggaaacagctatgaccGGAGGCTTGCCTTCTTCCGA
BRCA1_11.3F	11	Fwd	tgtaaaacgacggccagtTGCCAAAGTAGCTGATGTATTGGACG
BRCA1_11.3R	11	Rev	caggaaacagctatgaccACTGCTGCTTATAGGTTCAGCTTTCG
BRCA1_11.4F	11	Fwd	tgtaaaacgacggccagtTGATAAATCAGGGAACTAACCAAACGG
BRCA1_11.4R	11	Rev	caggaaacagctatgaccGGTTTCTGCTGTGCCTGACTGG
BRCA1_11.5F	11	Fwd	tgtaaaacgacggccagtTGAGGAGGAAGTCTTCTACCAGGCA
BRCA1_11.5R	11	Rev	caggaaacagctatgaccTCAAATGCTGCACACTGACTCACA
BRCA1_11.6F	11	Fwd	tgtaaaacgacggccagtTGCCAGTCAGGCACAGCAGA
BRCA1_11.6R	11	Rev	caggaaacagctatgaccGTGGTTAACTTCATGTCCCAATGGA
BRCA1_11.7F	11	Fwd	tgtaaaacgacggccagtTGTGAGTCAGTGTGCAGCATTTG
BRCA1_11.7R	11	Rev	caggaaacagctatgaccGAGCCTCCTTTGATACTACATTTGGCA
BRCA1_11.8F	11	Fwd	tgtaaaacgacggccagtTTCTCTGCCCACTCTGGGTCC
BRCA1_11.8R	11	Rev	caggaaacagctatgaccGGCCCTCTGTTTCTACCTAGTTCTGC
BRCA1_11.9F	11	Fwd	tgtaaaacgacggccagtTCACCTGAAAGAGAAATGGGAAATGA
BRCA1_11.9R	11	Rev	caggaaacagctatgaccTGTGTATGGGTGAAAGGGCTAGGA
BRCA1_11.10F	11	Fwd	tgtaaaacgacggccagtCAGAACTAGGTAGAAACAGAGGGCCA
BRCA1_11.10R	11	Rev	caggaaacagctatgaccCAAGTGTTGGAAGCAGGGAAGC
BRCA1_11.11F	11	Fwd	tgtaaaacgacggccagtGGAGTCCTAGCCCTTTCACCCA
BRCA1_11.11R	11	Rev	caggaaacagctatgaccTCACTCAGACCAACTCCCTGGC
BRCA1_11.12F	11	Fwd	tgtaaaacgacggccagtGCTTCCCTGCTTCCAACACTTGTTAT
BRCA1_11.12R	11	Rev	caggaaacagctatgaccGCACCTTAGGAGGAACATGTTTCAAG
BRCA1_12.2F	12	Fwd	tgtaaaacgacggccagtTGTCCCAAAGCAAGGAATTTAATCA
BRCA1_12.2R	12	Rev	caggaaacagctatgaccGCAAATGGGTTTCGAAGGTTTAGC
BRCA1_13F	13	Fwd	tgtaaaacgacggccagtGGGCATTAATTGCATGAATGTGG
BRCA1_13R	13	Rev	caggaaacagctatgaccTGCCTTGGGTCCCTCTGACTG
BRCA1_14F	14	Fwd	tgtaaaacgacggccagtGCATCTGTCTGTTGCATTGCTTG
BRCA1_14R	14	Rev	caggaaacagctatgaccCCATCAGTTTCCAAGCTTGTTCAGG
BRCA1_15v2F	15	Fwd	tgtaaaacgacggccagtTCATTTCTGATCTCTCTGACATGAGC
BRCA1_15v2R	15	Rev	caggaaacagctatgaccTGAGCTATTTTTCTAAAGTGGGCTTA
BRCA1_16.1F	16	Fwd	tgtaaaacgacggccagtGCTACTTTGGATTTCCACCAACACTG
BRCA1_16.1R	16	Rev	caggaaacagctatgaccGCTTCTCCCTGCTCACACTTTCTTC
BRCA1_16.2F	16	Fwd	tgtaaaacgacggccagtTCAACCTCTGCATTGAAAGTTCCC
BRCA1_16.2R	16	Rev	caggaaacagctatgaccCTGGTAAATTCACCCATGTGAGACAA
BRCA1_17F	17	Fwd	tgtaaaacgacggccagtACTAGTATTCTGAGCTGTGTGCTAGA
BRCA1_17.1R	17	Rev	caggaaacagctatgaccTCGATCTCCTAATCTCGTGATCTGC
BRCA1_18F	18	Fwd	tgtaaaacgacggccagtGCCTCTGATTCTGTCACCAGGG
BRCA1_18R	18	Rev	caggaaacagctatgaccGCTGCACATGGATTCCTGCC
BRCA1_19F	19	Fwd	tgtaaaacgacggccagtGGAATCCATGTGCAGCAGGC
BRCA1_19R	19	Rev	caggaaacagctatgaccGGCCTGCATAATTCTTGATGATCC
BRCA1_20F	20	Fwd	tgtaaaacgacggccagtCTGCAACCTCCACCTCCTGC
BRCA1_20R	20	Rev	caggaaacagctatgaccTGTGGTTGGGATGGAAGAGTGAA
BRCA1_21v2F	21	Fwd	tgtaaaacgacggccagtGCAGCAGAAATCATCAGGTGGT
BRCA1_21v2R	21	Rev	caggaaacagctatgaccTGCTGTTTTGTTTGGAGAGTGG
BRCA1_22F	22	Fwd	tgtaaaacgacggccagtCATGGCATATCAGTGGCAAATTGA

BRCA1_22R	22	Rev	caggaaacagctatgaccTTGGCACAGGTATGTGGGCA
BRCA1_23.3F	23	Fwd	tgtaaaacgacggccagtGGAGGCTGAGATGGAAGGAT
BRCA1_23.3R	23	Rev	caggaaacagctatgaccACCCCATGGAAACAGTTCAT
BRCA1_24.1F	24	Fwd	tgtaaaacgacggccagtCCAGGACCCTGGAGTCGATTG
BRCA1_24.1R	24	Rev	caggaaacagctatgaccTTAGGGAAACCAGCTATTCTCTTGAGG

Table S14. *TP53* primers used in Sanger sequencing of cell lines. Uppercase letters are *TP53* specific sequence, lowercase letters are M13 tails.

Name	Exon	Direction	Sequence 5'-3'
TP53ex2-4F1_m13	4	Fwd	tgtaaaacgacggccagtTCAGACACTGGCATGGTGTT
TP53ex2-4R2_m13	4	Rev	caggaaacagctatgaccAGGGTGTGATGGGATGGATA
TP53ex5-6F_m13	6	Fwd	tgtaaaacgacggccagtCACTTGTGCCCTGACTTTCA
TP53ex5-6R_m13	6	Rev	caggaaacagctatgaccGGGAGGTCAAATAAGCAGCA
TP53ex7-9F2_m13	7-9	Fwd	tgtaaaacgacggccagtTGGGACCTCTTAACCTGTGG
TP53ex7-9R2_m13	7-9	Rev	caggaaacagctatgaccTGTCTTTGAGGCATCACTGC
TP53ex7-9R1_m13	7-9	Rev	caggaaacagctatgaccAAGGAAACTGAGTGGGAGCA
TP53ex7-9F3_m13	7-9	Fwd	tgtaaaacgacggccagtCCTGCTTGCCACAGGTCT
TP53ex10F_m13	10	Fwd	tgtaaaacgacggccagtGACGAGAGTGAGACCCCATC
TP53ex10R_m13	10	Rev	caggaaacagctatgaccAAGGCAGGATGAGAATGGAA
TP53ex11F_m13	11	Fwd	tgtaaaacgacggccagtAAAGCATTGGTCAGGGAAAA
TP53ex11R_m13	11	Rev	caggaaacagctatgaccGCAAGCAAGGGTTCAAAGAC

Table S15. PCR reagent mix used in Sanger sequencing of endogenous *BRCA1* and *TP53* in cell lines.

Reagent	Volume	Concentration
MQ-H_2O	9.10 µL	-
360 Buffer, 10x	2.00 µL	1x
360 GC-enhancer, 10x	2.00 µL	1x
dNTP, 10 mM	1.60 µL	0.8 mM
$MgCl_2$, 25 mM	1.20 µL	1.5 mM
360 Polymerase, 5 U/µL	0.10 µL	0.025 U/µL
Primer Fwd+Rev	2.00 µL	0.25 µM of each
DNA, ~100 ng/µL	2.00 µL	~10 ng/µL

Table S16. PCR cycling parameters used with 360 polymerase during Sanger sequencing of endogenous *BRCA1* and *TP53.*

Segment	Temperature	Time	
Denature	95 °C	10'	
Denature	95 °C	30"	
Annealing	60 °C	30"	x 30
Extension	72 °C	60'	
Final extension	72 °C	7'	
Soak	10 °C	∞	

Table S17. Multiscribe™ Reverse Transcriptase cDNA reaction mixture for one reaction.

Reagent	Volume	Concentration
10x RT Buffer	5.0 µL	
25x dNTP Mix	2.0 µL	100 mM (25 mM of each)
10x RT Random Primers	5.0 µL	
MultiScribe™ Reverse Transcriptase	2.5 µL	
Nuclease-free water	10.5 µL	
Total	25 µL	

Table S18. cDNA cycling parameters.

	Step 1	Step 2	Step 3	Step 4
Temperature (°C)	25	37	85	4
Time (min)	10	120	5	∞

Table S19. Primers used for real-time quantification of *BRCA1*.

Name	Sequence
BRCA1_QPCR_14-15F	GAACCAGGAGTGGAAAGGTCAT
BRCA1_QPCR_15R2	TGGGTAGTTTCTATTCTGAAGACT

Table S20. SYBR green reaction mix used for qPCR of *BRCA1*. Volumes listed are for one reaction.

Reagent	Volume	Concentration
***Power* SYBR® Green PCR Master Mix**	5.0 µL	
cDNA	4 µL	Diluted 1:5
Primer: BRCA1_QPCR_14-15F	0.5 µL	5 pmol/µL
Primer: BRCA1_QPCR_15R2	0.5 µL	5 pmol/µL
Total	10 µL	

Table S21. TaqMan reaction mix used for qPCR of GAPDH. Volumes listed are for one reaction.

Reagent	Volume	Concentration
TaqMan® Gene Expression Master Mix	5.0 µL	
cDNA	5 µL	Diluted 1:5
GAPDH Oligo Mix (20x)	0.5 µL	
Total	10 µL	

Table S22. Cycling parameters RT-qPCR

	Step 1	Step 2	Step 3 (x 40)	
Cycle			1	2
Temperature (°C)	50	95	95	60
Time	2'	10'	15"	1'

Plasmid pcDNA3 GAL4 DBD:BRCA1 sequence of the GAL4 DBD:BRCA1 wild type insert. Sequence in dark grey are the *BRCA1* BRCT domain (aa 1396-1863), sequence in white are the GAL4 DBD, with the start codon (ATG) in red.

AAGCAAGCCTCCTGAAAGATGAAGCTACTGTCTTCTATCGAACAAGCATGCGATATTTGCCGACTTAAAAAGCTCAAGTGCTC
CAAAGAAAAACCGAAGTGCGCCAAGTGTCTGAAGAACAACTGGGAGTGTCGCTACTCTCCCAAAACCAAAAGGTCTCCGCTGA
CTAGGGCACATCTGACAGAAGTGGAATCAAGGCTAGAAAGACTGGAACAGCTATTTCTACTGATTTTTCCTCGAGAAGACCTT
GACATGATTTTGAAAATGGATTCTTTACAGGATATAAAAGCATTGTTAACAGGATTATTTGTACAAGATAATGTGAATAAAGA
TGCCGTCACAGATAGATTGGCTTCAGTGGAGACTGATATGCCTCTAACATTGAGACAGCATAGAATAAGTGCGACATCATCAT
CGGAAGAGAGTAGTAACAAAGGTCAAAGACAGTTGACTGTATCGCCGGAATTCCAGAGGGATACCATGCAACATAACCTGATA
AAGCTCCAGCAGGAAATGGCTGAACTAGAAGCTGTGTTAGAACAGCATGGGAGCCAGCCTTCTAACAGCTACCCTTCCATCAT
AAGTGACTCTTCTGCCCTTGAGGACCTGCGAAATCCAGAACAAAGCACATCAGAAAAAGCAGTATTAACTTCACAGAAAAGTA
GTGAATACCCTATAAGCCAGAATCCAGAAGGCCTTTCTGCTGACAAGTTTGAGGTGTCTGCAGATAGTTCTACCAGTAAAAAT
AAAGAACCAGGAGTGGAAAGGTCATCCCCTTCTAAATGCCCATCATTAGATGATAGGTGGTACATGCACAGTTGCTCTGGGAG
TCTTCAGAATAGAAACTACCCATCTCAAGAGGAGCTCATTAAGGTTGTTGATGTGGAGGAGCAACAGCTGGAAGAGTCTGGGC
CACACGATTTGACGGAAACATCTTACTTGCCAAGGCAAGATCTAGAGGGAACCCCTTACCTGGAATCTGGAATCAGCCTCTTC
TCTGATGACCCTGAATCTGATCCTTCTGAAGACAGAGCCCCAGAGTCAGCTCGTGTTGGCAACATACCATCTTCAACCTCTGC
ATTGAAAGTTCCCCAATTGAAAGTTGCAGAATCTGCCCAGAGTCCAGCTGCTGCTCATACTACTGATACTGCTGGGTATAATG
CAATGGAAGAAAGTGTGAGCAGGGAGAAGCCAGAATTGACAGCTTCAACAGAAAGGGTCAACAAAAGAATGTCCATGGTGGTG
TCTGGCCTGACCCCAGAAGAATTTATGCTCGTGTACAAGTTTGCCAGAAAACACCACATCACTTTAACTAATCTAATTACTGA
AGAGACTACTCATGTTGTTATGAAAACAGATGCTGAGTTTGTGTGTGAACGGACACTGAAATATTTTCTAGGAATTGCGGGAG
GAAAATGGGTAGTTAGCTATTTCTGGGTGACCCAGTCTATTAAAGAAAGAAAAATGCTGAATGAGCATGATTTTGAAGTCAGA
GGAGATGTGGTCAATGGAAGAAACCACCAAGGTCCAAAGCGAGCAAGAGAATCCCAGGACAGAAAGATCTTCAGGGGGCTAGA
AATCTGTTGCTATGGGCCCTTCACCAACATGCCCACAGATCAACTGGAATGGATGGTACAGCTGTGTGGTGCTTCTGTGGTGA
AGGAGCTTTCATCATTCACCCTTGGCACAGGTGTCCACCCAATTGTGGTTGTGCAGCCAGATGCCTGGACAGAGGACAATGGC
TTCCATGCAATTGGGCAGATGTGTGAGGCACCTGTGGTGACCCGAGAGTGGGTGTTGGACAGTGTAGCACTCTACCAGTGCCA
GGAGCTGGACACCTACCTGATACCCCAGATCCCCCACAGCCACTACTGA

Figure S1. Schematic representation of the pcDNA3 GAL4 DBD:BRCA1 plasmid. Dark purple represents the GAL4 DNA Binding Domain, and pink represents the *BRCA1* BRCT insert. Generated with SnapGene® 3.3.3

Section C

This section contains recipes for buffers and solutions used during transformation, plasmid amplification and western blotting.

Lysogeny broth (LB) medium
10 g tryptone
10 g NaCl
5 g yeast extract
900 mL MQ-H_2O
pH adjusted to 7.0 with 12 M HCl
Volume adjusted to 1 L using MQ-H_2O and autoclaved.

1x TGS buffer (western blot running buffer)
100 mL 10x TGS (Tris/Glycine/SDS)
900 mL MQ-H_2O

Blotting buffer (western blot)
3 g Trizma base
14.4 g glycine
100 mL methanol
900 mL MQ-H_2O

1x TBST (western blot)
100 mL 10x TBS buffer
900 mL MQ-H_2O
1 mL Tween® 20

5 % Bovine serum albumin (BSA, western blot)
2.5 g Bovine serum albumin
50 mL TBST

RIPA lysis buffer w/ inhibitor
1x RIPA buffer
1:100 100x Halt™ Protease & Phosphatase Inhibitor cocktail

Section D

This section contains unedited western blots, and evidence of band specificity on western (kindly provided by Elisabeth Jarhelle, 2017).

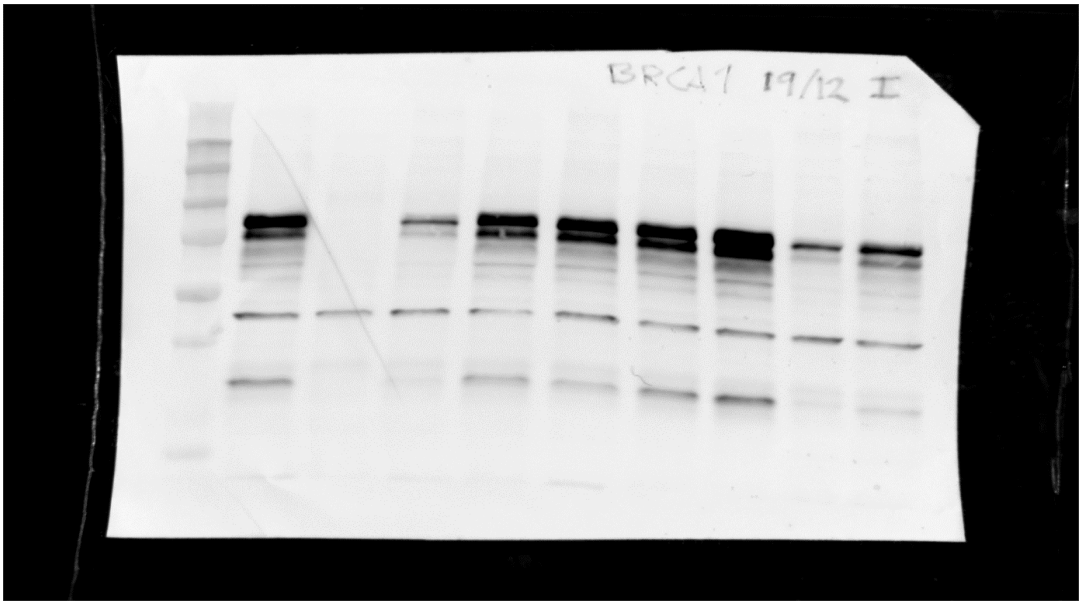

Figure S2. Unedited western blot of HEK293T cell lysates stained with primary antibody BRCA1 (C-20):sc-642 in a 1:2000 dilution, and secondary antibody m-IgGκ BP-HRP: sc-516102 in a 1:1000 dilution.

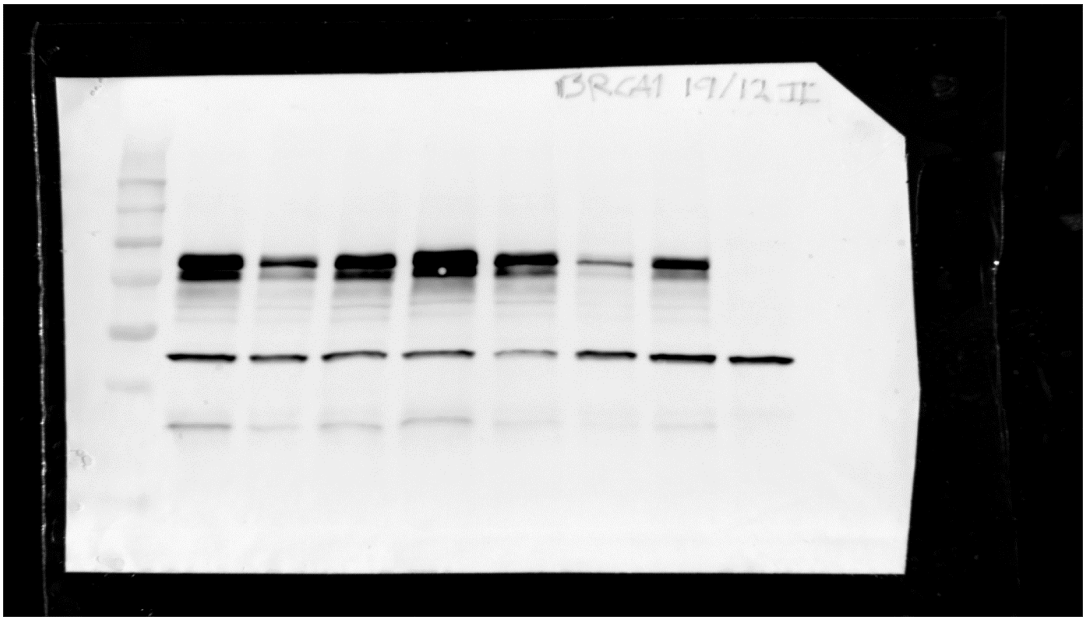

Figure S3. Unedited western blot of HEK293T cell lysates stained with primary antibody BRCA1 (C-20):sc-642 in a 1:2000 dilution, and secondary antibody m-IgGκ BP-HRP: sc-516102 in a 1:1000 dilution.

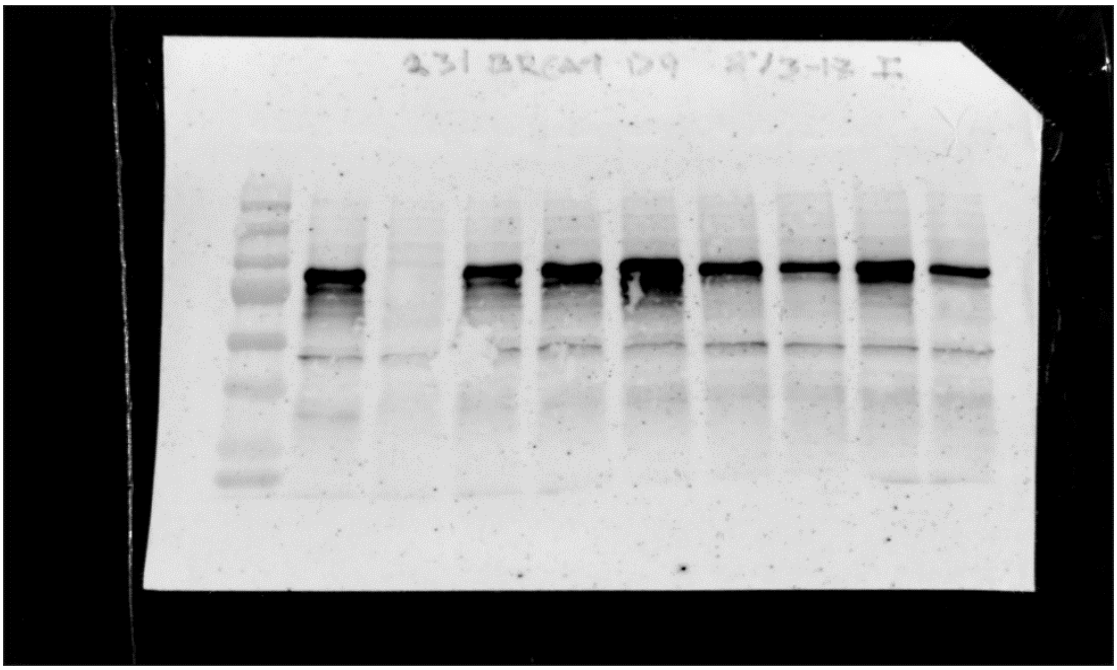

Figure S4. Unedited western blot of MDA-MB-231 cell lysates stained with primary antibody BRCA1 (D-9):sc-6954 in a 1:1000 dilution, and secondary antibody m-IgGκ BP-HRP: sc-516102 in a 1:1000 dilution.

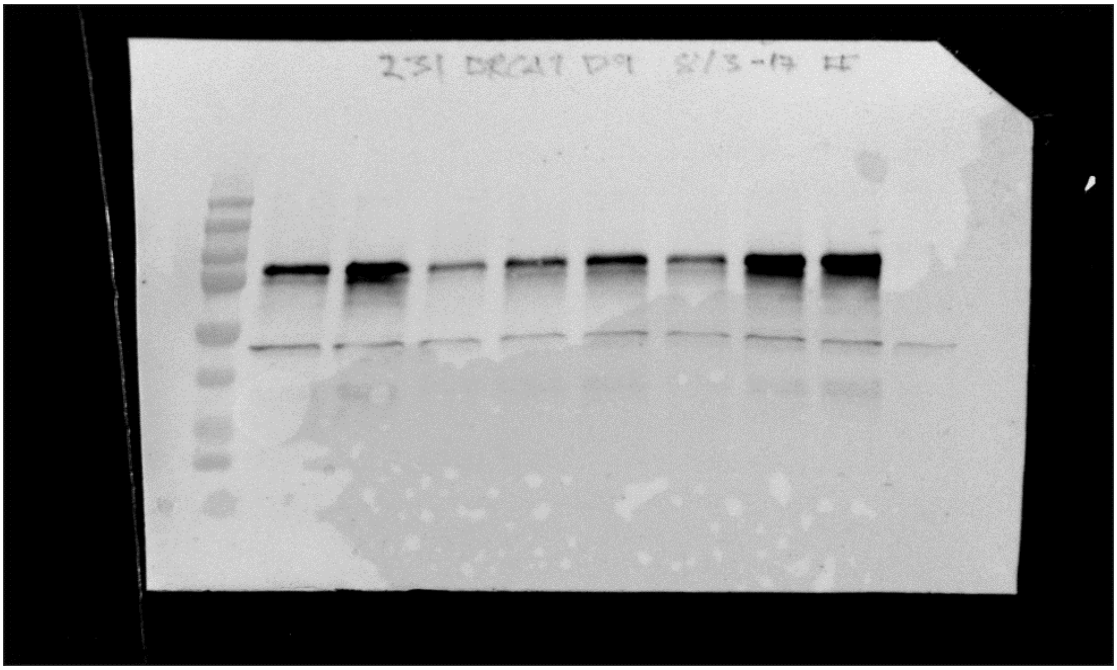

Figure S5. Unedited western blot of MDA-MB-231 cell lysates stained with primary antibody BRCA1 (D-9):sc-6954 in a 1:1000 dilution, and secondary antibody m-IgGκ BP-HRP: sc-516102 in a 1:1000 dilution.

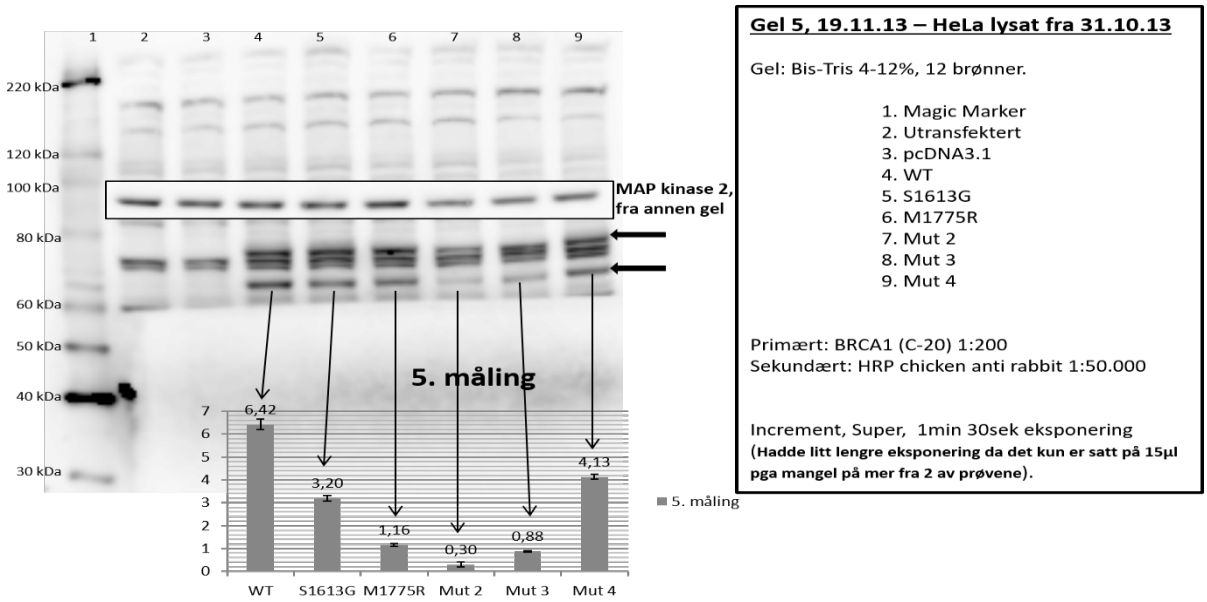

Figure S6. Evidence of band specificity provided by Elisabeth Jarhelle, illustrating that the two bands (indicated by bold black arrows) were specific for the GAL4 DBD:BRCA1 containing transfections.

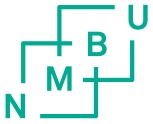

Norges miljø- og biovitenskapelig universitet
Noregs miljø- og biovitskapelege universitet
Norwegian University of Life Sciences

Postboks 5003
NO-1432 Ås
Norway